THE BREAKDOWN OF STAINLESS STEELS IN STRONG ACIDS

Nigel Mykura

Submitted for the Degree of

Doctor of Philosophy

to the

University of Aston in Birmingham

February 1982

NIGEL MYKURA

PhD 1982

SUMMARY

A study was made of the corrosion behaviour in the ASTM standard Nitric acid and Oxalic acid tests, of two commercial AISI type 304L steels in the as-received condition and after various heat treatments.

Optical microscopy and SEM, TEM and STEM in conjunction with energy dispersive x-ray analysis, were used to correlate the corrosion behaviour of these steels with their microstructure. Some evidence of phosphorus segregation at grain boundaries was found. The corrosion behaviour at microstructural level was studied by examining on the TEM thin foils of steel that had been exposed to boiling nitric acid.

Banding attack in the nitric acid and oxalic acid tests was studied using SEM and EPMA and found to be due to the micro-segregation of chromium and nickel.

Using two experimental series of 304L, one a 17% Cr, 9% Ni steel with phosphorus additions from 0.006% to 0.028%, the other a 20% Cr, 12% Ni steel with boron additions from 0.001% to 0.0085%, the effect of these elements on corrosion in the nitric acid test was studied. The effect of different cooling rates and different solution treatment temperature on the behaviour of these steels was examined. TEM and STEM in conjunction with energy-dispersive x-ray analysis were again used to study the microstructure of the steels. Phosphorus was found to affect the corrosion behaviour but no effect was found with boron.

Key words: austenitic stainless steel, intergranular corrosion, nitric acid, segregation

Contents

List of Plates

List of Tables

Page

List of Figures

Page

Introduction

The breakdown of stainless steels in strong acids as a result of intergranular corrosion occurs regularly and often unpredictably in practice. Despite much research work the mechanisms of such attack have not been fully explained.

This thesis covers experimental work on certain aspects of the intergranular corrosion (IGC) of austenitic stainless steel (mainly AISI 304L) performed by the author.

The first section of the work contains a review of the literature on IGC relevant to the study. This is followed by an experimental study of two commercial produced type 304L steels, one of which had shown an unusually high corrosion rate in the ASTM standard nitric acid test. The effect of various heat treatments on the performance of these two steels in this test was investigated, and the metallurgical structures of the steels studied using optical and electron methods.

The corrosion behaviour of two of the heat treated steels was investigated on a microscopic scale by exposing transmission electron microscopy (TEM) specimens to boiling nitric acid solution and then examining the microstructure of the exposed specimens.

As well as the nitric acid test, the oxalic acid etch test was used to assess the corrosion resistance of the treated commercial steels and the results from this test were correlated with the nitric acid test results on the same

steels.

A detailed optical and electron-optical study in conjunction with electron probe microanalysis (EPMA) was made of the micro-segregation that results in banded attack in the nitric acid and oxalic acid tests. This is followed be a review of the relevant literature on solute segregation, which leads into a study of such segregation in AISI 304L using scanning transmission electron microscopy STEM and enegy dispersive x-ray analysis.

The corrosion behaviour in the nitric acid test of two experimental casts of AISI 304L with controlled additons of phosphorus and boron were studied after they had been cooled at different rates from the solution treatment temperature.

Short discussion sections are included after each main experimental section and these are augmented by a general discussion. The main section of the thesis is followed by the conclusions and appendices which discuss various aspects such as specimen preparation.

1. Stainless Steels

One of the major reasons stainless steels are chosen for particular applications in industry is their high resistance to corrosion in a wide range of hostile environments. To be "stainless" an alloy must have a minimum of approximately 11% chromium. With a chromium content greater than this, an alloy will tend to form a tenacious, protective oxide in an oxidising environment such as air, and it is this oxide which endows it with its corrosion resistant properties.

Many other elements as well as chromium are used in stainless steels to give them a wide range of structures and properties. The main elements used are nickel, molydenum, titanium and niobium, and also sulphur and selenium when specific properties are required.

Chromium is a very strong ferrite stabiliser, i.e. increasing the amount of chromium in a stainless steel increases the tendency for that steel to produce a ferritic (body-centred cubic) structure. Silicon, molybdenum, vanadium, titanium and aluminium are also ferrite stabilisers.

Nickel, on the other hand, along with carbon, nitrogen, cobalt and manganese, are austenite (face-centred cubic atomic structure) stabilisers.

To achieve specific structure and properties it is essential to have the correct balance of alloying elements. The Schaeffler diagram (Fig. 1) illustrates the dependence of

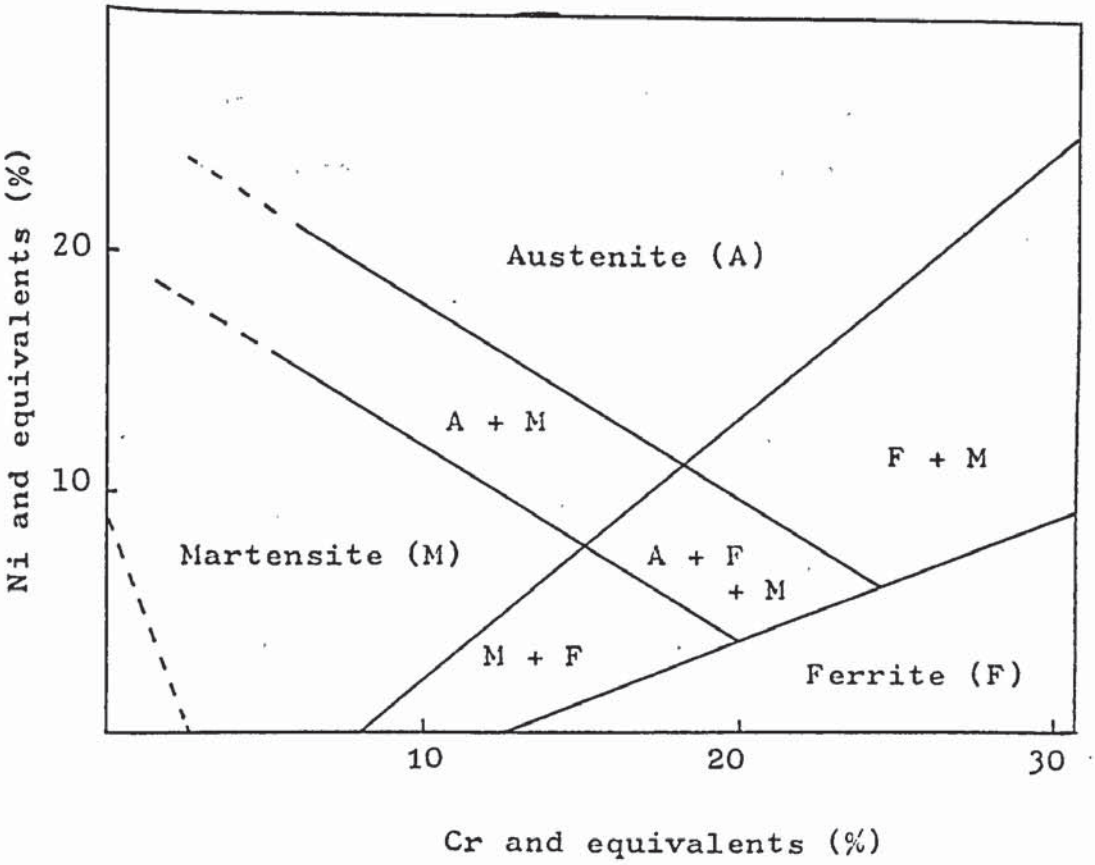

Fig. 1 Schaeffler diagram (Ref. 1 after Schaeffler and Schneider)

structure on composition. This is a non equilibrium diagram showing structures obtained after rapid cooling from 1050°C. The nickel and chromium equivalents can be obtained from the equations given by Pickering [110].-

$$\%\ \text{Ni equivalent} = \%Ni + \%Co + 30(\%C) + 25(\%N) + 0.5(\%Mn) + 0.3(\%Cu)$$

$$\%\ \text{Cr equivalent} = \%Cr + 2(\%Si) + 1.5(\%Mo) + 5(\%V) + 5.5(\%Al) + 1.5(\%Nb) + (1.5(\%Ti) + 0.75(\%W)$$

The differing compositions can result in four categories of stainless steel, defined by their structure: austenitic, ferritic, duplex (austenite + ferrite) and martensitic.

Of the four categories of stainless steel the largest by far in terms of production and utilisation, is the austenitic series. It is these steels which show the greatest general corrosion resistance and in particular the greatest resistance to corrosion in strong acids.

The austenitic steels consist of a single phase austenite at room temperature and this structure is maintained by having the correct balance of austenite and ferrite stabilizers. Commercial alloys of this type have compositions in the range (weight per cent)

Ni	6	-	22
Cr	16	-	26
C	0.03	-	0.25

All the austenitic alloys are variations of the classic 18/8 (chromium/nickel) theme with various compositional alterations made to provide different mechanical and chemical properties.

The austenitic stainless steels are typified by AISI type 304 steels with 18 to 20 per cent chromium and 8 to 12 per cent nickel, 0.08 per cent carbon, 2 per cent manganese and 1 per cent silicon. (Fig. 2). Overall it is the higher nickel type alloys that have the greatest corrosion resistance. The 304 type alloy is so widely used that the production for this type of alloy exceeds the combined production total for all the non-austenitic stainless steels [1]. The nickel is mainly responsible for the austenitic structure and increasing the nickel content

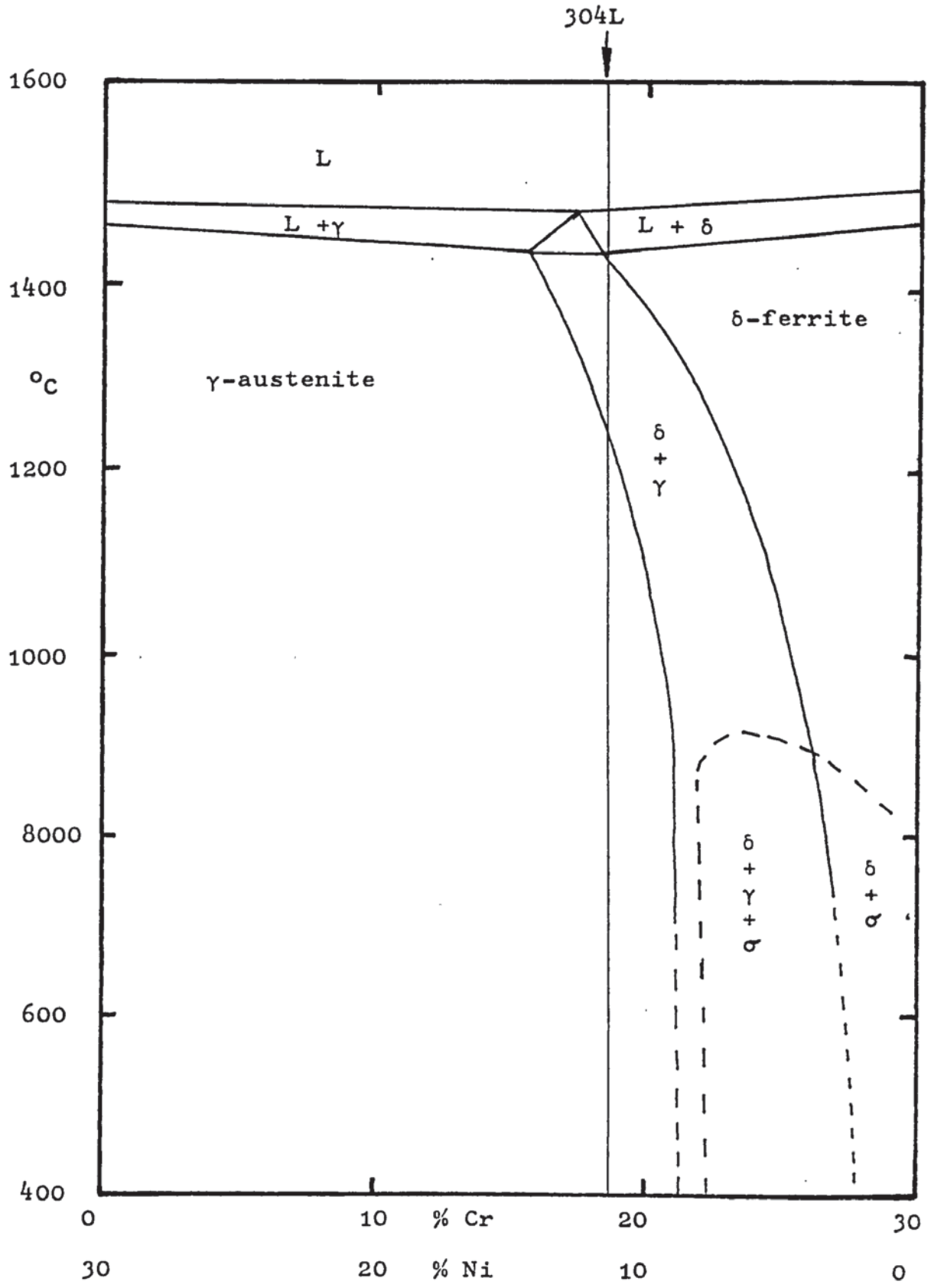

70% Fe vertical section of the Fe-Cr-Ni ternary phase diagram showing the approximate composition of AISI Type 304L stainless steel. (After Ref. 111)

Fig. 2

increases the stability of the austenite. The austenitic steels are more ductile, are easier to weld than the ferritic steels, and in general are easier to use.

Although the austenitic steels are superior in most aspects they have one drawback when being considered for use in low pH acids or very highly oxidising solutions.

It is now widely known and accepted that when an alloy of the 18/8 type is heated in the temperature range 425 - 800^{o}C, or is cooled through this range it can undergo certain metallurgical changes which result in a greatly increased susceptibility to intergranular corrosion if subsequently exposed to certain corrosive media, particularly highly oxidising acid solutions.

This treatment by which a steel becomes more susceptible to intergranular attack is commonly known as sensitization. In this work the word sensitization will be used to describe heat treatments that can result in susceptibility, but this does not necessarily imply susceptibility.

It is the effect of various heat treatments on the sensitization of AISI 304L, the low carbon version of AISI 304, and the subsequent corrosion of such steels in boiling nitric acid, that this work is mainly concerned.

1.1 Intergranular Corrosion in Austenitic Stainless Steel

Intergranular corrosion in austenitic steels nearly always occurs in steels that have been sensitized, usually by heating within the sensitizing range, although it can occur after cooling through this range.

The temperatures most likely to result in susceptibility to intergranular corrosion are those in the middle of the sensitization range, but this is also dependent on the time of exposure. Long times may be required in the lower part of the range while very short times may result in susceptibility in the upper part of the range. For an 18/8 steel containing 0.08 per cent carbon, heated for one minute, the most dangerous temperature is 750°C [2]. (Fig. 3). If the heating time is one hour the critical range will extend from 550 to 740°C, and if of the order of one thousand hours the range of maximum susceptibility shifts to 550 to 650°C.

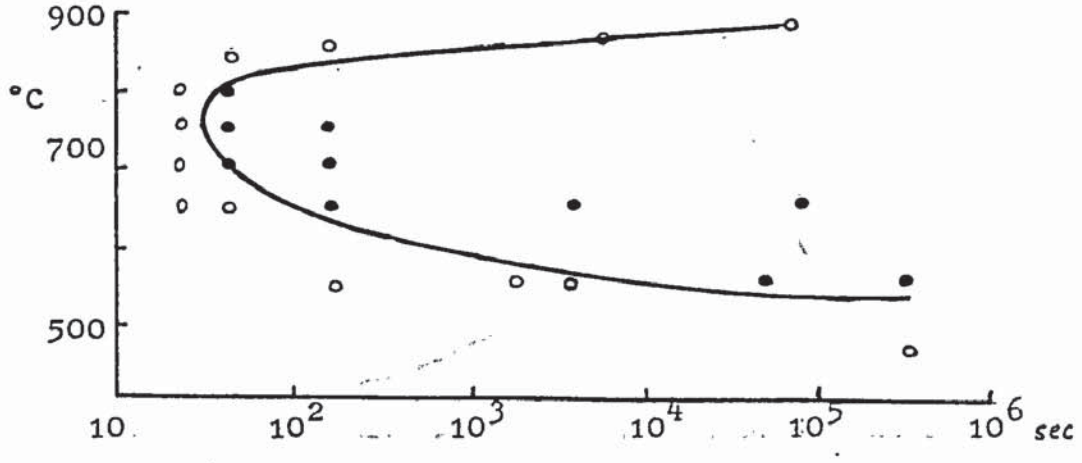

Fig. 3 Effect of time and temperature on sensitization of an 18/8 steel.

Slow cooling through the sensitizing range can induce susceptibility but rapid cooling such as quenching prevents this occurring.

Sensitization can also arise during welding and when failure due to intergranular corrosion results, it usually occurs along a line parallel to the weld, but a slight distance from it, where the sensitization temperature has been reached. This type of failure is commonly referred to as weld decay.

If an 18/8 steel is held for various lengths of time at a given temperature it is found that sensitivity at first increases, reaches a maximum and then falls off. Thus at 650^{o} the maximum sensitivity is reached after 100 hours, and on holding at that temperature for 1000 hours or longer the sensitivity will decrease so as to be negligible.[3].

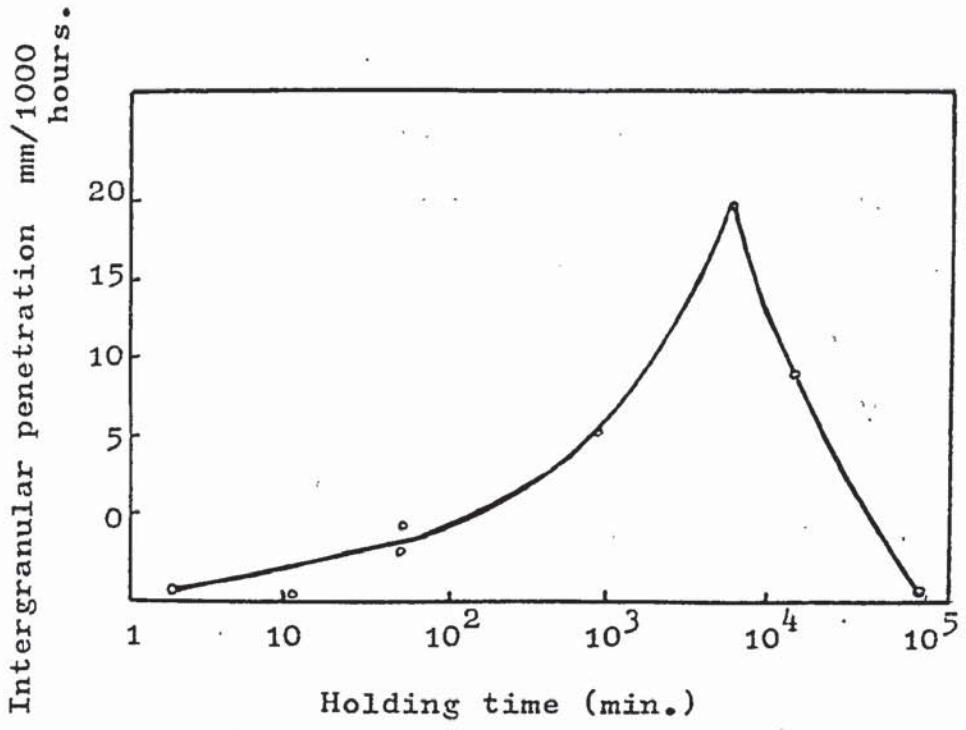

Fig. 4 Sensitisation and recovery of 18/8 steel.

Intergranular corrosion susceptibility in the austenitic steels increases with increasing carbon content. Whereas the carbon solubility during the annealing of an 18/8 austenitic steel is about 0.15 per cent at 1000°C, it has very restricted solubility at lower temperatures. At 900°C the solubility limit is 0.06 per cent, at 800°C it is 0.03 per cent and at 500°C it is about 0.01 per cent [4]. Rapid cooling by quenching from the annealing temperature results in supersaturation of carbon in solution in austenite. As we shall see, the susceptibility to intergranular corrosion is strongly associated with the precipitation of chromium carbides formed as a result of the carbon coming out of solution. An 18/8 steel containing 0.1 per cent carbon may be severely sensitized after five minutes at 600°, whereas a similar alloy containing 0.03 per cent carbon and given the same treatment, may suffer no appreciable damage when exposed to a highly corrosive environment such as hot nitric acid.

Other alloying elements can also have an effect on the sensitization behaviour of austenitic steels. The susceptibility to intergranular attack increases with increasing nickel content. This is due to nickel lowering the solubility of carbon in austenite. This was demonstrated by Tedmon et al [5] and Cihal [6] who also demonstrated that chromium increases the solubility of carbon.

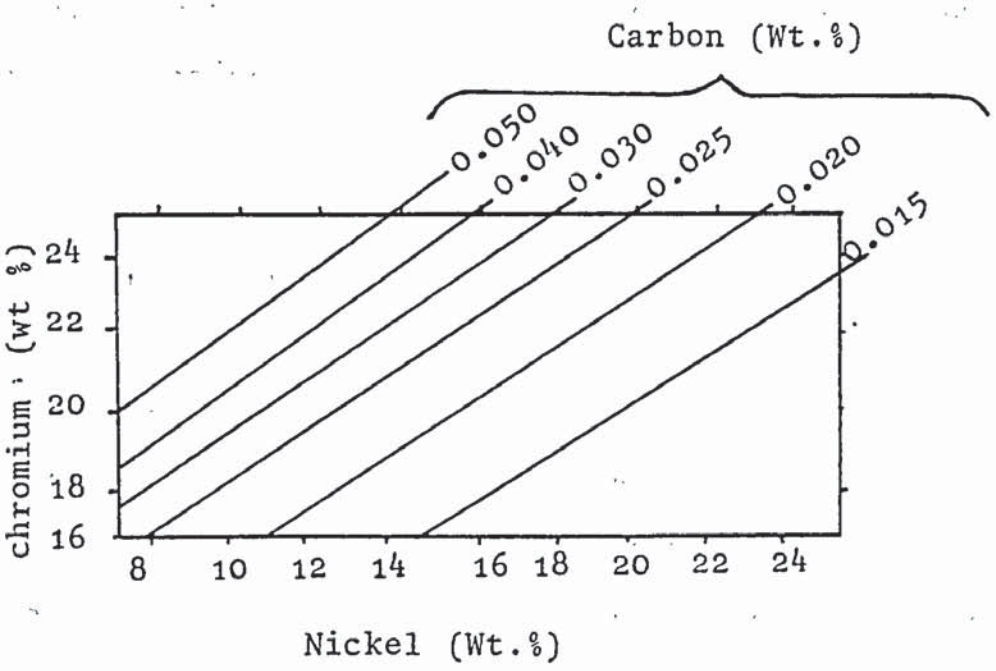

Effect of Cr and Ni content on % carbon needed to avoid intergranular attack in sensitized stainless steel in the Strauss test. (Ref. 6)

Fig. 5

Molybdenum is usually added to steels such as AISI type 316 at the 2 to 3 per cent level to increase resistance to pitting attack. In acidified copper sulphate solution (such as the Strauss test) this level of molybdenum will reduce the tendency to sensitization [7]. However, in nitric acid solutions such as the Huey test, high rates of intergranular attack can be observed in sensitized 316 even at very low carbon levels when carbide precipitation would not be regarded as a problem [8]. Although the molybdenum slightly decreases carbide precipitation, it does enhance the formation of sigma phase [9,10], but there is still considerable doubt as to whether the attack is due to attack of the so called "sub-microscopic" sigma, or to a solute segregation effect. Molybdenum containing grades such as 316L and 317L are not usually selected for

nitric acid service as type 304L (which is cheaper) has a better resistance to corrosive attack in nitric acid.

Niobium and titanium are frequently used alloying additions in austenitic stainless. Their main role is as "carbon getters", to combine with carbon and thus prevent the precipitation of chromium carbides associated with intergranular corrosion. Titanium has a strong affinity for carbon and it produces titanium nitride and carbide both of which may be deleterious in steels used in strong oxidising media such as nitric acid due to possible dissolution [11,12]. This carbide will usually result in a pitting mode of attack, though close to the fusion temperature such as found in welding, a continuous film of titanium carbide (TiC) can form along the weld/parent metal interface which may result in subsequent intergranular attack.

Niobium also combines strongly with carbon to form its carbide NbC which by reducing the level of free carbon is beneficial. The NbC can however form stringers during hot working which enhance the possibility of end grain attack. Although this is not likely to give problems under service conditions, it may lead to spurious results in laboratory tests [13], such as the Huey test where a relatively large end grain area is exposed. If an excess of niobium is present intermetallics such as Fe_2Nb may be formed, and this may lead to enhanced attack. Niobium is preferred to titanium as a carbon getter by steelmakers as it can be

added in the melting furnace allowing time for analysis and corrections whereas titanium has to be added to the ladle at the pouring stage, due to its high activity. The amount of titanium or niobium required to ensure complete stabilisation are higher than indicated by the formulae of the carbides. In the carbide TiC the ratio Ti : C is 4 : 1, but a proportion of titanium remains in solution in the steel, and some reacts with nitrogen. Rosenburg and Darr [14] indicated that a Ti : C ratio of 6 : 1 would be required to ensure complete elimination of the $M_{23}C_6$ reaction during sensitization.

Nitrogen is added in small quantities (typically 0.15 per cent) to stainless steels mainly as an austenite stabiliser or to increase the strength of the alloy. The effect of the nitrogen on sensitization depends markedly on the amount present. Binder et al [7] found that for a 304 steel containing 0.02 - 0.03 per cent carbon, a maximum intergranular penetration rate was found at 0.04 per cent nitrogen. Scharfstein [13] found that doubling and tripling the nitrogen content of 304L had no deleterious effect in the Huey test, although he concluded that precipitated nitrides were probably harmful to corrosion resistance.

Silicon, always present in the steel as it is a widely used deoxidising agent, can act both for and against corrosion resistance. Several workers [15-18] have shown it to decrease resistance to intergranular corrosion.

Armijo [18] considered that the deleterious effect of silicon on the corrosion rate peaked at approximately 0.7 per cent when investigating high purity Fe-Cr-Ni alloys. Providing the silicon remains in the matrix and does not form harmful silicates or induce the formation of ferrite 3-4% silicon will enhance the resistance of austenitic steels to intergranular attack, but few of these steels are produced commercially due to difficulties in hot working.

The effect of phosphorus on the intergranular corrosion of austenitic stainless steel is one area in which much work has been done. It is only present in the steels as a residual element and most workers agree on its deleterious effect on intergranular corrosion. Armijo [18] in his work on high purity alloys with controlled levels of phosphorus found that the corrosion behaviour changed from general corrosion at P < 0.01%, to intergranular attack when the concentration exceeded that figure. Briant [19] found that high purity 304 and 304L alloys doped with phosphorus showed a greatly increased corrosion rate over undoped alloys when subjected to the Huey test. This attack was intergranular and was most pronounced in a 304 steel sensitized at 600°C. Similar steels sensitized at 650°C and 750°C showed a lower corrosion rate and a "healing" effect" after 500 and 1000 hours sensitization. Overall the sensitized 304L had a lower corrosion rate than the 304, with the sensitization at 600°C giving the highest corrosion rate in in both cases. The phosphorus doped 304L steels sensitized at 650° and 700°C gave a corrosion rate similar to or lower

than that of the high purity alloys given a similar treatment. This indicates that the action of phosphorus is more harmful in the higher carbon 304 type steels, when measured by the Huey test although the phosphorus additions were found not to affect the corrosion behaviour of these steels in the Strauss test ($CuSO_4/H_2SO_4$). Joshi [20] has shown that in a 304 type steel phosphorus will tend to segregate at grain boundaries resulting in a change in boundary chemistry.

Aust et al [21] suggested, as a result of grain boundary hardening measurement, that phosphorus was a species that segregated to grain boundaries of a high purity, solution-treated austenitic stainless steel.

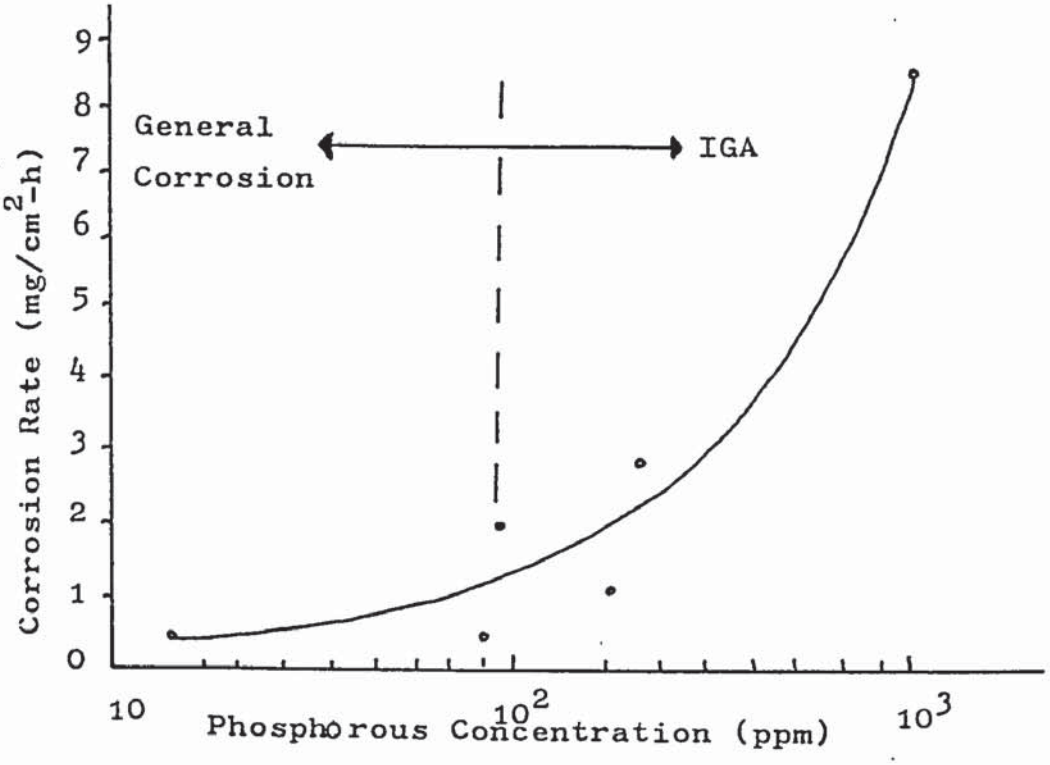

Fig. 6 Effect of phosphorus additions on the intergranular corrosion resistance of annealed high purity 14/14 Cr/Ni stainless steel in $HNO_3 + Cr^{+6}$ (after Ref 18)

Sulphur on the whole does not appear to be deleterious with respect to intergranular corrosion, the main problem being the formation of sulphides which can result in pitting. Briant [19] found that the rate of corrosion in the Huey test of sensitized 304 and 304L steels doped with 0.03% S, and sensitized at temperatures between 600°C and 700°C, did not differ significantly from the rate of corrosion of a high purity specimen, similarly treated.

The effect of boron on the intergranular corrosion of austenitic steels is not at all clear, and there is considerable disagreement. It is usually found in concentrations of < .001% although it may be added to improve hot workability. Voeltzel [22] found that a boron level greater than .006% was detrimental in 304 while Farrell [23] found that for 304 in boiling nitric acid a level of .007% boron gave the minimum corrosion rate. Robinson [24] compared two 304 type steels one with no boron, the other with 4 ppm boron. There was little difference in Huey test corrosion behaviour of the two steels in the solution treated state, but when the steels had been sensitized at 750°C and 650°C the corrosion resistance of the boron containing steel was vastly superior. This was attributed to the boron retarding the carbon precipitation during sensitization. Costello [25] stated that boron increased resistance to sensitization of a type 304 alloy containing additions of 0.0016 per cent boron and 0.15 per cent niobium, over a 304 containing only niobium additions, which in turn had increased resistance over a standard 304 with no additions. Boron contents above 0.002 per cent were found

to intensify intergranular precipitation of carbides.

Although no Huey test results for alloys containing more than 0.0016 per cent boron are quoted, hot nitric/hydrofluoric (10%/3%) tests on welded 304 sheet showed increasing intergranular weld decay (associated with carbide precipitation) with increasing boron levels above 0.0016 per cent. However there was some variation in the carbon level of these steels.

Several workers [26, 27] have shown that boron tends to segregate to grain boundaries in heat treated 316 austenitic stainless steels containing less than 100 ppm boron. No precipitates were visible by electron microscopy and the presence of the boron at the grain boundaries was detected by auto-radiography. The segregation was found only when the steel was slow cooled, and the segregation increased on cooling from higher temperatures. This is discussed in more detail later.

While investigating pure iron containing 25 - 100 ppm boron Brown et al [28] found continuous segregation of boron at the grain boundaries in steels quenched from the γ field and the degree of segregation decreased with increasing temperature.

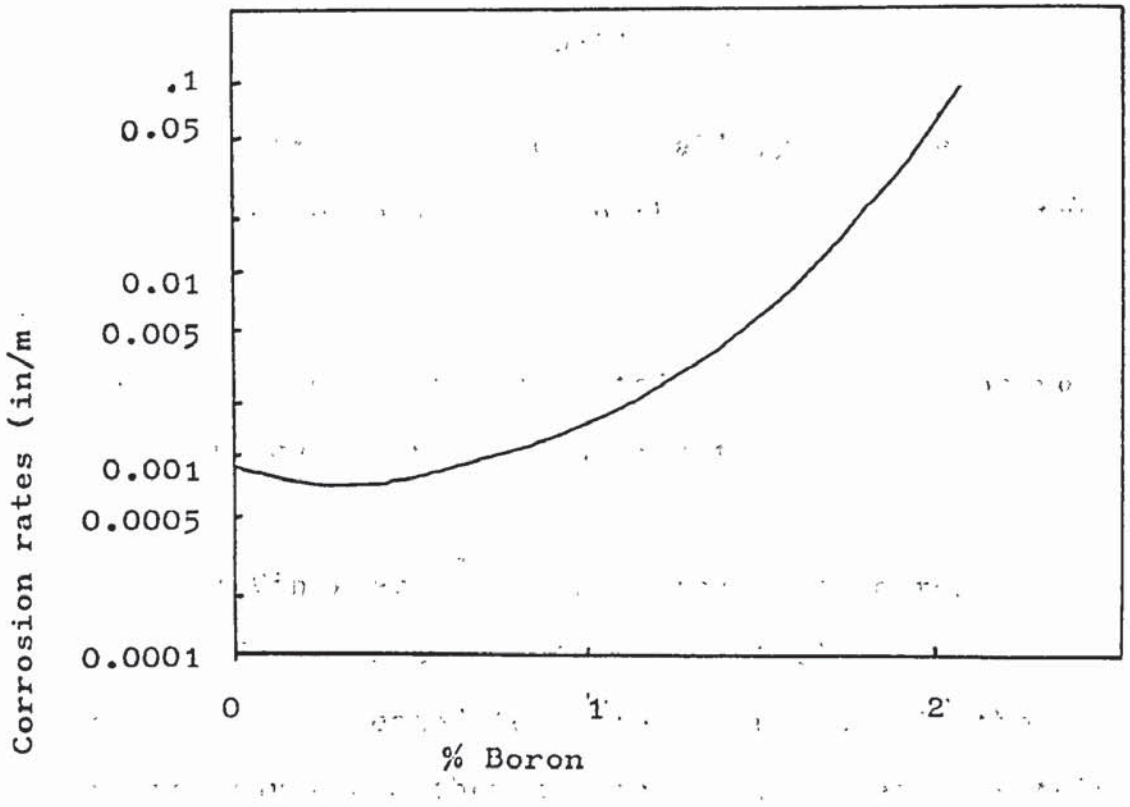

Effect of boron on type 304 stainless steel as measured by Huey tests. Specimens annealed at 1950 F and water treated. (Ref. 13)

Fig. 7

Levitin [29] showed that when the boron level exceeded 0.01 per cent it can form complex chromium (60 %) iron (25%) carboborides at the grain boundaries on solidification from the melt. He also considered that the effect of boron increases as the carbon content of the steel is reduced. Sumner [30] considered that the effect of boron is due to its interaction with dislocations to provide nucleation sites for carbide precipitation.

During sensitization the physical metallurgy of the austenitic steels and their mechanical properties change only slightly. They become slightly stronger and if any precipitation of carbides occurs at the grain boundaries, they become slightly less ductile. Even though precipitated carbides are present a steel need not show subsequent intergranular corrosion in

service. Damage to a steel will depend on

1. The chemistry and physical metallurgy of the grain boundaries being in a favourable condition for attack, and

2. The environment that the metal is exposed to being likely to cause intergranular attack.

Stickler and Vinckier [31] showed that the corrosion resistance of a sensitized stainless steel will return when the steel is heated for extended periods in the sensitizing range and they attributed this recovery to a change in morphology of the grain boundary carbides from a thin sheet formation along the boundaries to arrays of thick geometrical particles. Similar results were found by Aust [21] whose work will be discussed in more detail later on.

For a given steel damage will only occur when exposed to specific corrosive environments. The severity of the attack will depend on the environment as well as the prior heat treatment and alloy composition. When the attack is only superficial, its effects are confined to shallow penetration along grain boundaries and slight cracking upon bending the material. If the penetration is very deep, so much grain boundary material may be removed that "grain dropping" can occur and in cases of very severe sensitization this can result in the metal disintegrating into powder.

Many solutions will result in intergranular attack of sensitized stainless, and some will even cause intergranular

attack of solution treated stainless steels.

Hot nitric acid solutions with more than 50 per cent nitric acid, sulphuric acid media especially those containing copper salts or ferric ions, and mixtures of nitric acid with sulphuric acid or hydrofluoric acid are liable to cause intergranular attack in sensitized steels. Intergranular attack of solution treated stainless steels has only been found in highly oxidising acid solution such as boiling nitric acid with dichromate ion addition. Chaudron [32] and Armijo [18] in showing that high-purity steels were immune to attack in such solutions, demonstrated that the attack on the grain boundaries of solution treated steels cannot be attributed to geometric factors at the boundaries alone.

Warren [9, 10] compiled a comprehensive list of media that have been reported to have caused problems; sea water, crude petroleum, chlorinated solvent, as well as lactic, acetic, oxalic, citric and phosphoric acids, were among the media found to result in intergranular corrosion and accompanying deterioration of AISI type 316 steel. However, although such lists of dangerous media have been published, the ability of a corrodent to cause problems is dependent on the specific alloy, its degree of sensitization, and corrodent variables such as concentration, temperature, impurity levels and so on. Most examples of intergranular corrosion in practice have occurred in oxidising organic or inorganic acids [33].

Much work has been done on the intergranular corrosion of austenitic stainless steels and several theories have been proposed to account for all the different observations that have been made. None of the theories successfully accounts for all the known facts. The main points to be accounted for to enable a theory to be plausible are:-

1. Susceptibility to attack arises after heating within or slow cooling through the temperature range 400°C to 850°C (sensitization)

2. Rapid cooling of the metal (quenching) through the above range usually prevents susceptibility arising.

3. The degree of intergranular attack in a given medium depends on the sensitization temperature, time at temperature and alloy composition.

4. The degree of intergranular attack subsequent to sensitization is strongly dependent on the carbon content of the alloy, high carbon alloys being more easily sensitized and strongly attacked.

5. Sensitization is characterized by the formation of $M_{23}C_6$ carbide precipitates at the grain boundary.

6. A healing effect occurs, restoring corrosion resistance, after long heat treatments at the sensitizing temperature.

7. Solution treated steels with no visible precipitation at the grain boundary undergo intergranular attack in highly oxidising acids, although high purity alloys do not exhibit such attack.

The earliest theory, and the most plausible to account for these observations was the chromium depletion theory proposed by Bain et al [3], although, at that time not all of the above observations had been made. These workers suggested that sensitization of austenitic stainless steel occurs as a result of chromium carbide precipitation, accompanied by chromium depletion in regions adjacent to the boundary.

After solution treatment at 1100 °C followed by quenching all the carbon is in solution in the austenite. The system is no longer in equilibrium below the carbon solubility line and on reheating to a temperature above 450 C, the carbon atoms are able to diffuse and form chromium carbide in the higher energy regions of the grain boundary. The formation of the chromium carbide particles results in the austenite immediately adjacent to the carbide being denuded of chromium. The diffusion of chromium is too slow to replenish the denuded areas with chromium from the bulk. The denuded area with its lower chromium levels has a lower resistance to corrosion and is attacked preferentially in certain media.

Bain considered that once the chromium level had fallen below 12 per cent in the denuded area subsequent intergranular attack could take place.

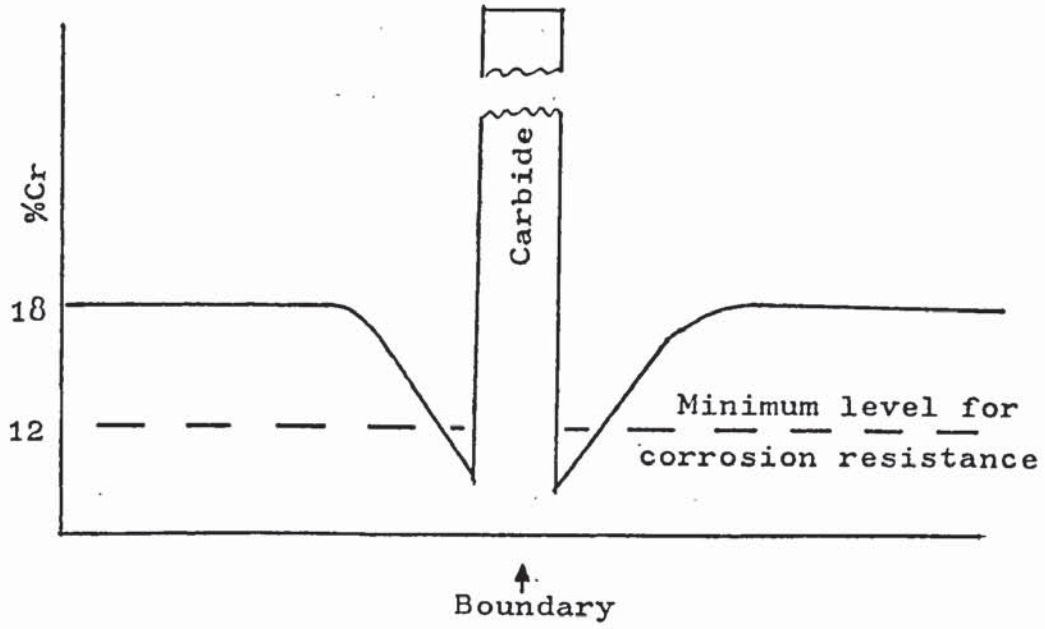

Diagram showing chromium concentration in region of a carbide particle in a sensitized 18/8 steel.

Fig. 8

If the heating is continued for long periods, chromium diffusion will continue, although only slowly and the denuded zones will be replenised. Much work has been done to establish the existence of a chromium depleted zone, but so far the results have been conflicting in the support of this theory and there is no direct evidence of a depleted zone. Alm and Kiessling [34] detected regions of chromium depletion in steels treated to exaggerate the effect using electron probe micro-analysis (EPMA). Fleetwood [35] using micro radiographic measurements

indicated that such depletion existed although Weaver [36] using EPMA could detect no depletion in treated steels.

Stickler and Vinckier [31] considered that the width of metal attacked in intergranular corrosion was too wide to be attributed to attack of depleted material. Although the depleted zone is narrow, once attack has commenced there may not be sufficient resistance to passivate an actively corroding surface and the band of metal being attacked could widen.

One of the main objections of the chromium depletion theory is that it does not satisfactorily explain the sensitization of steels in very short times. In some cases during welding operations it is possible for this to occur in a few seconds and this would preclude the diffusion of chromium ions.

The second theory proposed to account for intergranular corrosion associated with precipitated carbides was the electrochemical theory proposed by Kinzel [4] and supported by Stickler and Vinckier [31]. They suggested that the intergranular attack is an electrochemical reaction between the carbide particles and the matrix, which proceeds rapidly along the grain boundaries. There is some contradiction between researchers [4, 37, 38] as to whether chromium carbides are more noble than the bulk material, but it is known that the nobility depends on the corrodent involved. For example in the Huey test solution of boiling

nitric acid, the austenite is more noble than the carbide, the reverse being true in the Strauss (acidified copper sulphate) test solution. The main objection to the electrochemical theory is that in an aqueous oxidising solution the carbide and the matrix should be at essentially the same potential. Aust et al [66] pointed out that it is possible to heat treat a steel so that grain boundary carbides precipitate while the steel remains immune to attack. The electrochemical theory does not account for this but the chromium depletion theory does: the chromium concentration in the alloy adjacent to the carbide has not been depleted to a level below that required for passivity. However where depletion has occurred beyond this level there will be a difference in potential and this could be an accelerating factor in intergranular attack.

The third theory in the strain theory proposed by Kinzel [4]. He observed that the intergranular corrosion of sensitized austenitic stainless was accompanied by narrow edge attack on one side of the carbide/matrix interface. This attack is attributed to corrosion of the distorted crystal lattice adjacent to the precipitate. Streicher [39] also suggested that the strain energy provided the driving force for intergranular corrosion. This theory is difficult to prove or disprove, but it is known that the corrosion rates in the bulk material do not alter much with applied strain.

The most recent theory described by Aust et al [21] is the solute segregation theory which associates intergranular

corrosion with the presence of a continuous grain boundary path of either second phase particles e.g. carbides, or solute segregants other than carbon e.g. nitrogen, phosphorous, sulphur, boron or silicon. The theory was put forward to account for attack in non-sensitized steels and only secondary consideration is given to sensitized steels. It is known that some highly oxidising solutions such as nitric acid containing dichromate ions, cause intergranular attack in solution treated steels even when carbon 'getters' such as niobium or titanium are present or the carbon content is very low. Streicher and Coriou [40] considered that the oxidising ions present in those solutions tend to act as cathode depolarisers, raising the open circuit potential of the system and thus accelerating the anodic attack in the grain boundary region. Aust considers that in austenitic steels in the solution treated condition there would be a continuous grain boundary path for attack provided by the solute segregation. This is shown diagramatically in Fig. 9a Providing the composition is within the necessary limits, when the steel is quenched from the sensitizing temperature range (450 - 800°C) continuous grain boundary carbides or second phase are formed, producing a continuous path for intergranular corrosion (Fig. 9b). In steel heat treated and quenched from 900°C isolated carbides are formed at the grain boundaries (Fig. 9c). This treatment reduces intergranular corrosion as there is no continuous path. In a high purity alloy with no segregation or precipitation at the grain boundaries, a low corrosion rate would be expected (Fig. 9d).

(a) Segregated

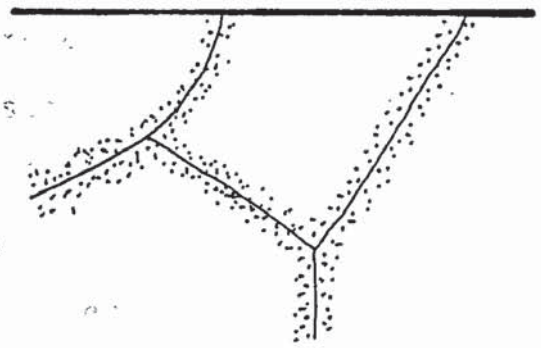

(b) Sensitised

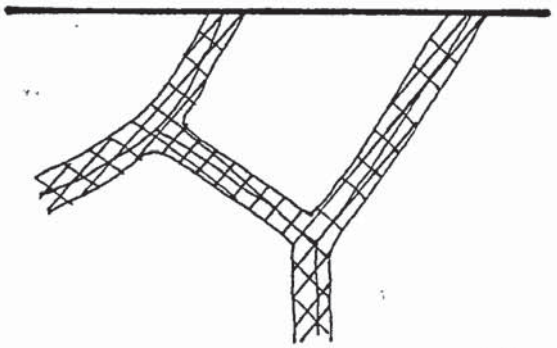

(c) Stabilised

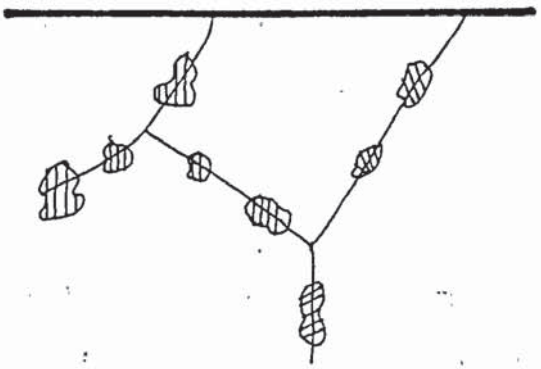

(d) Clean

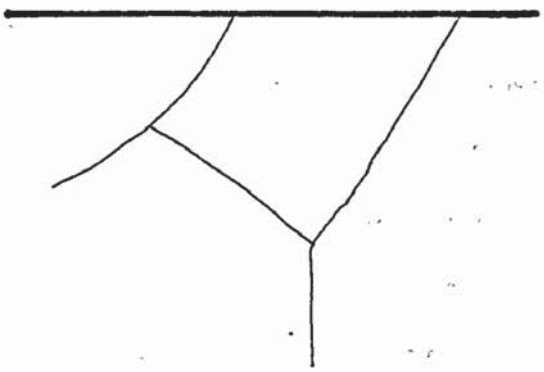

Schematic illustration of intergranular corrosion mechanism proposed by Aust et al. (Ref. 21)

Fig. 9

Several workers [18, 41, 42] have emphasised the need to keep the residual elements present in the steel as low as possible, to prevent any segregation to the grain boundaries that may increase intergranular attack. There is very little direct evidence to associate solute segregation of any particular species with intergranular attack, although more recently acquired analysis techniques such as electron probe microanalysis (EPMA), and scanning transmission electron microscopy (STEM), Auger spectroscopy, are changing this situation due to their high spatial resolution.

None of the theories so far proposed can account for all the known facts. The chromium depletion theory is based mainly on tests using the weakly oxidising Strauss test solutions, while the solute segregation theory is based on strongly oxidising solutions such as that used in the Huey test and variations of it.

Joshi and Stein [43] considered that the mechanism operating depended strongly on the corroding solution and the impurities present in the solution. They found chromium depletion was supported by Strauss tests and that the corrosion properties in a highly oxidising nitric/dichromate solution related well with the solute segregation theory. It is most probable that intergranular corrosion can occur due to a combination of the proposed theories, the predominance of a given mechanism being governed by the nature of the metal and the nature of the corroding solution.

In this work it is with the solute segregation theory that the work is most closely involved and this theory will be examined in more detail later on.

1.2 Need to determine Susceptibility to Intergranular Corrosion

As we have seen, in certain circumstances, usually when the steel has become sensitized, austenitic stainless steels can become susceptible to intergranular corrosion. Prior to using austenitic steels in environments that could result in, or have in the past produced intergranular attack it is essential to test the steel to ascertain its susceptibility. Because failure under service conditions may not occur for months or even years after installation it is impractical to perform the test under such conditions and time limitations dictate that an accelerated test must be used. It is essential to have a test that can be performed rapidly on a laboratory size test specimen that will give a reliable indication of the corrosion resistance of the steel to intergranular attack. This invariably means that a much more aggressive medium must be used for testing than exists in service conditions.

Most tests that have been devised do not attempt to duplicate service conditions but are intended to indicate in a short time the existence of metallurgical factors that may result in increased intergranular attack.

These conditions may arise in steels actually in service if the wrong grade (e.g. 304 instead of 304L) is used, or if the final works annealing and quenching operations have been ineffective or even non existent and have thus not kept all the harmful carbides and nitrides in solution. Incorrect or insufficient use of 'carbon getters' such as

Nb and Ti, and heating of the steel during welding or fabrication can also result in sensitized steels being used in service conditions.

1.3 Tests for Susceptibility to Intergranular Corrosion

Ideally, a test for susceptibility to intergranular corrosion must be quick, easy to perform and inexpensive. It must pass all steels that would show no intergranular attack under service conditions, and must fail any steels that would show such attack.

Because of the widely varying nature of media which can result in intergranular attack it is almost impossible to develop a test that will conform to the ideal. Several different tests have been developed over the years to detect susceptibility to intergranular corrosion and these vary in severity and in sensitivity to different metallurgical conditions.

The first tests devised were Hatfield's [106] in 1926 using sulphuric acid containing copper sulphate, and Huey's boiling 65 per cent nitric acid test in 1930 [44]. These tests were at first developed to detect susceptibility to intergranular attack due to the presence of grain boundary chromium carbides, but it was soon found that the nitric acid test was sensitive in some cases to the presence of another component of the steel. As we shall see some workers attributed this to "sub-microscopic" sigma phase at the grain boundaries. Gillette [45] in 1949 considered that the methods in use at that time for evaluating susceptibility to intergranular corrosion were incapable of truly appraising the steel for a given service condition as such tests may discard perfectly satisfactory material. The nitric acid test and the sulphuric acid/copper sulphate test

sometimes known respectively as the Huey and Strauss tests, both take a considerable time, the actual testing time for the Huey test being ten days. The nitric acid test is also very sensitive to dissolved impurities in the acid.

More recently, the oxalic acid etch test and the ferric sulphate/sulphuric acid etch-test were devised to detect the presence and extent of chromium depletion associated with chromium carbide precipitation whilst overcoming some of the problems of the nitric acid and sulphuric acid/ copper sulphate tests. These tests have been standardised by ASTM and incorporated into ASTM A262-79 [46]

As can be seen from Table 1, the standard tests vary in nature and sensitivity. The oxalic acid test is a very rapid etching test to screen out specimens that would pass the nitric acid test with no difficulty. The Ferric sulphate/sulphuric acid test is a severe test which is fairly quick, insensitive to "sub-microscopic sigma" and is unaffected by build up of corrosion products. The nitric acid test, although widely used for many years in America as one of the severest tests, has several disadvantages. It is sensitive to the existence of some phases other than chromium carbides, it is affected by build up of corrosion products, and it is comparatively lengthy and expensive. The nitric-hydrofluoric acid test does not attack sigma phase and is used to differentiate between the effects of chromium carbides and sigma in molybdenum steels such as 316, 316L, 317, 317L. The current sulphuric acid/copper sulphate test involves contact of specimen with metallic

Table 1 ASTM Standard A262-70 (after Ref 1)

Practice	Test Media + Conditions	Evaluation	Phases attacked
A Oxalic etch	10% Oxalic acid. Electrolytic 1.5 mins at 1A/cm^2 anodic	Nature of attack	Various carbides
B Streicher	50% H_2SO_4 + 2.5% $Fe_2(SO_4)_3$ 120h. Boiling	Wt loss per unit area	Chromium depleted area
C Huey	65% HNO_3 Boiling 5 x 48h. Acid changed every 48h	Ave wt loss per unit area	Chromium depleted area sigma and carbides
D Warren	10% HNO_3 70°C 2 x 2h	Wt loss per unit area	Chromium depleted area in Mo bearing steels
E Strauss	15.7% H_2SO_4 + 5.7% $CuSO_4$ Boiling 24h Specimen in contact with Cu	Appearance after bending	Chromium depleted area

copper during testing which increases the severity of testing over the original Hatfield/Strauss test.

Each of the corrosion tests operates at a different potential and they cover a wide range of potentials.

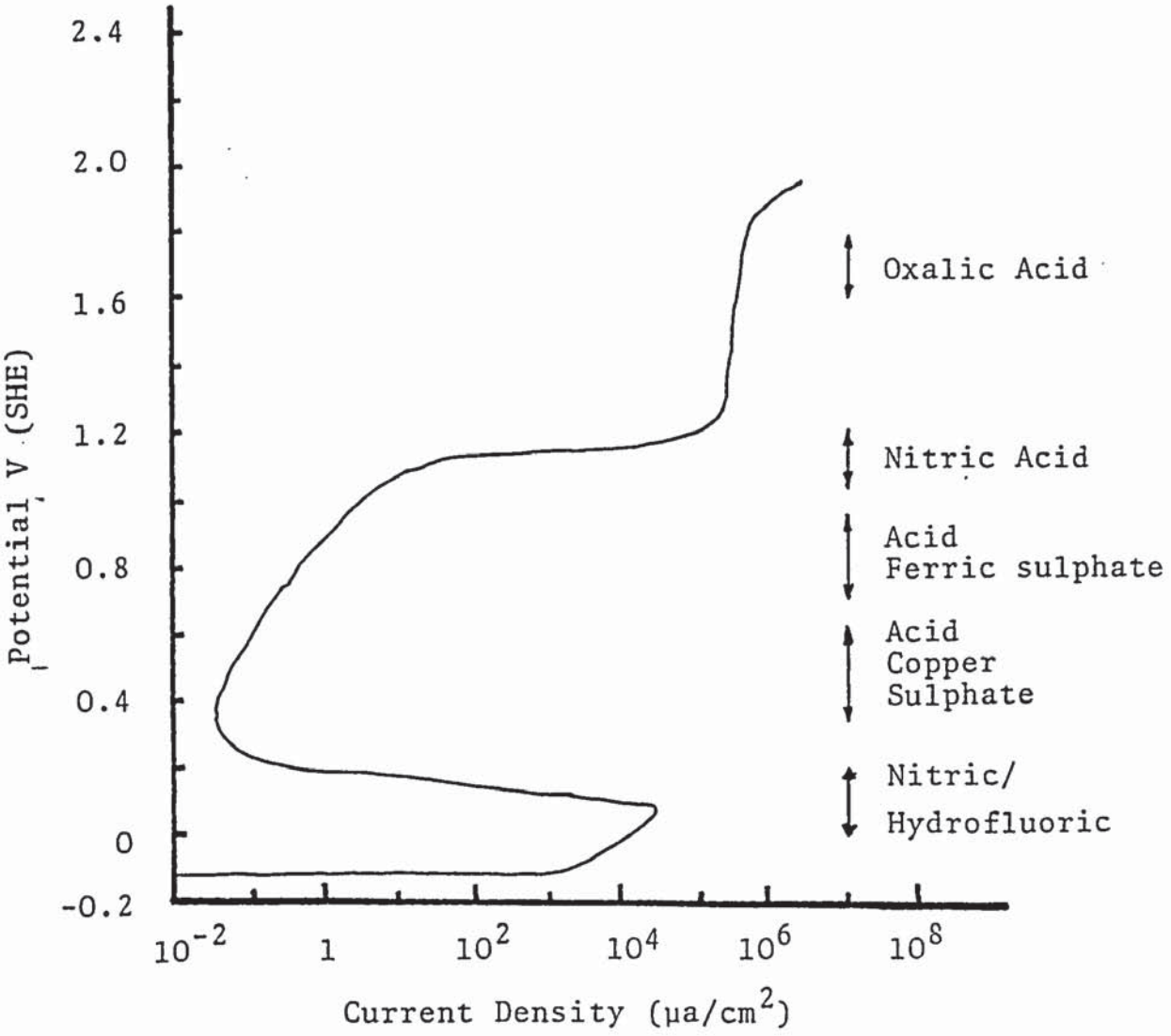

Fig. 10 Operating potentials of the tests for susceptibility to intergranular corrosion, for a sensitized 18/10 stainless steel in a hot reducing acid. (after Ref. 60)

The oxalic acid test operates in the high transpassive region, the nitric acid test on the boundary between the passive and transpassive region, the ferric sulphate/ sulphuric acid and the copper sulphate/sulphuric acid operate in the passive region and the nitric/hydrofluoric test operates close to the boundary of the passive/active

regions. The actual test selected for use will depend on requirements and past practice.

The nitric acid test has been the most widely used since its inception in the 1930's as it is a severe test that gives a quantitative result. It is most useful for assessing steels for nitric acid service. The ferric sulphate/sulphuric acid test is more recent and also gives a quantitative result. The $Fe_2(SO_4)_2$ inhibits general attack on the grain surfaces whilst grain boundary regions with lowered resistance due to chromium carbide precipitation are attacked. The oxalic acid test and the copper sulphate/sulphuric acid tests are both assessed qualitatively by surface appearance after the test. The oxalic acid test does not reject material, it only passes steel that is resistant to intergranular attack. Any steel that does not pass must be tested by one of the other standard tests, usually the nitric acid test. The nitric/hydrofluoric test is used only for Mo containing steels. The hazards due to HF and the high rate of general corrosion during this test have limited its popularity.

Streicher [47] in his paper on evaluation tests concluded that because of problems such as end grain attack connected with build up of hexavalent chromium, and the time and expense involved, the nitric acid test should be used primarily as a simulated service test for alloys to be used in nitric acid. He also concluded that there was much duplication with all the different tests and that some could be removed such as the nitric-hydrofluoric test.

1.4 The Boiling 65% Nitric Acid Test

With the occurrence of intergranular corrosion in austenitic steels in certain media during the first half of the present century, the need arose for a test that would identify affected steels prior to their being put into service. In response to the need to evaluate the susceptibility of these alloys to sensitization, many evaluation tests have been devised.

The 65% Nitric Acid or Huey test which utilized boiling 65 per cent nitric acid was described by W.R. Huey [44]. It has been the most widely used of all the evaluation tests and it has been adoped as an ASTM standard test (A262-79 Practice C) [46]. The test is performed on a specimen of known weight and surface area in a wide mouthed Erlenmeyer flask with a cold-finger condenser to prevent evaporation loss. The specimen is held in the acid in a glass cradle.

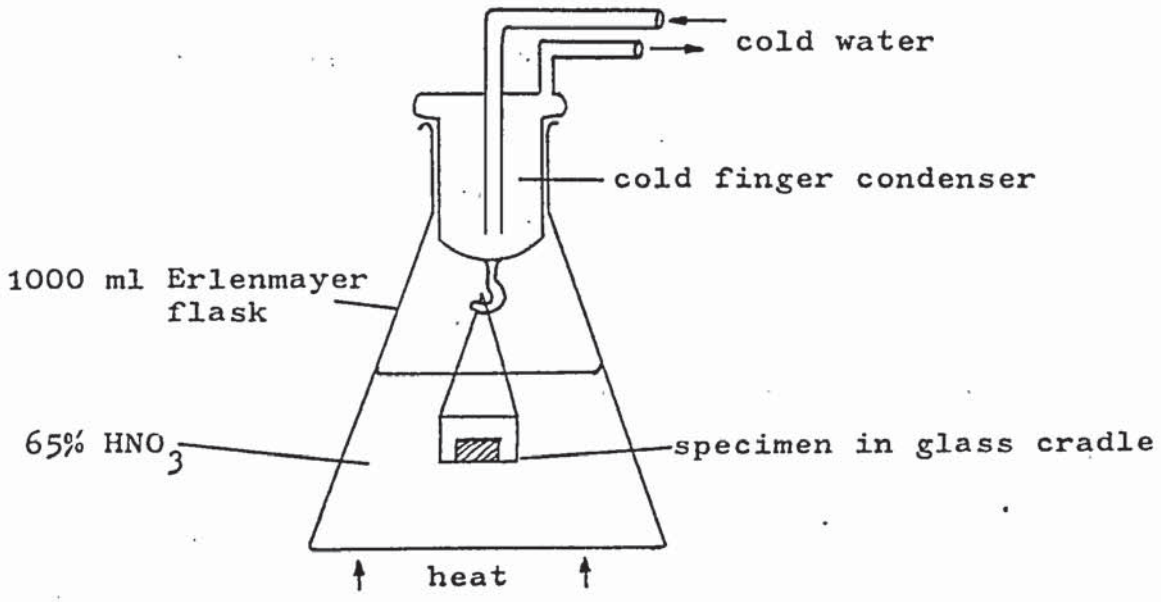

Fig. 11 Experimental set-up for Boiling 65% Nitric Acid Test.

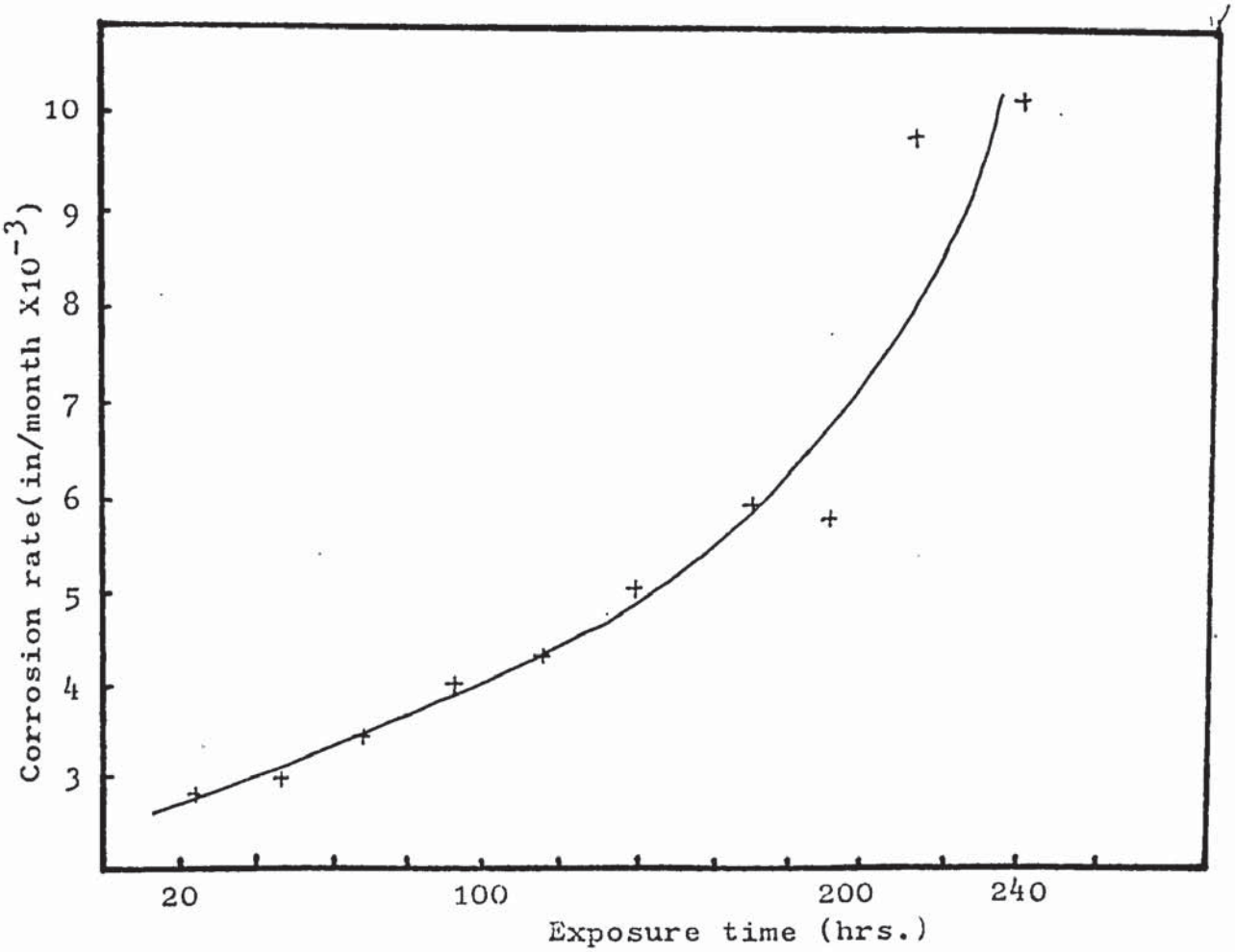

Increase in corrosion rate of AISI 316 in boiling 65% nitric acid due to build-up of corrosion products in the acid.

(Experimental data obtained by the author, 1979)

Fig. 12

Evaluation of susceptibility is based on two parameters, corrosion rate calculated from weight loss readings, and visual appraisal of specimen surface with respect to grain dropping. The test is performed over five 48 hour periods in the boiling 65 per cent nitric acid solution. The test solution volume to specimen surface area ratio should be a minimum of 125 ml/in^2 and the acid solution should be changed for fresh solution at the end of each 48 hour period. This changing of acids is necessary to prevent build-up of impurities, as the corrosion rate of stainless steels in boiling nitric is sensitive to the

level of chromium present in solution as shown by DeLong [49], and Shirley and Truman [50]. Other investigators [51-54] have shown that the cause of accelerated corrosion in such situations is the presence of the hexavalent chromium ion Cr^{6+}. This ion is formed by the chromium entering the nitric acid as divalent ions which are rapidly converted to trivalent ions, which in turn are oxidised to the hexavalent state. The critical level of chromium in solution above which rapid acceleration of the corrosion rate occurs was shown [49] to be 0.004%. With an 18.5 per cent Cr specimen of 19.3 cm^2 surface area in 600 ml of test solution, the 0.004% chromium level in the solution would be reached after 48 hours, with a corrosion rate of approximately 0.0071 in/month [55]. This level of corrosion rate is unlikely to be approached in typical tests.

Delong [49] devised a method of the multiple testing of specimens simultaneously in the same container. His apparatus consisted of a double container, an inner vessel holding the specimens surrounded by an outer vessel, both containing boiling nitric with a common condenser. The pure condensate is returned to the inner vessel which overflows, carrying the corrosion products into the outer vessel, thus preventing the build up of corrosion products in the testing solution and the associated problem of accelerated corrosion rates.

Because of the variation in attack between the top, end and edge faces the dimensions of the specimens are chosen to

limit the amount of end and edge faces exposed to the acid. End grain attack can be quite catastrophic due to localised attack on inclusion stringers resulting in the formation of pits where corrosion products such as Cr^{6+} can build up and cause accelerated attack. ASTM standard A262 stipulates that the exposed cross section shall be less that 50% of total surface area.

A typical test specimen would be 25 x 40 x 3 mm. The specimen is ground over the complete surface to give a 180 mesh grit finish and it is then measured accurately, degreased in a non-chlorinated solvent, and then weighed accurately prior to the test. At the completion of each 48 hour test period the specimen is washed and dried, degreased and then reweighed. Individual weight losses are recorded for each of the five 48 hour periods and the average corrosion rate is calculated giving a quantitative measure of the degree of sensitization for compartive purposes.

The Nitric acid test has been used over many years to detect the presence of harmful carbides usually chromium carbides that had precipitated on the grain boundaries. It was thought at first [56] that austenitic stainless steels that contained no precipitated carbides would be free from intergranular attack in the Nitric acid test. However in certain circumstances the low carbon grades of austenitic stainless steel, specifically designed to have a carbon content below that required for formation of grain boundary carbides such as 316L, 304L have shown intergranular attack in the Nitric acid test. Some

workers [8, 57, 39] assumed this attack to be due to the presence of sub-microscopic sigma. Although concrete evidence for such a phase is lacking, it can be identified in the 316L type alloys after long heat treatment at the sensitizing temperature. However sigma phase in this form has no effect on the corrosion rate.

The grain size of the metal can have an effect on the corrosion rate in the Nitric acid test and Tupholme and Bouchier [59] showed that a large grained structure was more resistant in the Nitric acid test than a small grained one, in both AISI 316L and 304L. They state that grain size ASTM 4 is a desirable size with regard to inter-granular corrosion resistance. Streicher [13] also found a greater corrosion rate in nitric acid with a small grain size, although Couriou [58] found the opposite effect.

The ASTM standard A262 stipulates a surface polished to a 120 mesh finish prior to testing in the Nitric acid test. Tupholme et al [59] found that the corrosion rate in these tests was lower with a polished surface that with than a plain descaled surface. Streicher [39] studied the effect of several different surface finishes on the Huey test corrosion rates (Fig.13). A sand blasted surface gave the highest corrosion rate, an 80 mesh grit ground surface an intermediate rate, and the smooth surface obtained by polishing or bright pickling gave the lowest corrosion rates. He attributed these differences to absolute surface area exposed by each method of preparation and not to any surface stress involved,

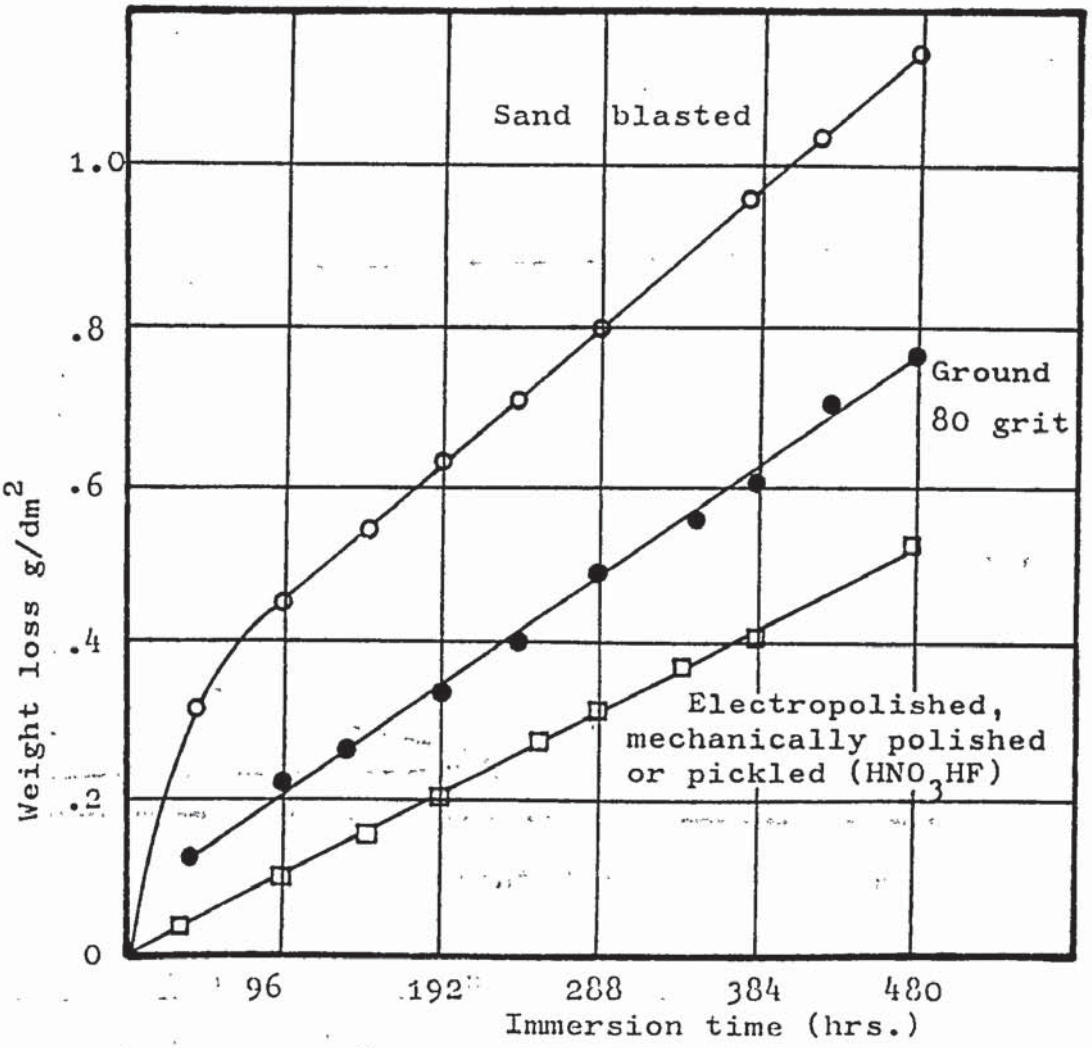

Influence of surface finish on the corrosion of an annealed and water quenched AISI 304 steel in boiling 65% nitric acid. (After Ref. 39)

Fig. 13

and noted that the different surface finishes did not affect the electrode potential of the steel in the nitric acid solutions.

The Nitric acid test operates at a electrochemical potential of approximately 1.10 V_{SHE} although Briant [19] states that this potential can alter during the test. This potential is very close to the transpassive region.

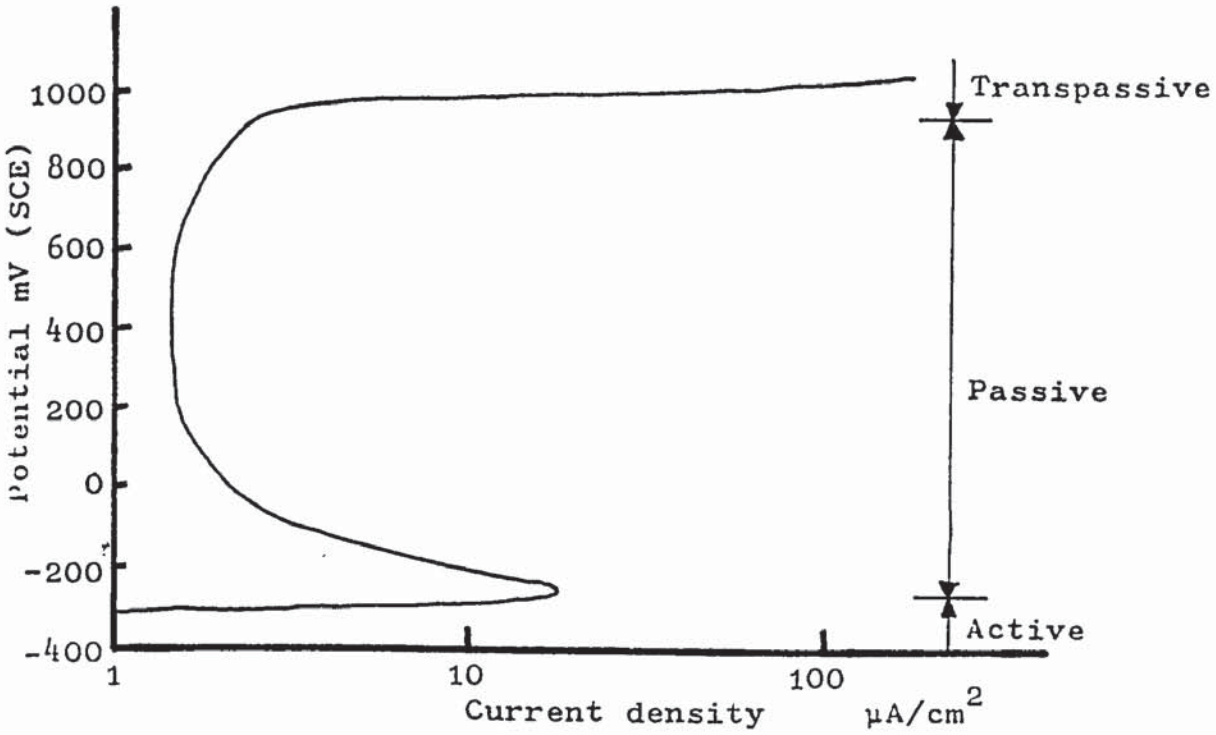

Fig. 14 Potentiodynamic anodic polarization curve for type 304 in 1N H_2SO_4 showing wide passive range. (after Ref. 114).

and a small change in potential can lead to a large change in the current density.

Figures for corrosion rates in the nitric acid tests are quoted either as a weight loss per unit area e.g. $mg/cm^2/hr$ or as a rate of penetration e.g. in/month or mm/year. The penetration rates, calculated from weight loss measurements are misleading as the nature of the attack is intergranular and is not uniform. Considerable penetration along the grain boundaries can occur without any accompanying large scale weight loss.

The calculation for penetration figures mm/year is

$$\text{mm/y} = \frac{87488 \times W}{A \cdot d \cdot t}$$

where t = exposure time in hours

A = specimen surface area in cm^2

W = weight loss in grams

d = density (g/cm^3) of specimen

The Du Pont Co[55] adopted maximum permissible corrosion rates in the nitric acid test which have shown good correlation with subsequent service experience. For various grades of steel, these rates are:

		Max. corrosion rate		
Grade	Condition	mm/y	in/mth	$mg/cm^2/48h$
304	As received	0.45	0.0015	1.98
304L	1h at 677°C	0.61	0.0020	2.68
316	As received	0.45	0.0015	1.98
347	1h at 677°C	0.61	0.0020	2.68

The nitric acid test can be performed with either an Allihn condenser or a cold-finger condenser. Truman[52] showed that the cold-finger condenser gives a lower rate of corrosion assuming all other factors are the same. He attributed the lower corrosion with the cold-finger condenser to the retention of a gaseous oxide of nitrogen which kept the concentration of hexavalent chromium down in the nitric. The Allihn condenser allows the gaseous products to escape more easily.

In this work the figures for corrosion rates in the nitric acid test are mainly quoted as a weight loss per unit area in a 48 hours period. A given test result will normally be the arithmetic mean of the weight losses per unit area (mg/cm^2) in the five consecutive 48 hour periods that constitute the nitric acid test.

2. Variations in Results from Nitric Acid Tests on AISI 304L

Many consumers of austenitic steel intended for use in environments known to cause intergranular attack still specify that steel must be tested using the standard nitric acid test ASTM A262-79 Practice C for evaluation. It is essential that the steel supplied should perform consistently well in the test from both the supplier's and the consumer's point of view. However, variations can occur between different melts of steel due to causes which are not readily recognisable. These variations can cause a wide spread of corrosion rates in the nitric acid test results, some tests actually resulting in corrosion rates higher than the accepted level which are usually agreed between supplier and consumer.

Two commercially produced casts that showed this variation were two type 304L steels produced by the AOD process. Both casts had followed the same production route and had been made to the same specification. The only ostensible difference was that they were produced by different shifts.

The composition of the steels, analysed by wet analysis* was as follows

	C	Si	Mn	P	S	Cr	Mo
Cast A	.019	.25	1.69	.020	.006	18.06	.10
Cast B	.017	.25	1.45	.026	.007	18.10	.21

*Carried out by the British Steel Corporation, Sheffield Laboratories.

	Ni	Cu	Sn	Al	N	Ti	W	B
Cast A	11.8	.05	.02	.06	.043	.005	.04	.0025
Cast B	11.68	.10	.02	.011	.037	.010	.04	.0015

After the hot rolling to the required section both casts were given a works softening treatment of 20 minutes at 1090°C followed by quenching in water sprays.

2.1
Experimental Procedure

Previous investigation* of these casts indicated that Cast B had a much lower resistance to intergranular corrosion when tested in the nitric acid test. Both casts were tested in the standard ASTM nitric acid test in the as received condition, having been works softened. The steel was cut to suitable size for the test, taking care that no excess heating of the sample occurred during the cutting operation. The surface on all faces of the sample was ground on wet SiC papers to a 180 mesh grit finish to ensure that all traces of oxide and other surface defects such as rolled in inclusions had been removed. This also ensured that all the samples had an identical surface finish for comparison purposes.

In the tests the procedure followed was that laid out in the ASTM standard ASTM A-262-79, practice C [46]. An acid volume of 125 ml/in^2 (19.4 ml/cm^2) of sample surface area was used to give a constant acid volume/specimen surface area ratio for all tests. Analar grade nitric acid, supplied by BDH was used and this was diluted with deionised water

*Carried out by the British Steel Corporation, Sheffield Labs.

to give a 65% nitric acid solution. (see appendix 3)

After grinding and inspection the specimens were degreased in an ultrasonic cleaner using a non-chlorinated solvent such as acetone. They were then dried and weighed to ± 0.25mg. The specimens were then suspended in the required volume of nitric using a glass cage. All glassware was thoroughly cleaned in nitric acid prior to the test, and care was taken to avoid contamination of the sample prior to the test. The loss in weight was calculated after each 48 hour period of the test and this enabled a corrosion rate for each period to be calculated. At the end of the fifth test period an average corrosion rate was calculated and the surface condition of the corroded sample was examined for any trace of grain dropping or end grain attack.

2.2
Results

Two specimens of each cast were tested and the results were as follows

	Corrosion Rate $mg/cm^2/48$ h	Average
Cast A	0.92, 1.45	1.19
Cast B	11.48, 9.85	10.65

There was a considerable difference in corrosion rates between cast A and cast B and this difference was found in both tests. Examination of the surface of both steels showed that the nitric acid test had resulted in much more severe attack in cast B with more grain dropping, and end grain attack. The difference in corrosion rates was far

greater than would be expected from experimental spread, or the slight difference in composition that existed between the two metals. The two steels were examined metallographically to establish the cause of the differing corrosion behaviour.

Specimens of the two steels in the as received condition were mounted and polished and then etched to reveal the structure. Several different etchants were tried (see appendix 2) to reveal the most information about the structure, and the most effective was found to be an electrolytic anodic etch in 10% Oxalic acid.

In the as-received condition there was no obvious difference in metallurgical structure. There was an equi-axed grain structure with numerous annealing twins. During etching some pitting was observed on the grain boundaries of both steels although no grain boundary particles were visible under optical examination. One or two larger pits were found within the body of the grains and these had probably occurred where particles had been attacked. (Plates 1, 2)

Samples of the steel that had been subjected to the Nitric acid test were then examined. They were mounted and polished and then given a light electrolytic etch in oxalic acid. Both steels showed massive surface attack although cast B was far worse and the corroded surface was far more irregular. Considerable grain dropping had occurred with cast B whilst it was minimal in cast A. Penetration along grain boundaries had occurred in both steels and where twin boundaries (both coherent and incoherent) had become exposed to

the nitric acid solution, penetration had occurred along these as well. Once the corrosion attack had penetrated the grain itself, for instance, along a twin boundary, it often branched out along certain crystallographic planes within the grain. This occurred to such an extent that large amounts of the interiors of these grains could be dissolved. Both the intergranular and intragranular attack were worse in cast B. (Plates 3, 4, 5)

In both casts massive pits that were parallel to the rolling direction formed during the nitric acid test. These pits were as much as 5 mm to 8 mm long and were 5 - 8 grain diameters in width. At pit initiation sites intergranular penetration would occur to a much greater depth than general surface intergranular penetration. General surface intergranular penetration could be detected to a depth of 1 - 3 grain diameters before grain dropping occurred, but at pit initiation sites the penetration was 8 - 10 grain diameters for cast B and 10 to 12 grain diameters for cast A. The pits appeared to an equal extent in both steels with five pits appearing in one particular cross-section with an area of 3 cm^2. (Plate 6)

As well as optical examination, the two steels in the as-received condition were examined using the transmission electron microscope (TEM). The specimens for use with the TEM, 3 mm diameter discs thinned down in the centre to electron-transparency thickness, were prepared by the method detailed in the appendix 1.

This method was found to give reasonably good thin electron-transparent areas, although in several specimens the thin areas were found to have fractured during electro-thinning procedures in a manner that resulted in a step-like specimen edge. Penetration and cracking also occurred along the line of stacking faults, but not however along the grain boundaries. Both steels had a relatively high dislocation density.

Examination of the grain-boundary regions of cast A and cast B by TEM showed that both of the steels were quite clean. Cast B showed one or two small precipitates on the grain boundaries but these were quite widely spaced and a good search was necessary to reveal any. The precipitates were very narrow, of the order of 0.05 μ wide and they extended along the grain boundary. The dislocations in the as received metal tended to be arranged in linear arrays across the grains. Most of the particles were too small to obtain selected area diffraction patterns with the available instrument. (Plates 7, 8)

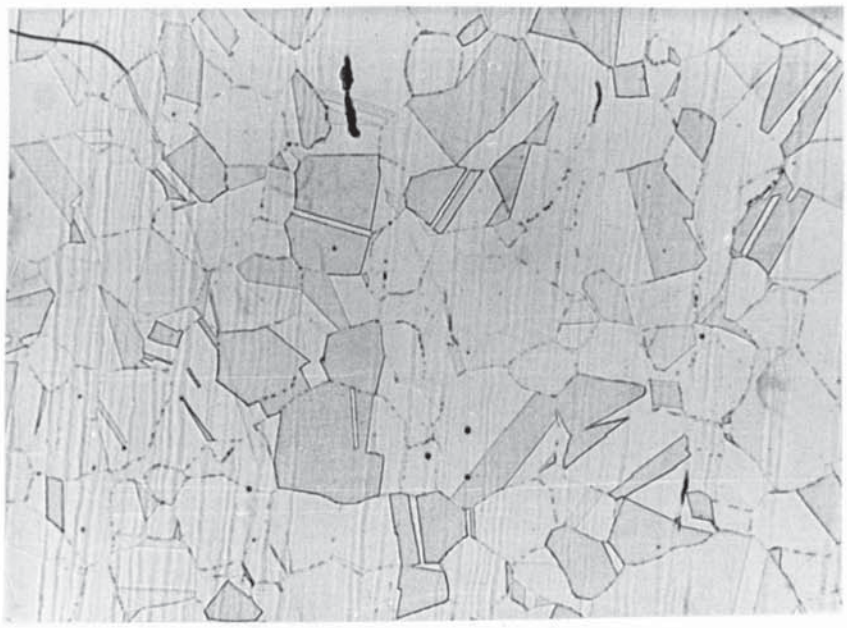

Plate 1 Cast A, 304L. As-received, works-softened condition. Etched electrolytically in 10% oxalic acid for 30 sec. at 4 volts x300

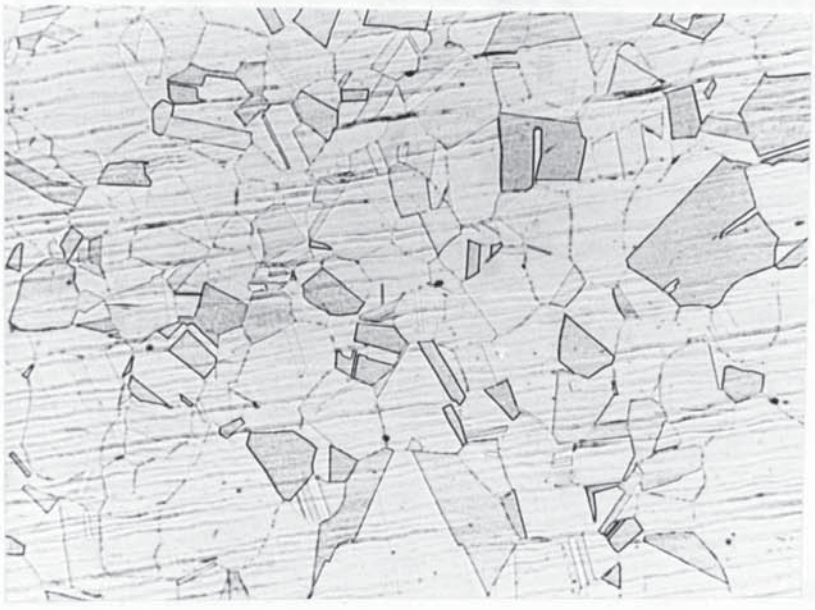

Plate 2 Cast B, 304L. As-received, works-softened condition. Etched electrolytically in 10% oxalic acid for 30 sec. at 4 volts x300

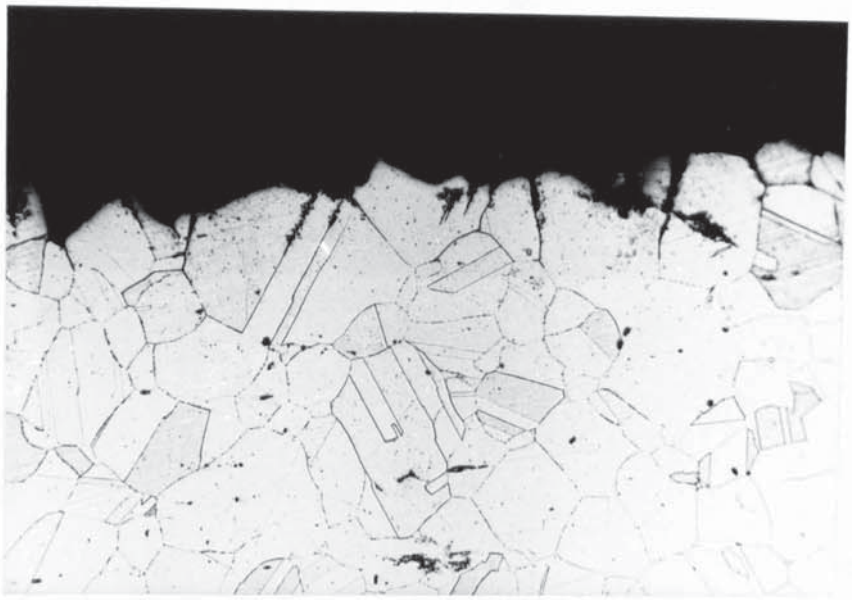

Plate 3 Cast A, 304L. As-received, works-softened condition. Cross-section of specimen surface after nitric acid test. Etched electrolytically in 10% oxalic acid for 30 sec. at 4 volts

x300

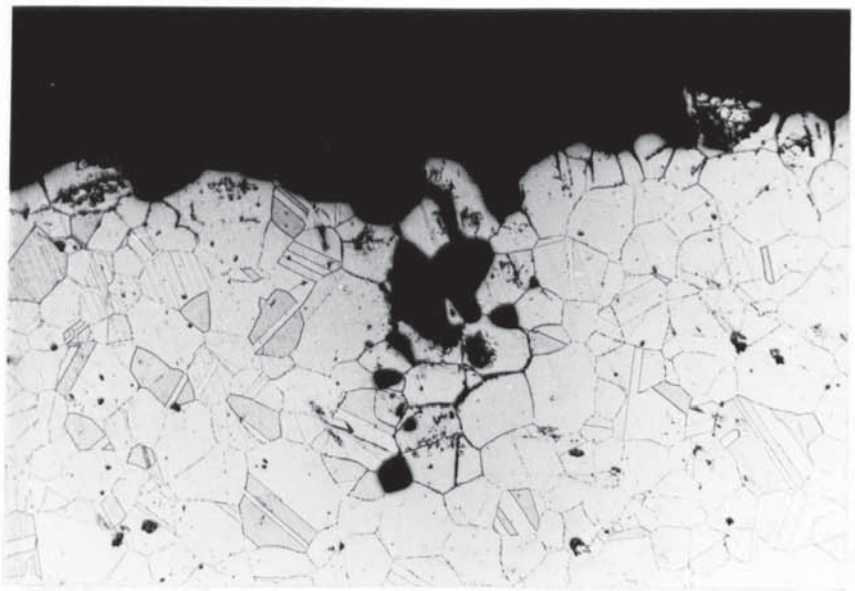

Plate 4 Cast B, 304L. As-received, works-softened condition. Cross-section of surface after nitric acid test showing pit initiation site. Etched electrolytically in 10% oxalic acid for 30 secs. at 4 volts. x300

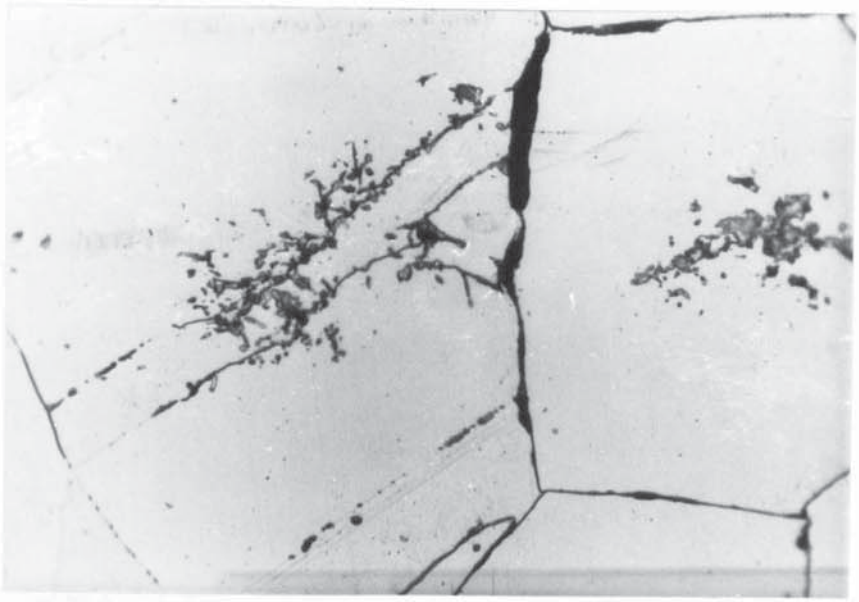

Plate 5 Cast A, 304L. As received, works-softened condition. Cross-section of specimen after nitric acid test showing attack along grain boundaries, twin boundaries and in grain interior. Etched electrolytically in 10% oxalic acid for 30 sec. at 4 volts. x1500

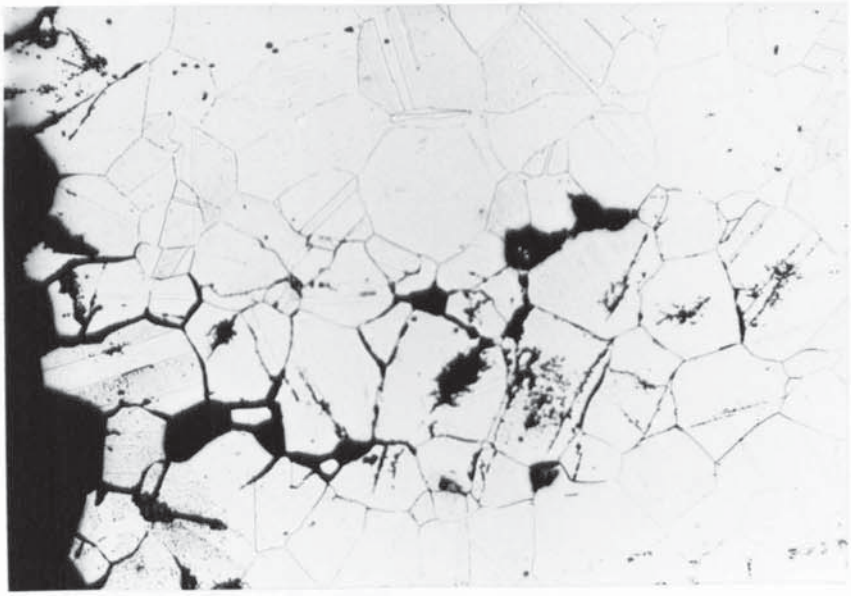

Plate 6 Cast A, 304L. As received, works-softened condition. Cross-section of specimen after nitric acid test. Pit has formed parallel to rolling direction. Etched electrolytically in 10% oxalic acid for 30 secs. at 4 volts.

x 300

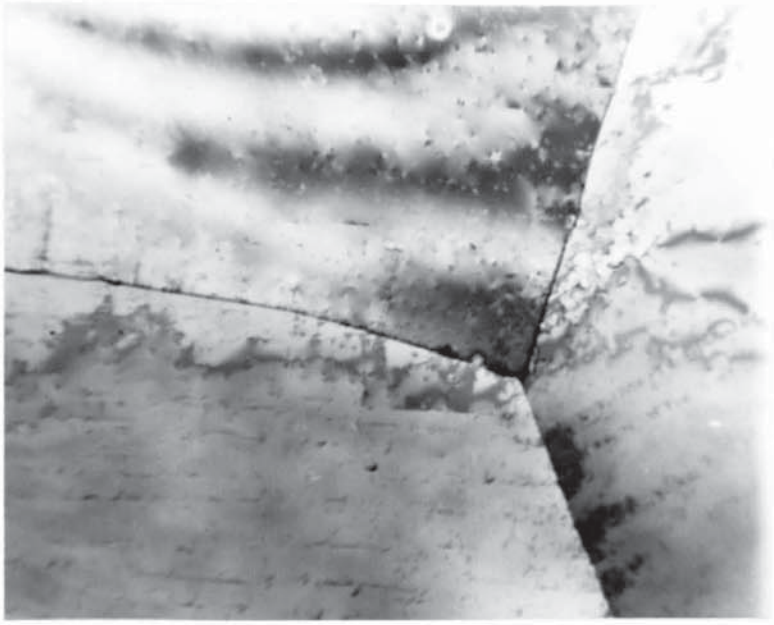

Plate 7 Cast A, 304L. As received, works-softened condition. TEM micrograph of triple point with arrays of dislocations within the grain. Several small particles can be seen on boundary at left. x2.6K

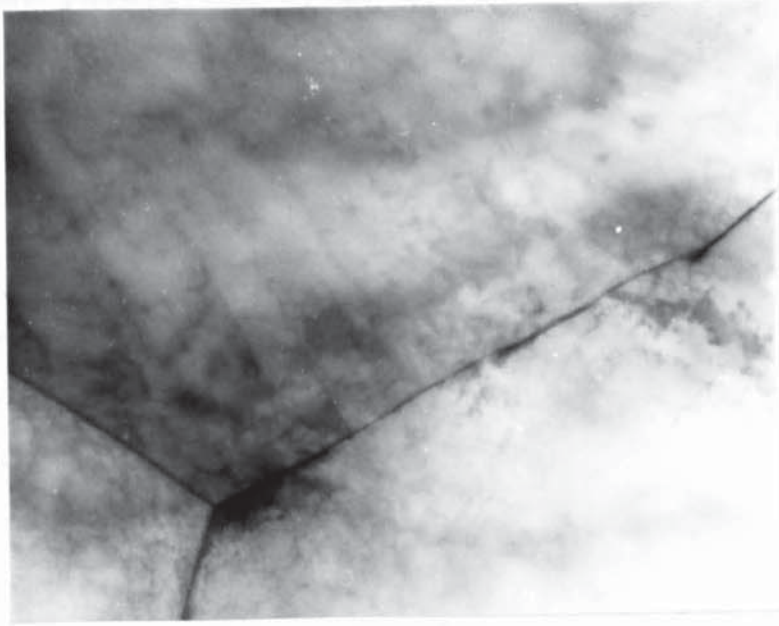

Plate 8 Cast B, 304L. As received, works-softened condition. TEM micrograph showing triple point. Some particles can be seen extending along the boundary on the right. X2.6K

2.3 Causes of Intergranular Attack and the Difference in Severity of Attack Between Two 304L Steels

The difference in corrosion rate between A and B is greater than can be accounted for by compositional difference alone. The nature of the attack on cast B and to a certain extent on cast A indicated that there was a factor operating at the grain boundary lowering the resistance to intergranular attack. The incidence of precipitated particles on the grain boundaries of cast B was very low and almost non-existent in cast A. Although the presence of such particles is indicative of diffusion of a solute species to the grain boundary, there is such a small number of precipitates that they alone, or a depleted zone connected with them, would not be sufficient to account for the massive intergranular attack that occurred.

As well as the intergranular attack on the steels during the nitric test, there was considerable penetration and attack of the interior of grains close to the surface of the specimens. Very few of the surface exposed grains escaped this internal attack which was very often initiated by penetration along twin boundaries. Once it had penetrated the interior of grains the attack would branch out along certain crystallographic planes so that the dissolution of the metal had a dendritic appearance. The crystallographic nature of the grains, and the nature of the grain and twin boundaries with their higher energy due to atomic misfit, alone would be insufficient to account for the attack. It is almost certain therefore that there are small precipitates, not easily detectable, or some solute

segregation not visible by optical or electron-optical means, which are distributed at the grain boundaries and on certain crystallographic planes within the grains, and which greatly reduce the resistance to attack during the nitric acid test. Once the attack has penetrated into the metal along a grain or twin boundary, the severity of attack and rate of dissolution can increase. This is because the nitric acid within the crevices will have a rising level of dissolved chromium, undiluted by the bulk solution, so that the critical level of dissolved hexavalent chromium, above which metal dissolution increases rapidly will be reached relatively quickly.

The massive pits that were found in both steels after the nitric acid test must have resulted from some micro-segregation that occurred as a result of the hot rolling operation. Although faint marks parallel to the rolling direction could be seen on the specimen surface prior to the test, in the places where pits subsequently formed, metallographic examination revealed no difference in structure or precipitation between the steel ahead of the tip of the pit and the bulk of the metal. Similarly to the deep intergranular attack, once a pit has formed, we would expect it to extend more rapidly than general surface attack due to build-up of corrosion products at the crack tip.

Solute segregation is a possible explanation for these observations because as a result of heat treatment or process operation, deleterious species may have segregated

to grain and twin boundaries and to certain crystallographic planar defects within the grains, altering their composition and chemical behaviour, but not altering metallographic appearance.

The higher corrosion rate of cast B can be accounted for by it having inadvertently received an unspecified or incorrectly applied heat treatment during processing. This could possibly have given rise to conditions where diffusion and segregation of a deleterious species took place.

To try to establish if the corrosion of cast B was due to incorrect heat treatment, a series of heat treatments was devised to see if a similar large difference in corrosion rate between cast A and cast B could be achieved under laboratory conditions.

3.1 Effect of various heat treatments on the susceptibility to intergranular corrosion of two casts of 304L in the nitric acid test

The two steels were heat treated either at the solution treatment temperature of 1050°C or the sensitizing temperature of 650°C or a combination of the two.

Table 2

Sample	Cast	Treatment	
1	A	10 mins 1050°C	WQ
2	A	100 mins 1050°C	WQ
3	A	10 mins 1050°C	AC
4	A	100 mins 1050°C	AC
5	A	100 mins 650°C	WQ
6	A	10 mins 650°C	WQ
7	A	100 mins 1050° WQ, 100 mins 650°	WQ
12	A	100 mins 1050° WQ, 10 mins 650°	WQ
9	B	10 mins 1050°C	WQ
10	B	100 mins 1050°C	WQ
11	B	10 mins 1050°C	AC
13	B	100 mins 650°C	WQ
14	B	10 mins 650°C	WQ
15	B	100 mins 1050° WQ, 100 mins 650°C	WQ
16	B	100 mins 1050° WQ, 10 mins 650°C	WQ
17	B	100 mins 1050°C	AC

WQ - Water quenched AC - Air cooled

The cooling rate of the air cooled specimens was measured using a thermocouple attached to the face of the specimen.

This gave an approximate figure for cooling rate as the temperature varied slightly from that at the centre of the specimen.

Table 3 Average cooling rates of air cooled specimen

				°C/sec
Between	1000	and	900°C	18.3
	900		800	14.2
	800		700	10.0
	700		600	6.6
	600		500	4.6
	500		400	3.2

Where possible the heat treatment was performed in a vacuum furnace. This was not possible for some specimens which were treated in an electric muffle furnace. In the muffle furnace an air-formed oxide resulted and this was entirely removed afterwards by surface grinding.

The susceptibility to intergranular corrosion was assessed using the standard Nitric Acid test using the procedure detailed in previous chapters. The specimen surfaces were ground to a 180 mesh grit finish prior to the test. An acid/specimen surface area ratio of 20 cm^3/cm^2 was used. A specimen size was chosen to give a test volume of approximately 500 ml acid. The weight loss for each specimen was determined to establish the corrosion rate. Each test was performed twice.

During the nitric acid tests it was noted that the colour of the boiling acid varied considerably from colourless through straw to dark yellow. This is most probably due to the tightness of fit of the condenser into the test flask.

A tight fitting condenser will prevent the escape of gaseous oxides of nitrogen (a yellow gaseous product could often be seen in the flask) which Truman [52] considers may act as an inhibitor to corrosion, whereas a loose fitting condenser will allow the gaseous products to escape and will allow access of air into the flask.

Table 4

Nitric acid test corrosion rates of Cast A and B after heat treatment

Corrosion rates in $mg/cm^2/48h$ (average of five periods)

Sample	Cast A	Sample	Cast B
1	0.57, 0.74	9	0.57, 0.57
2	0.53, 0.13	10	0.57, 0.66
3	0.78, 1.53	11	0.66, 0.96
4	0.53, 0.61		
5	1.13, 1.1	13	0.96, 1.58, 0.92
6	0.83, 1.75	14	3.02, 5.78, 5.08
7	0.88, 2.11	15	0.61, 0.70
12	0.96, 0.87	16	0.57, 0.70

Extended Heat Treatment

As well as the shorter heat treatments detailed previously, three specimens of Cast B were given extended heat treatments at the sensitizing temperature of 650°C as shown in Table 5.

Table 5 Extended heat treatments Cast B

Specimens	Treatments		
1E	68 hours	650°C	WQ
2E	168 hours	650°C	WQ
3E	700 hours	650°C	WQ

These treatments were performed in an electric muffle furnace and the specimens were prepared and then subjected to the nitric acid test in the same manner as those given the shorter heat treatments.

Table 6 Nitric acid test corrosion rates. Cast B extended heat treatment

Specimen	Corrosion Rate $mg/cm^2/48h$
1E	3.37
2E	22.03, 4.38
3E	4.86, 5.7

After the nitric acid tests had been completed, all of the specimens were examined by scanning electron microscopy (SEM) to assess the extent of the surface attack for comparison with the quantitative weight-loss results of the nitric acid test. The main factors investigated during the SEM examination were depth of attack, width of boundary ditching and extent of grain dropping.

3.2 Results

3.2.1 Shorter Heat Treatments on Cast A and B

The nitric acid test results showed a wide variation in corrosion rates between heat treatments and occasionally between specimens that had received the same heat treatment. As would be expected, the lowest corrosion rates were found in the specimens that had been given a solution treatment with a water quench (Nos 1, 2, 9 and 10). Both Cast A and Cast B showed similar corrosion rates except one specimen of cast A which had been given the longest solution treatment and had the lowest corrosion rate of all specimens tested. SEM examination of these specimens revealed that the surface attack was very light. Preferential attack had occurred in some specimens at the grain boundaries but there was no grain dropping, and two specimens of the longer solution heat treatments showed very little grain boundary attack whatsoever. The centre of the grains showed some sign of attack and pitting, though this was less marked with the specimens given the longer heat treatment (100 mins) and on these specimens the original abrasion marks were still visible. The 100 minutes solution heat treatment resulted in a lower corrosion rate than the 10 minute treatment although the weight loss results for cast B did not decrease as much as those for cast A. (Plate 9)

The specimens that had been solution treated and air cooled instead of quenching (3, 4 and 11) showed a slightly higher corrosion rate generally. This is to be expected as on cooling the steel will pass more slowly through the

sensitization temperature range and there will be more time for diffusion and segregation to take place. As well as having a higher weight loss, the severity of the surface attack was greater with one or two small grains dropping from the surface. One test on specimen 3 resulted in a much higher weight loss and more severe attack of the grain boundaries, with an increased amount of grain dropping. In this specimen attack in the centre of the grains was more localised than usual with one or two wide mouth pits forming. Another feature of this specimen was the occurrence in one or two places of intergranular attack along very straight lines. The straight lines of attack were parallel with the rolling direction indicating that this type of attack was occurring at the site of a second phase stringer that had resulted from the hot rolling of the steel. (Pl. 10)

A TEM examination of several of the water quenched and air cooled cast B steels was made. The specimens for the TEM were prepared using the process detailed in appendix 1. There was approximately a 50 per cent success rate in obtaining an area of steel sufficiently thin for TEM examination.

The solution treated and water quenched specimen which had the lowest corrosion rate in the nitric acid test was very clean when examined on the TEM. There was no evidence of any precipitates at any of the grain boundaries.

The grain boundaries of the air cooled specimen were not as clean as those of the water quenched specimen, with precipitates forming at several places. The precipitates were only found on some of the grain boundaries, often being found in small groups. They were most often lenticular in shape with the long axis running along the plane of the grain boundary. The precipitates were of the order of up to 5 μ across and 5 to 50 μ in length. Selected area diffraction patterns of the precipitates showed that they were carbides of the type $M_{23}C_6$. (Plates 12,13,14)

In several places there were small holes in TEM specimens approximately 0.5 μ in diameter where particles appeared to have dropped from the foil during electro-thinning. This was confirmed when some particles still in the foil were found. The metal immediately surrounding the particles was much thinner than the rest of the specimen and in some cases the metal had been dissolved away leaving a hole adjacent to the particle. This could either arise due to local changes in composition round the particle, or an inherent difference in electrode potential between the particle and the matrix resulting in preferential attack of the region round the particle.

The specimen which had been sensitized from the as-received condition (5, 6, 13, 14) generally showed the highest weight loss in the Nitric acid test with one, No. 14 showing catastrophic intergranular attack in all three specimens exposed to the nitric acid test. There was attack at the grain boundaries with all these heat treatments and

only one (No. 6) showed no evidence of grain dropping. Although No. 6 which had been sensitized at 650°C for 10 minutes showed no grain dropping it appeared to be far more surface active with a greater degree of attack at the centre of the grains. This attack was crystallographic in nature, preferentially attacking along certain planes of atoms within the grains. This is most probably associated with micro-segregation within grains (Pl. 15,16) Specimen 14 which had also been sensitized for 10 minutes at 650°C showed massive attack at the grain boundaries and at the centre of grains with considerable grain dropping. The attack however was not uniform with regions on the surface where large amounts of grain dropping had taken place, adjacent to regions where grain dropping was negligible. This dual behaviour was found only in No. 14, and in all three specimens subjected to the nitric acid test. The region of heavy grain dropping coincided with heavy grain-centre attack, and this grain-centre attack was crystallographic in nature. From a weight loss aspect the corrosion of No. 14 greatly exceed that of any of the other steels given in a short heat treatment. (Pl. 17)

The specimens which had been given a solution treatment prior to sensitization (7, 12, 15, 16) showed generally lower weight loss in the nitric acid test than those that had been sensitized from the as received works softened condition. This is as expected as the sensitization due to diffusion of segregants will be less in the solution treated steel where deleterious species such as carbon, phosphorus, silicon, etc, will be in solution, than in

the as-received steel where some diffusion/segregation may already have occurred. Contrary to expectations from previous specimens Cast B showed a lower corrosion rate in these specimens than Cast A. The longer sensitization time as expected gave the higher corrosion rates although the difference was never very large. The SEM studies on these specimens showed that none of them exhibited extensive grain dropping. It was apparent from these studies that the longer sensitization times resulted in more attack on the grain boundaries and less attack on the centre of the grains. One specimen of No. 12 showed the same straight-line attack as that found in No. 3. It appeared to be of a similar nature, the width and direction indicating that it had occurred where a second phase stringer had existed.

3.2.2 Extended Heat Treatment Cast A and B

The weight-loss results from the nitric acid test on specimens of Cast B that had been given extended heat treatments at the sensitizing temperature of 650°C were much higher than those given shorter heat treatments. In all cases there was massive intergranular attack with considerable grain dropping. Treatment 2E, 168 hrs at 650°C showed a considerable disparity between consecutive specimens which had been cut from the same bar of cast B and had been given identical treatment, the worse of the two having the highest corrosion rate of any specimen tested of either cast A or cast B. (Plate 18)

In all cases where there had been massive intergranular attack, the high corrosion rate was maintained in all of the five 48 hour test periods, although the acid was changed after every period. As more grains drop from the metal surface, the total surface area exposed to the nitric acid solution increased. There did not appear to be a clear trend of corrosion rate with time of heat-treatment. However, if the very high corrosion rate of 2E is regarded as a spurious result the corrosion rate did show an increase with heat-treatment time. However there were insufficient results for significance of any large degree to be placed on this trend.

Examination by TEM of the specimens that had been given extended treatments showed that all had a larger number of grain boundary particles than those that had been given the shorter sensitizing treatments or those that had been solution treated and air cooled. The particles were of the same lenticular shape as previously, with the long axis along the boundary, and selected area diffraction confirmed them to be of the same type $M_{23}C_6$. There also occurred some precipitation within the grains themselves. In two separate cases 2E and 3E (168h and 600h), a band of a large number of small precipitates associated with a higher dislocation density than normal was observed. Within the band itself the precipitates had a preferred orientation along two planes that were at an angle of approximately 110^{o} to each other within the plane of the foil. The particles were elliptical in shape with axes of approximately 0.25 μ and 0.08 μ. As with the other TEM specimens containing precipitates, the specimens with extended sensitization showed preferential attack round some of the grain boundary particles that had occurred during electro-polishing, with some of the particles actually dropping out of the foil or being dissolved. This often left holes in the foil, although some particles were found with no localised attack or perforation.

The type of precipitates found in the extended heat treatments are shown in Plates 19, 20, 21.

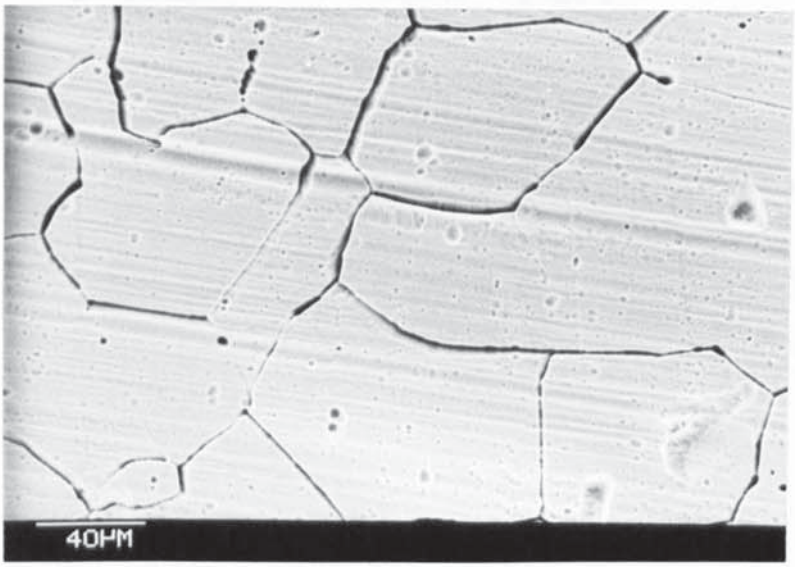

Plate 9 Cast A 304L Solution treated 100 minutes at 1050°C and water quenched. SEM micrograph of surface after nitric acid test showing low level of surface and intergranular attack.

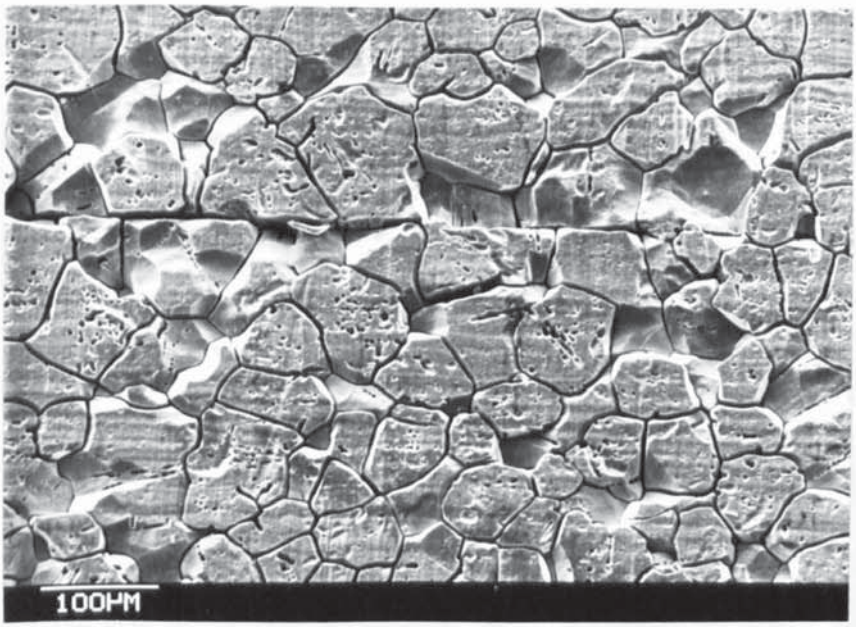

Plate 10 Cast A 304L Solution treated 10 minutes at 1050°C and air cooled. SEM micrograph of surface after nitric acid test showing moderate surface and intergranular attack with some grain dropping.

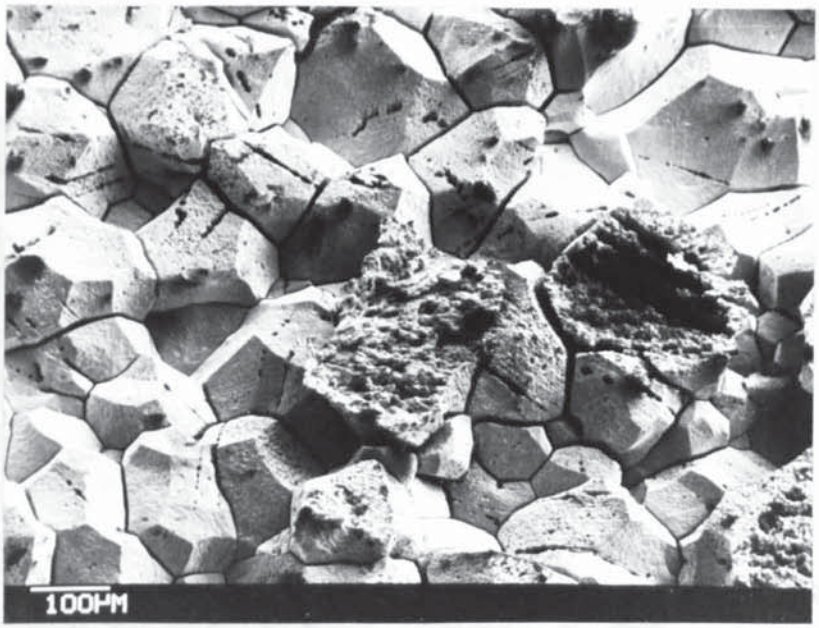

Plate 11 Cast B, 304L. Sensitized 10 mins. 650°C, water quenched SEM micrograph of surface after nitric acid test showing massive grain dropping. Less than 10% of original surface grains remain.

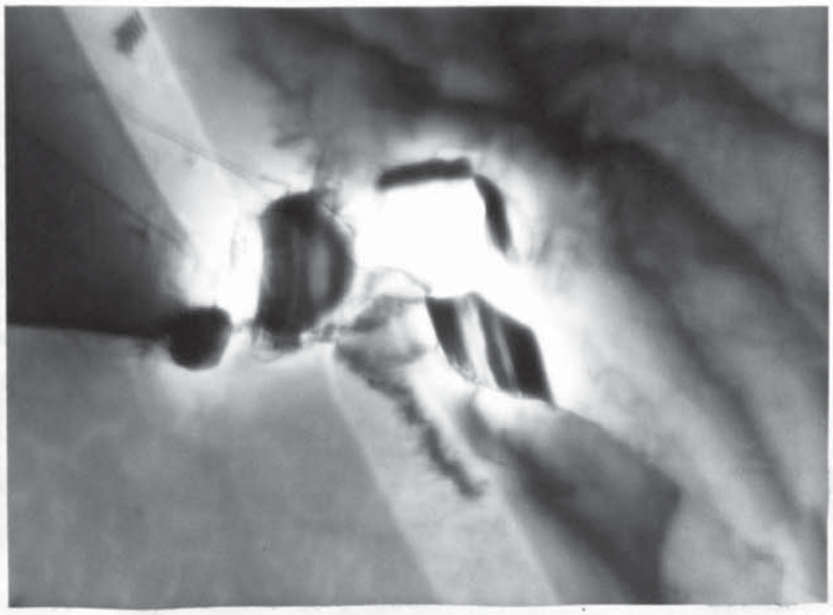

Plate 12 Cast A, 304L. Solution treated for 10 min. at 1050°C and air cooled. TEM micrograph showing precipitates of $M_{23}C_6$ on the boundary.

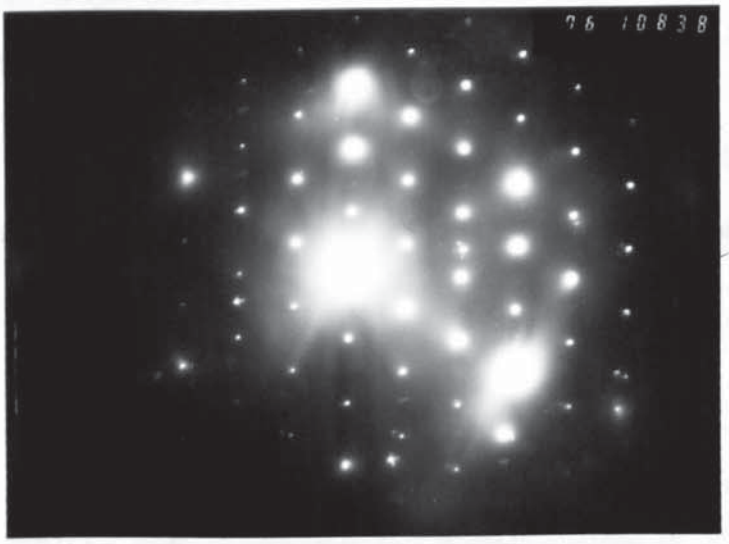

Plate 13 Electron diffraction pattern of grain boundary carbide in solution treated and air cooled specimen of cast A. A parallel orientation relationship exists between the matrix (bright spots) and the carbide (faint spots) $M_{23}C_6$.

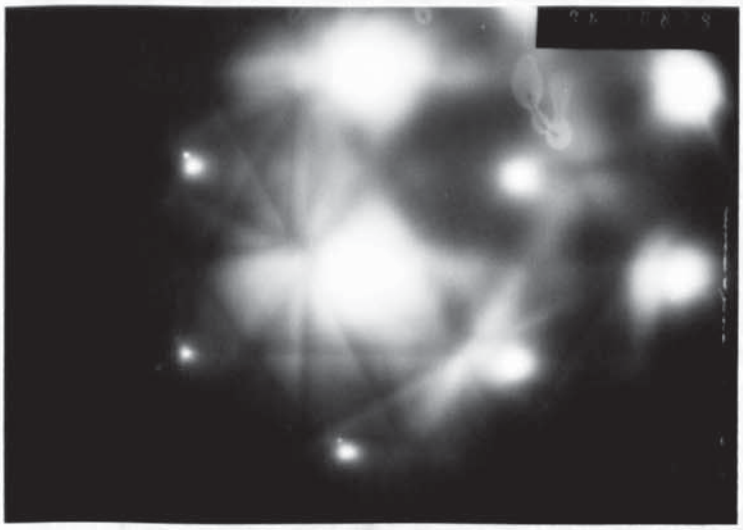

Plate 14 Electron diffraction pattern of matrix adjacent to grain boundary carbide. (see above).

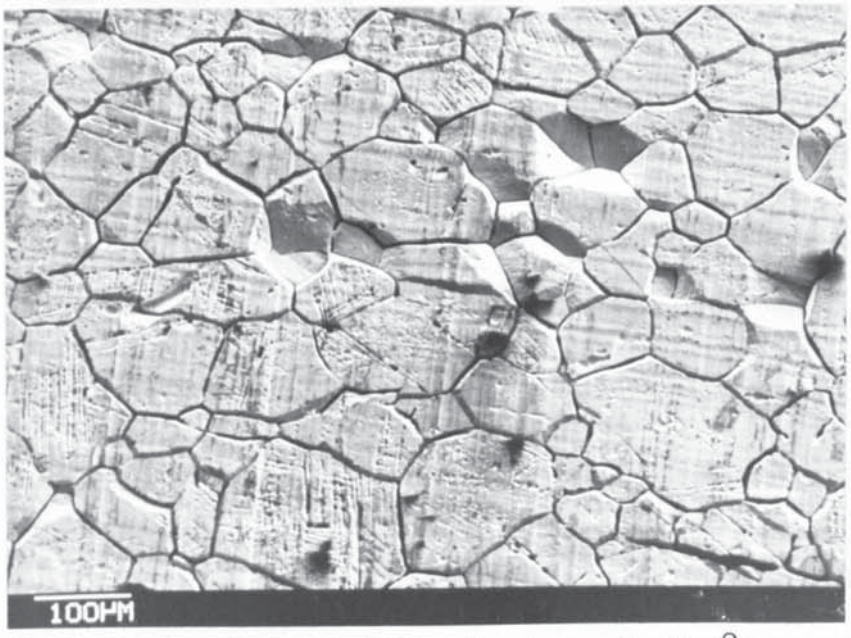

Plate 15 Cast B sensitized 100 minutes at 650°C, water quenched SEM micrograph of surface after nitric acid test showing abrasion marks from grinding process (vertical marks), banding due to segregation (horizontal marks), and attack within grains revealing orientation effects.

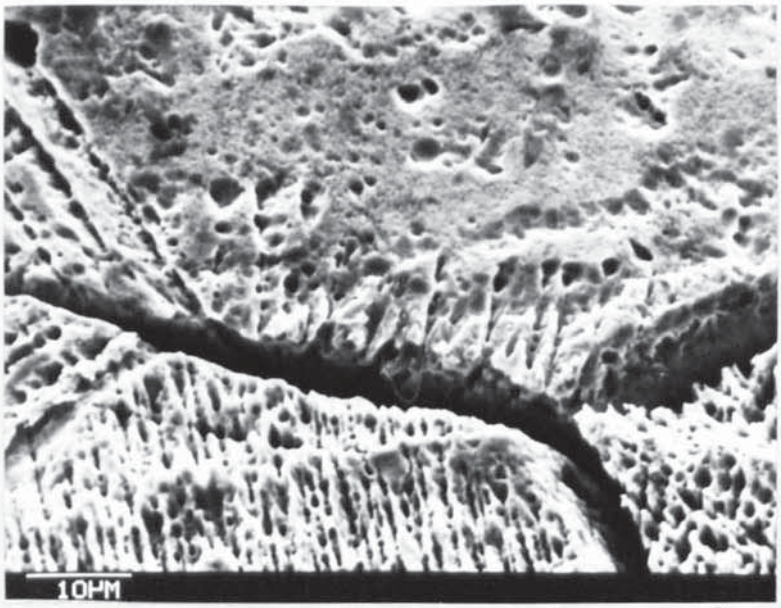

Plate 16. Cast A sensitized 100 minutes at 650°C, water quenched SEM micrograph of specimen surface after nitric acid test showing orientation dependent attack within individual grains.

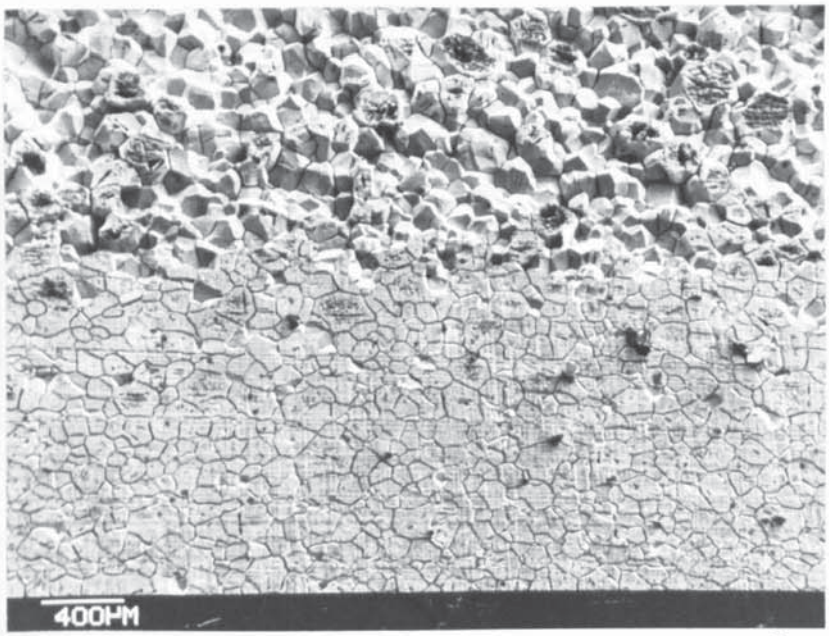

Plate 17 Cast B. Sensitized for 10 min. at 650°C and water quenched. SEM micrograph of surface after nitric acid test showing dual attack. One portion showing ∿ 90% grain dropping, the other less than 10%. The separating line between the two regions runs parallel to the rolling direction.

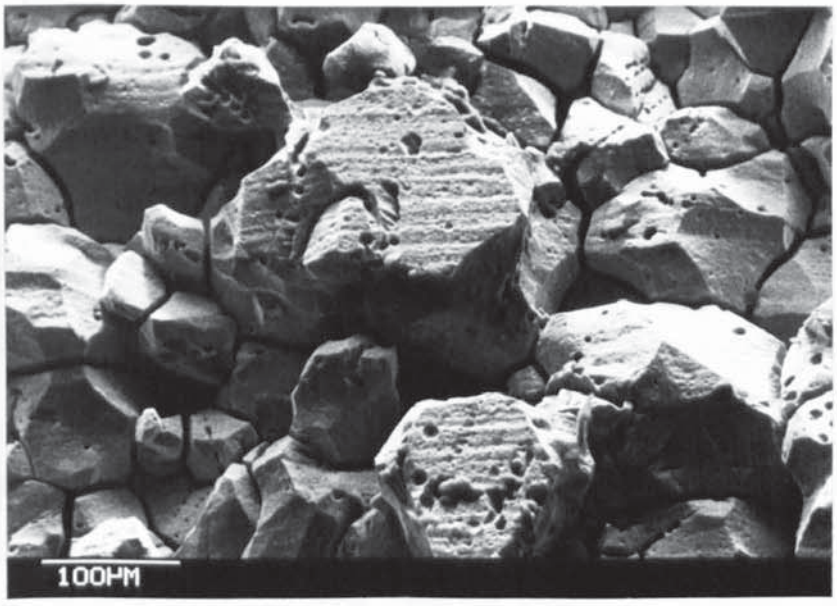

Plate 18 Cast A sensitized 168 hours at 650°C water quenched. SEM micrograph of surface after nitric acid test showing massive intergranular attack and grain dropping.

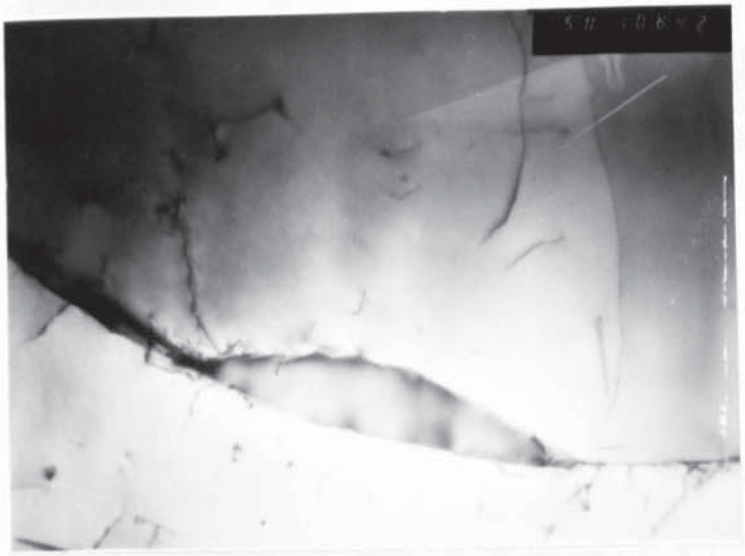

Plate 19 Cast B sensitized 700 hours at 650°C., water quenched
TEM micrograph showing carbide $M_{23}C_6$ on a grain boundary
x 50K

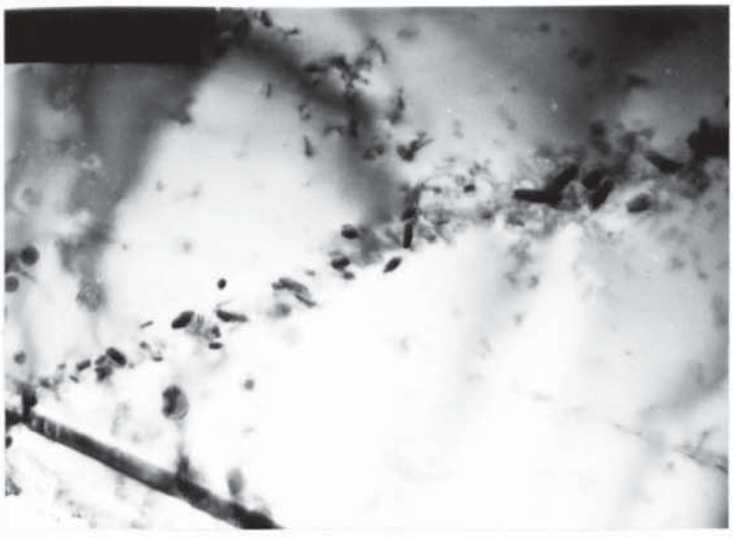

Plate 20 Cast B sensitized 700 hours at 650°C, water quenched.
Narrow band of precipitates. X 33K

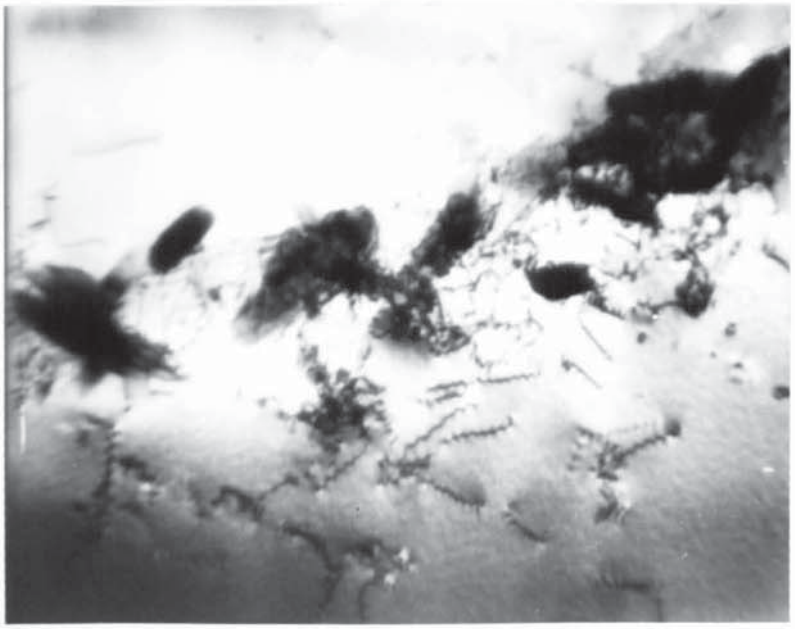

Plate 21 Cast B sensitized 700 hours at 650°C, water quenched TEM micrograph showing preferred orientation of small precipitates on apparent low angle boundary.

x 200K

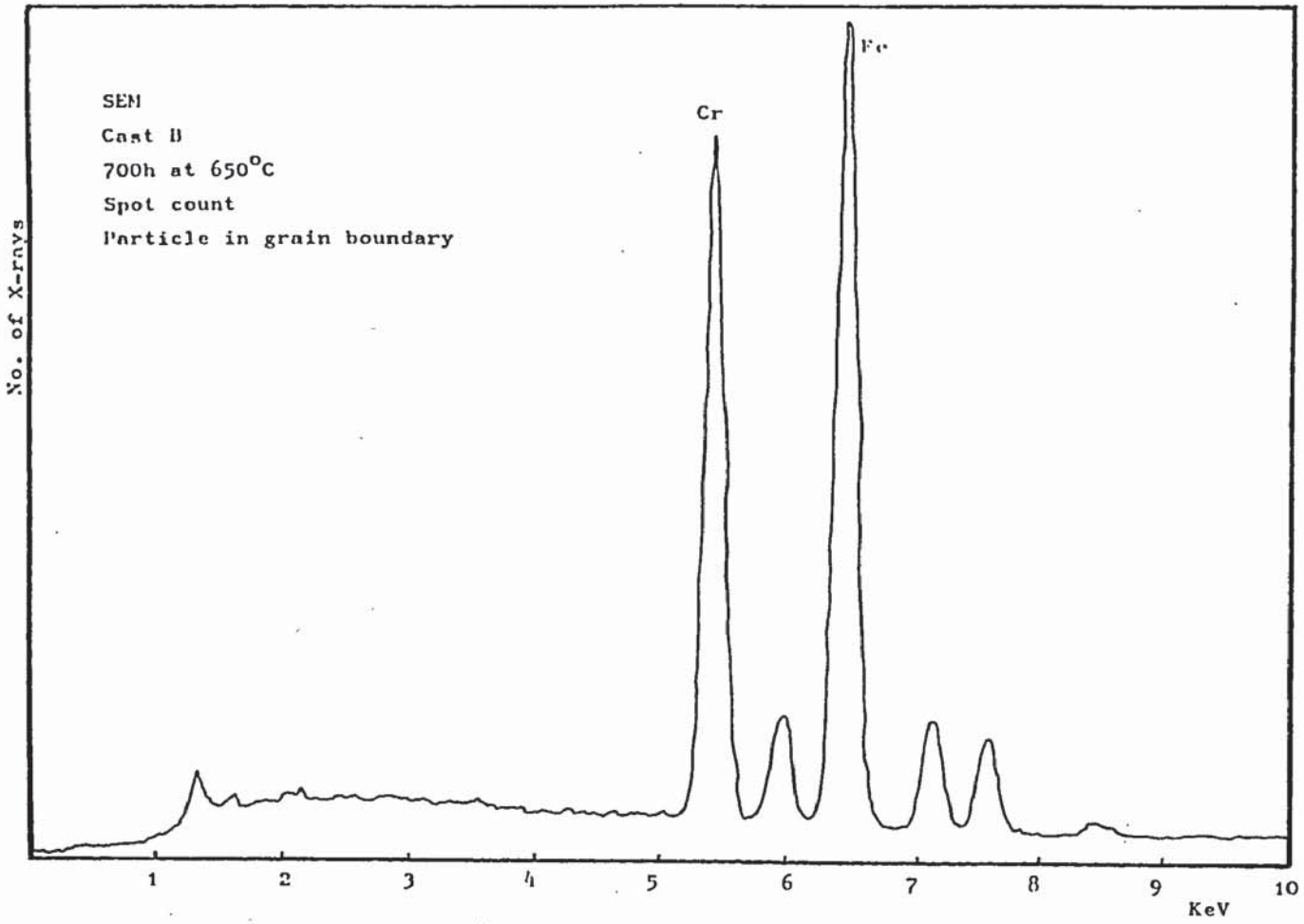

Fig.15 Energy dispersive x-ray spectrum, showing high level of chromium in grain boundary particle ($M_{23}C_6$) in cast B after 700h sensitization.

3.3 Examination of TEM Specimens of 304L Subjected to the Nitric Acid Test After Different Heat Treatments

To try and relate the corrosion behaviour of 304L with microstructure, TEM foils of cast A were exposed to boiling 65% Nitric Acid, and the nature of the attack studied. The two steels studied were cast A in the solution treated and water quenched condition, and the same steel after solution treatment and air cooling (Nos. 1 and 3 respectively as designated earlier in this work, see Table 2, p.59)

The TEM specimens were prepared and electropolished to electron transparent thickness. (See appendix 1)

The specimens were then immersed in boiling 65% nitric acid (as used in the ASTM standard test)[46] using a specially made glass specimen holder. The holder consisted of a narrow glass tube with a perforated bulb at one end to accommodate the specimen. The holder, with specimen, was inserted into the side port of a twin-necked round-bottom flask containing the boiling nitric acid. The other part of the flask was connected to a reflux condenser, which condensed the nitric acid vapours and returned them to the flask.

3.3.1 Experimental

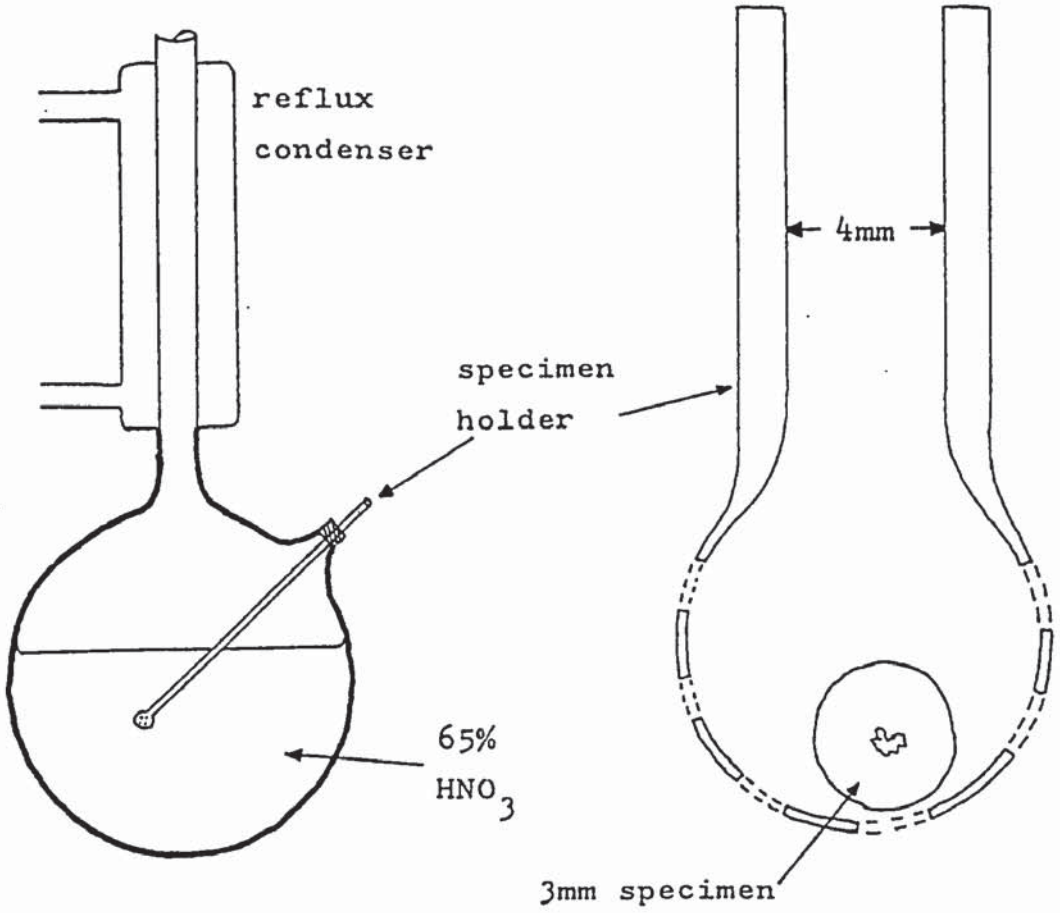

Fig. 16

Experimental set up for immersion of TEM specimens in boiling nitric acid with detail of specimen holder

The perforated bulb allowed free circulation of the nitric acid round the specimen. On removal from the acid the specimen was washed in water and then in ethanol prior to examination on the TEM.

The specimens were exposed to acid for various times, starting with only a few seconds, and they were examined after each exposure on the TEM.

3.3.2 Results

The specimen that had been water quenched from the solution treatment temperature showed very little attack whatsoever at the shorter exposure times (less than 1 minute). There was some slight general dissolution at the edge of the specimen where the metal was at its thinnest and some broadening of the cracks that had occurred during electropolishing.

At longer times (1 to 10 minutes) the cracks broadened even more and there was noticeable attack on one or two of the visible grain boundaries. The attack on the grain boundaries and in some cases twin boundaries, manifested itself as perforations on the boundaries. The perforations were only found on some of the boundaries and tended to be linear. They started out quite short and narrow and increased in length with increasing immersion time. The rate of extension was quite slow, after twenty minutes exposure the holes were approximately 0.1 μ in length and 0.015 μ in width.

Some perforation was observed on a twin boundary and it was only the coherent boundary that was attacked. The incoherent boundary was not attacked in this manner. (Plate 22)

The air cooled specimen, as in the nitric acid test, showed a higher rate of attack and the attack was more widespread. More dissolution of the cracks that had arisen during the electropolishing operation occurred. These were widened

considerably during the exposure, although very little penetration occurred along grain boundaries that had not already cracked.

The nature of the attack in air cooled specimens differed to that in the water quenched specimens.

In the air cooled, the boundaries that perforated did so in a very regular fashion. At a large number of points along the attacked boundary, small holes usually round in shape, formed. These holes were small (0.015 μ after 10 seconds in the nitric acid) and were fairly evenly spaced along the boundary with a separation of approximately 0.04 μ. There was a slight variation in the size and shape of the holes and this was unrelated to position on the boundary. (Plates 23, 24)

One boundary on the air cooled specimen appeared to have parallel lines along the grain boundary with a separation of 50 Å between the lines. (Plate 25)

The holes did not run the full length of the boundaries but were only found where the metal foil was reasonably thin.

3.3.3 Discussion

The type of intergranular attack occurring depended on how the metal had been heat treated. The steel that had been solution treated showed a slow rate of intergranular attack and relatively long lengths of boundary perforated, while

in the air cooled steel perforation occurred at regularly spaced points along the boundary and small round holes formed.

The attack on the solution treated steel can be explained by the presence of segregated solute impurities on the grain boundaries while in the air cooled steel precipitation, presumably of carbides, has occurred on the boundary. It was observed that air cooling does result in some grain-boundary precipitates although on the boundaries that had perforated the precipitates were very difficult to detect.

This type of attack was observed by Armijo [73] in 304 solution treated at 1000°C and exposed to nitric-dichromate and was attributed to the formation of globular carbides.

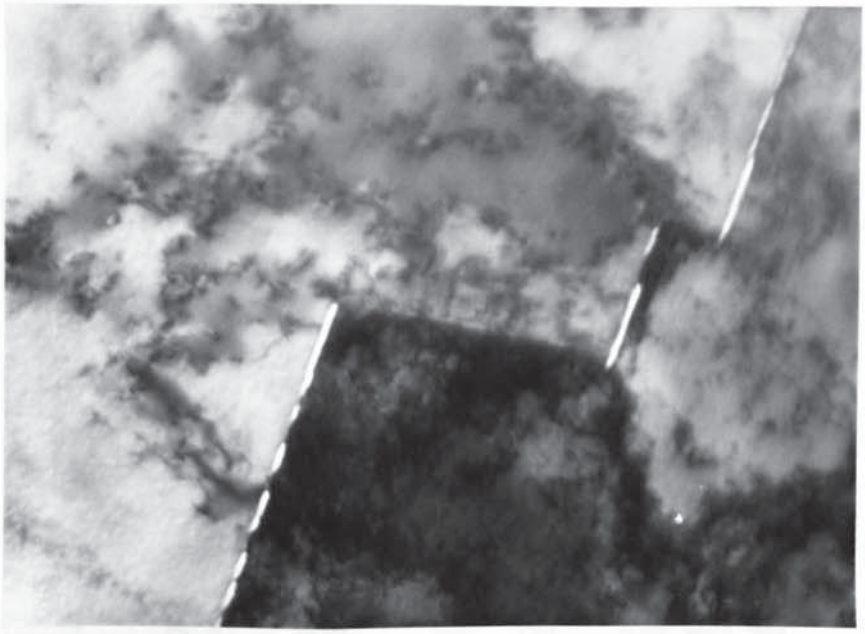

Plate 22 Cast A solution treated 100 minutes at 1050°C. Water quenched. TEM specimen immersed in boiling 65%/HNO_3 for 20 minutes. The grain boundary has perforated in linear sections.

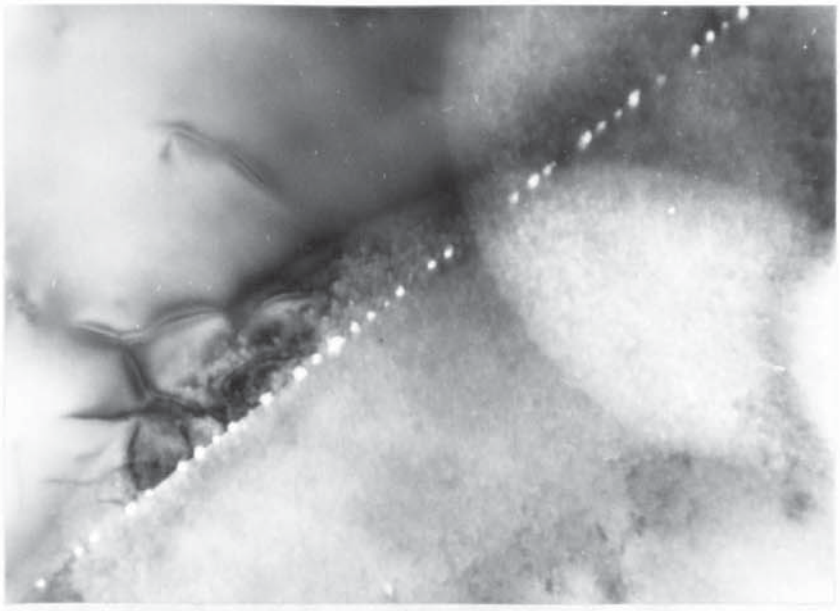

Plate 23 Cast A solution treated 100 minutes at 1050°C air cooled. TEM specimen immersed in boiling 65% nitric acid for 10 seconds after electro-thinning operation. The grain boundary has perforated at regular intervals.

X 27K

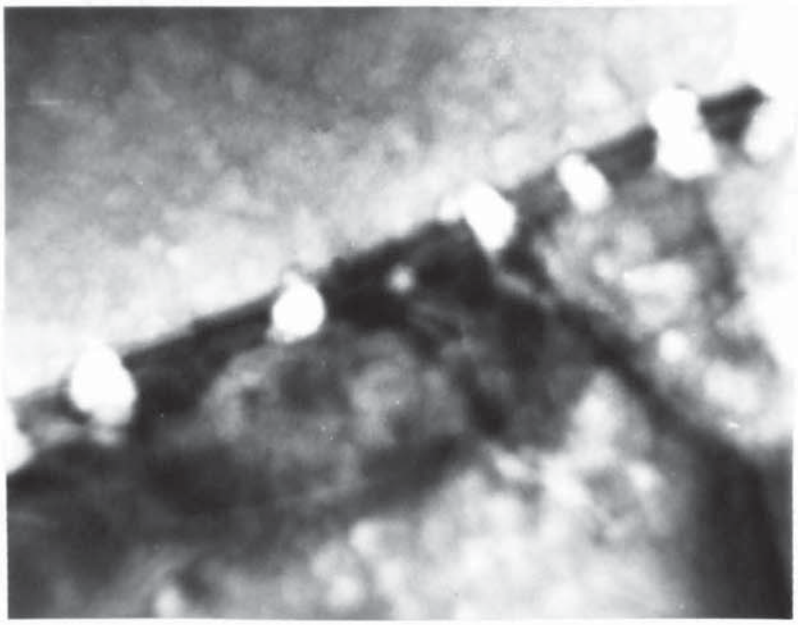

Plate 24 Cast B solution treated 100 minutes 1050°C air cooled. Perforation of grain boundary after immersion of TEM specimen in boiling nitric acid test solution. X 40K

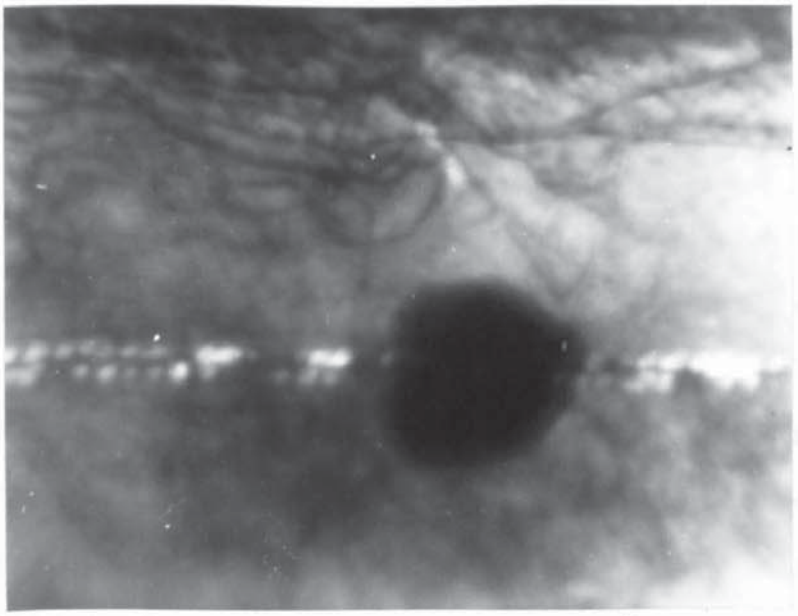

Plate 25 Cast B solution treated 100 minutes 1050°C air cooled. Perforation of grain boundary after immersion of TEM specimen in boiling nitric acid test solution. Dark region is a contamination spot caused by the electron beam during microanalysis. x 8K

4. Assessment of Intergranular Corrosion Resistance using the Oxalic Acid Etch Test of Two AISI Type 304L Steels

The behaviour of the two casts A and B were investigated using the ASTM standard oxalic acid etch test. This test is normally used for screening austenitic steels prior to the nitric acid test or any other prolonged standard test . If a steel passes the oxalic acid test it will not need to undergo the more prolonged test. It is intended to show positively those steels which have not been sensitized. According to Cowan and Tedmon [60] this test "will only show the absence of chromium depletion sensitization and does not test for 'sub-microscopic sigma' susceptibility" and Streicher [39] states the presence or absence of grain boundary chromium carbides will be shown by this test.

For grades of steel such as 304L, 316L the test normally is conducted on sensitized specimens, usually 1 hour at 650°C. This treatment should be sufficient to render a steel susceptible to intergranular corrosion if the possibility of any such susceptibility arising exists. Therefore, if any susceptibility has arisen during the heat treatment of casts A and B of 304L we would expect this to be shown by the oxalic acid test. The test itself is far quicker, less hazardous and is easier and cheaper to perform than the nitric acid test.

4.1 The Oxalic Acid Etch Test

The test used was the ANSI/ASTM standard A262-79, Practice A [46]. The assessment of the degree of attack in this test does not allow for a quantitative result, and it is assessed by the classification of etch structure after the test. In the test, a known area of the steel, ground and polished to a 1 micron finish is subjected to an anodic current of $1A/cm^2$ for 1.5 minutes in a 10 per cent (w/w) solution of oxalic acid in de-ionised water at ambient temperature. This results in the surface of the steel being electro-etched. The nature of the etched surface structure resulting from this test depends on the chemical and metallurgical make up of the steel. Based on the degree of etch attack on the grain boundaries the steel is deemed either resistant to, or susceptible to, intergranular attack.

The three basic classifications of surface morphology arising from the test are:-

1. Step type structure. This is typified by general surface attack with no preferential attack at grain boundaries. The differential attack from one grain to another results in the steps between adjacent grains on the surface. This structure is indicative of resistance to intergranular corrosion, and a steel that passes the test by showing such a structure would not show heavy grain boundary attack in the nitric acid test.

2. Ditch type structure. This surface structure is produced by preferential attack and etching of grain boundaries. Where this occurs to a considerable extent the removal of metal from the grain boundaries results in deep inter-connecting ditches surrounding all the grains of the metal. This structure is indicative of lowered resistance to chemical or electro-chemical attack of the grain boundary regions. This may be due to precipitated particles or to segregation of deleterious atom species at the grain boundaries. A test specimen is considered to have the ditch structure when one or more grains is completely surrounded by ditches.

3. Dual structure. This occurs when, although there are some ditches at grain boundaries in addition to steps, no one grain is completely surrounded with ditches.

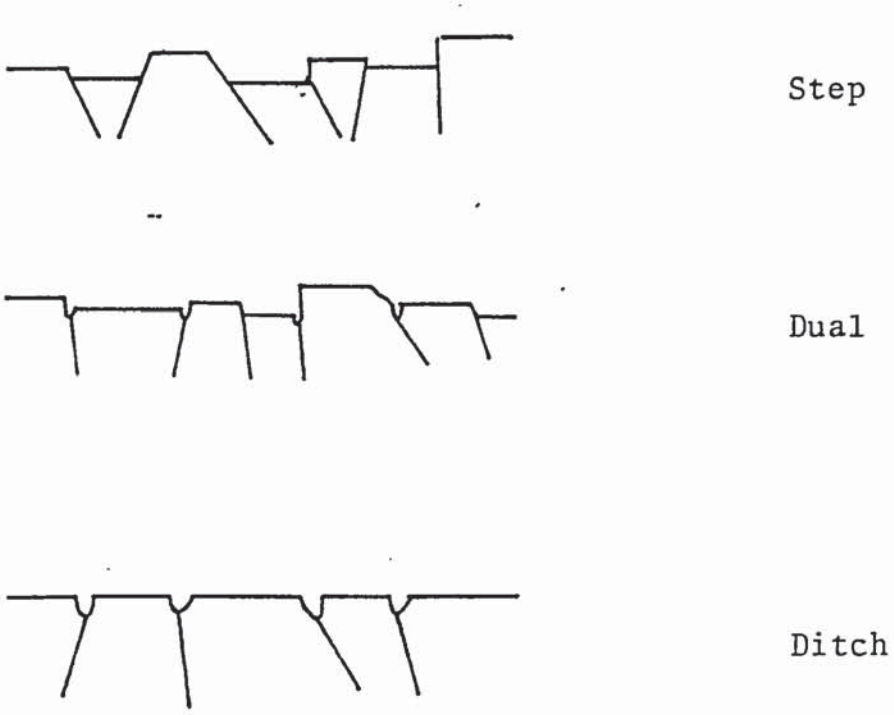

Fig. 15 Diagrammatic representation of the surface type classifications in the oxalic acid etch test.

4.2 Performance of 304L Casts A, B in Oxalic Acid Test after heat treatment

The two steels A,B, were tested after they had been heat treated as detailed earlier in this work. The specimens were mounted in Bakelite, ground on SiC papers and then polished on diamond wheels to a 1 micron finish. They were then washed in acetone, and dried prior to testing. From the surface area of each specimen the correct current to give a current density of $1A/cm^2$ was calculated. Using a stainless steel beaker as the cathode, an anodic current

was held for 1.5 minutes.

4.3 SEM Examination

The etched structures of the specimens after the test were examined using Scanning Electron Microscopy (SEM). Nos. 1 and 2 (Cast A) which had been solution treated and quenched showed the typical step type structure, with no dissolution at the grain boundaries. However 9, 10 (Cast B) which had been given identical heat treatments to 1, 2 did show some grain boundary attack on SEM. The grain boundary attack was worse on No. 9 which had the shorter solution treatment of the two. However, in all the solution treated specimens, some metal dissolution had occurred where stringers of a second phase had been exposed. (Plate 26)

The solution treated specimens that had been air cooled (Nos. 3, 4, 11) showed a greater degree of grain boundary attack than the water quenched specimens. This attack started as small etch pits on the boundary which grew and joined together resulting in a ditch. There was little or no attack on twin boundaries, except where a twin band terminated within a grain resulting in an incoherent twin boundary. These regions seemed very susceptible to localised attack in all specimens. Most of the grains were almost completely surrounded by etched grain boundaries which still showed the shape of the pits that had formed first. These pits would eventually become ditches if the etching time were extended. Not many of the grains were surrounded. Nos. 3, 4 (cast A) showed a dual structure while No. 11 (cast B) showed a ditch structure. (Pl. 27, 28)

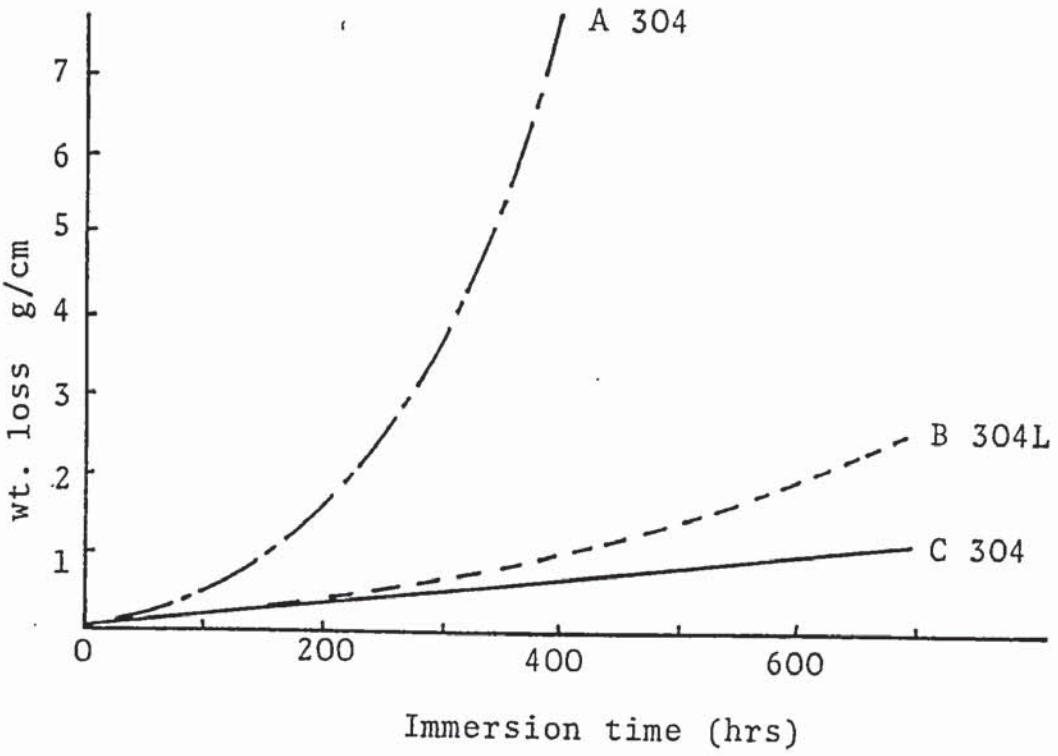

Fig. 16 Corrosion of 304 and 304L in boiling 65% HNO_3. A and B which have both been sensitized (1h @ 677°C), show a ditch structure in the oxalic acid test, but B has a corrosion rate similar to C (solution treated) which shows a step structure. B has a lower level than A of precipitated carbide. (Ref. 56)

The specimens of the steels that had been sensitized from the as received condition (5, 6, 13, 14) showed attack at the grain boundaries that was usually deeper and more continuous, although not all of the grains were completely surrounded by ditches. No. 13, which had been sensitized for 100 minutes had deeper ditching than No. 14, which had only been sensitized for 10 minutes although in the nitric acid test No. 14 had consistently shown a much higher corrosion rate. The steels again showed quite heavy localised directional attack where particles or stringers

had existed. No. 13 showed a ditch type structure while the others had a dual type structure.

The etch structure of the specimens that had been solution treated prior to sensitization (7, 12, 15, 16) were not as severe as those that had been sensitized from the as-received condition, and No. 12 (cast A) which was sensitized for 10 minutes, showed very little grain boundary attack at all, and had a step type structure. The other three showed dual type structure with more severe grain boundar- dissolution.

As well as the grain boundary attack, all the steels showed two other types of attack to a greater or lesser extent. (Plates 29, 30)

The general surface attack consisted of two types of pits. There were small geometrically shaped ones which covered the whole grain surface which resulted from the crystallographic nature of the grains. More widely dispersed through the grains were larger, deeper, round pits resulting from end grain attack. The nature of the crystallographic attack could be seen clearly where a crystal had twinned.

The other attack found on all specimens was the variable attack due to segregation banding in the steel. This resulted from segregation of the components of the steel during production hot-rolling processes. The banding was directional and the severity of attack depended on which face was being tested. Associated with the banding were

particles and stringers which dissolved preferentially. Segregation banding in the oxalic acid test resulted in the same surface appearance as it did in the nitric acid test. It is discussed more fully later.

Table 7 Comparison of Nitric Acid and Oxalic Acid Test Results on Casts A, B

No. and Cast	Heat Treatment (mins) 1050°C	650°C	Nitric Acid Test $mg/cm^2/48h$	Oxalic Acid Test Structure	Ditching
1A	10 WQ	-	0.66	Step	-
9B	10 WQ	-	0.57	Dual	Slight
2A	100 WQ	-	0.33	Step	-
10B	100 WQ	-	0.62	Dual	Slight
3A	10 AC	-	1.15	Dual	Moderate
11B	10 AC	-	0.81	Ditch	Slight
4A	100 AC	-	0.57	Dual	Slight
17B	100 AC	-	0.49	Step	-
7A	100 WQ +	100 WQ	1.50	Dual	Moderate
15B	100 WQ +	100 WQ	0.66	Dual	Slight
12A	100 WQ +	10 WQ	0.92	Step	-
16B	100 WQ +	10 WQ	0.63	Dual	Slight
5A	-	100 WQ	1.11	Dual	Moderate
13B	-	100 WQ	1.15	Ditch	Moderate
6A	-	10 WQ	1.29	Dual	Slight
14B	-	10 WQ	4.62	Dual	Moderate

Table 8 Comparison of Nitric Acid and Oxalic Acid Test Results on Casts A, B after extended heat treatment

Cast	Heat Treatment	Nitric Acid Test	Oxalic Acid Test	
			Etch Structure	Ditching
A	68h 650°C WQ	N/A	Ditch	slight
A	135h 650°C WQ	N/A	Ditch	slight
A	700h 650°C WQ	2.03	Ditch	slight
B	68h 650°C WQ	3.37	Ditch	slight
B	135h 650°C WQ	4.38	Ditch	slight
B	700h 650°C WQ	5.7	Ditch	slight

4.4 Discussion of Oxalic Acid Test and Nitric Acid Tests on Casts A, B of 304L

The corrosion rates in the nitric acid test of the air cooled and sensitized specimens of cast A were of the same order of magnitude as those of the as received material. The same test on similar specimens of cast B resulted in a corrosion rate approximately one tenth of that found with the as-received material. Only No. 14 (Cast B sensitized 10 min 650°C WQ) with a corrosion rate of 4.62 mg/cm^2/48h (average 3 tests) was anywhere near approaching the 10.65 mg/cm^2/48h of cast B in the as-received condition. In the nitric acid test there was very little difference overall between the performance of Cast A and Cast B after heat treatment. In some treatments Cast A had the lower weight loss and in others Cast B was the more resistant. However, the lowest

individual corrosion rate by far was in cast A and the highest in Cast B.

The oxalic acid test results differentiated more sharply between casts A and B. In all the heat treatments except one cast B showed the worse result. The standard oxalic acid test has only three categories of behaviour, although further classification of the severity of attack may be made within the dual and ditch categories. Degree of grain boundary attack within these two categories was classified as either slight or moderate. This enabled distinction to be made between etch structures that would otherwise have had the same classification. Cast A had three specimens which showed a step type structure, including one that had been sensitized for 10 minutes after solution treatment, while not even the solution treated specimens of cast B showed this structure. Cast B had two specimens which showed the ditch structure, one of them air cooled after 10 minutes at 1050°C, the other sensitized for 100 minutes. None of the cast A specimens showed a ditch structure. The worst classification of cast A was found after 10 minutes solution treatment followed by air cooling, and also after sensitizing for 100 minutes at 650°C. Most of the specimens fell into the dual surface structure classification.

The difference in the two casts is therefore shown up much better by the oxalic acid test than the nitric acid test. Test conditions are far more critical in the nitric acid test and small variations in composition of the acid such

as chromium content can lead to large weight loss differences. Once severe attack has occurred in the early stages of the nitric acid test, it will continue in later stages due to increased surface area and formation of crevices at the grain boundaries which can result in a build up of Cr^{6+}. As mentioned previously differing corrosion rates may also result from retention or escape from the flask of oxides of nitrogen which may act as inhibitors.

Cast B is the less resistant of the two casts to intergranular attack. This is shown most clearly when the steels are in the as-received works-softened condition, but is also evident after several different heat treatments including a 100 minute solution treatment. However, none of the laboratory treatments resulted in a corrosion rate as high as the steel that had been work softened, when subjected to the nitric acid test.

Both air cooling and sensitization resulted in increased attack in both tests compared with solution treatment. TEM examination showed that although some precipitates were found in these specimens they were insufficient in number to build up a continuous grain boundary region of chromium carbide particles with accompanying chromium depleted zones that could act as a corrosion path. Even in the solution treated condition where no precipitates were visible at the grain boundaries using TEM, the nitric acid test resulted in some intergranular attack, though this was limited with only one or two per cent of the grains dropping from the surface.

The most interesting effect observed was that all the heat treatments including sensitization decreased the susceptibility of cast B to intergranular corrosion compared with the as-received condition. Only one specimen which was sensitized for 168h. showed a higher corrosion rate. This condition that existed in the cast B as-received was sufficiently transient to be removed by a ten minute heat treatment either at 1050°C or 650°C. These treatments however made very little difference to the number of visible precipitates on the grain boundaries indicating that the as-received sensitivity was caused directly or indirectly by an atom species in solution that was able to diffuse to, or away from, the grain boundaries relatively easily. This appeared to be a separate phenomenon, although of a similar solute segregation type, to the susceptibility to intergranular attack that resulted from 650°C sensitization after a solution treatment.

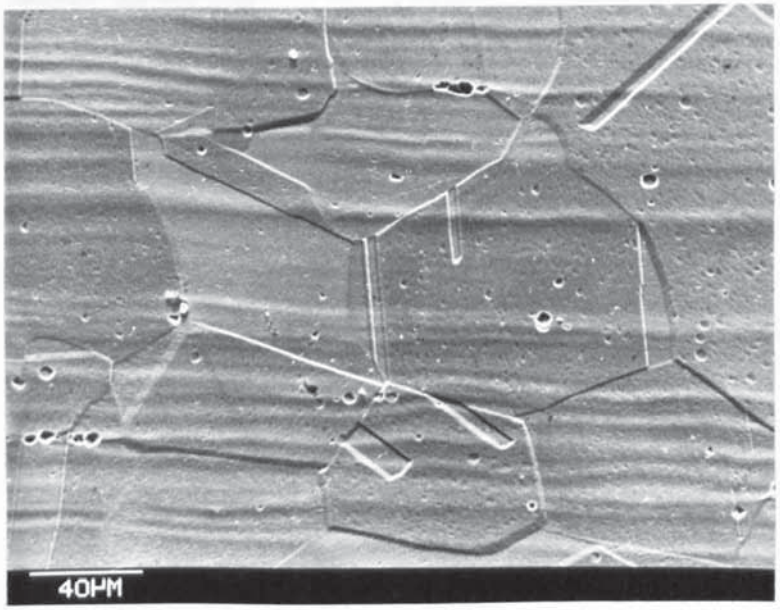

Plate 26 Cast A solution treated 100 minutes 1050°C water quenched. SEM micrograph of surface after oxalic acid etch test. Shows typical "step" structure and segregation banding.

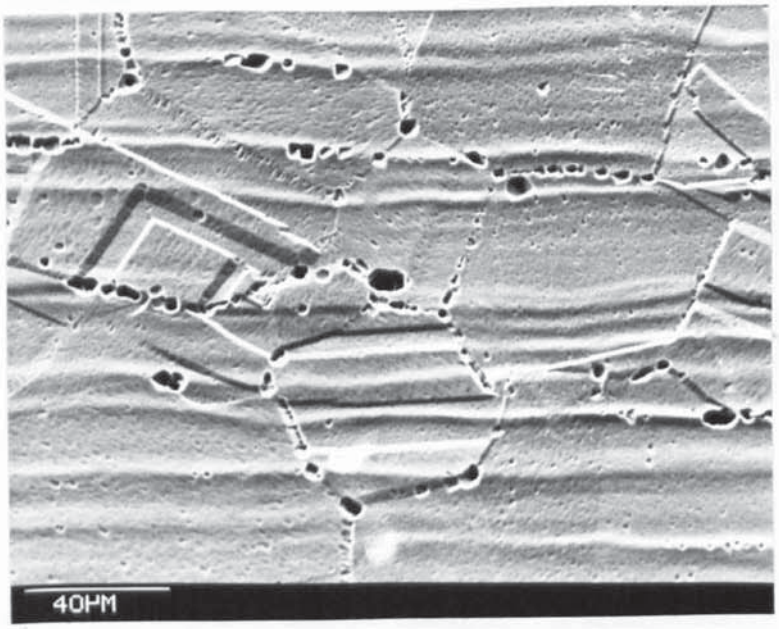

Plate 27 Cast B solution treated 100 minutes 1050°C water quenched. SEM micrograph of surface after oxalic acid etch test. Shows typical "dual" structure, some grain boundary pitting and segregation banding.

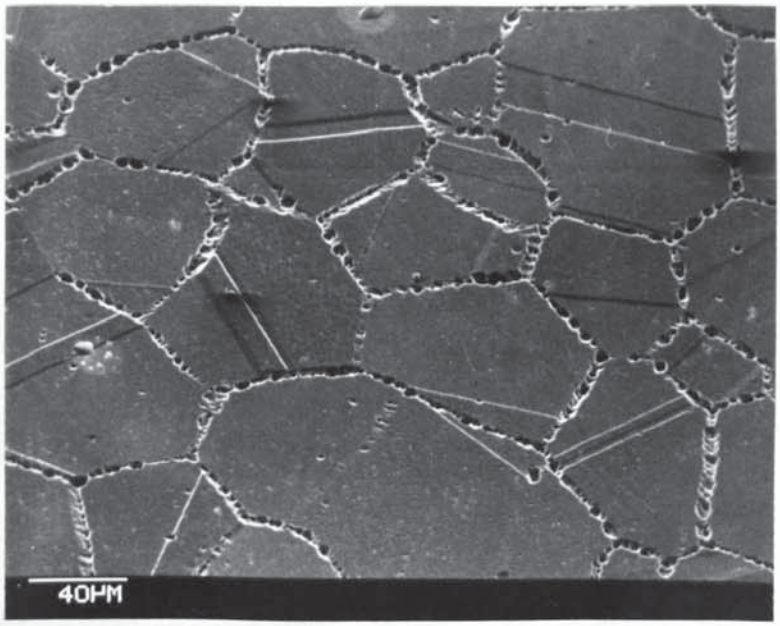

Plate 28 Cast B solution treated 10 minutes 1050°C air cooled. SEM micrograph of surface after oxalic acid etch test. Shows the start of ditching at the grain boundaries.

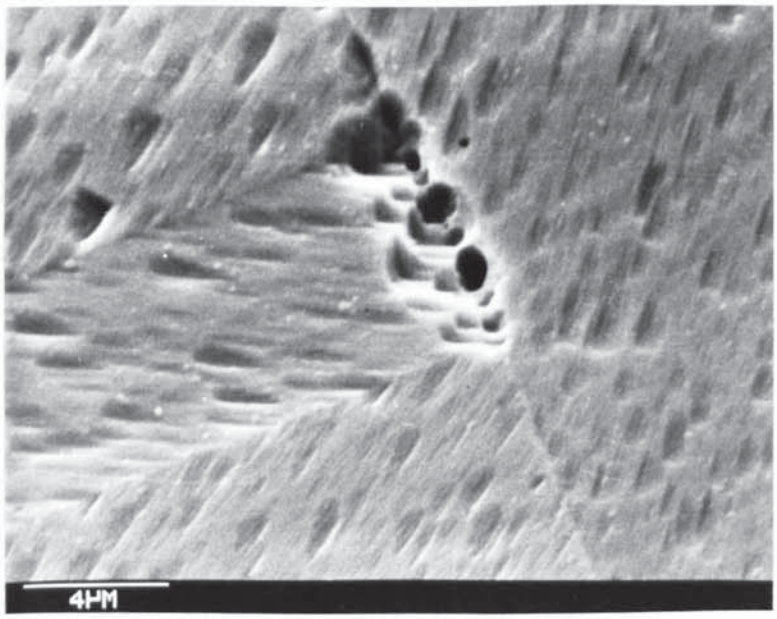

Plate 29 Cast A solution treated 100 minutes 1050°C, then sensitized 10 minutes 650°C water quenched. Shows preferential dissolution on segment of grain boundary and crystallographic orientated etch pits.

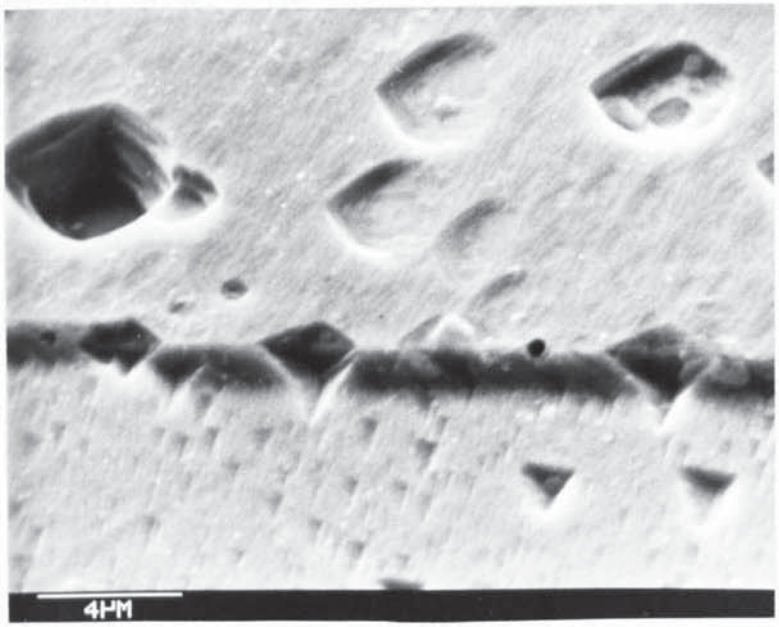

Plate 30 Cast A sensitized 100 minutes 650°C water quenched. SEM micrograph of surface after oxalic acid etch test. Shows differential etching at coherent twin boundary, crystallographic etching and formation of rectangular pits.

5. Segregation Banding in Cast B

During the nitric acid tests on Cast A and B it was observed that as well as the intergranular attack, surface pitting, and attack of inclusions, there was on some specimens banding attack which resulted in linear variations in attack that covered the surface. The bands were all parallel and ran parallel to the rolling direction.

This banding was observed more easily in stainless steel after exposure to an electrolytic etch in oxalic acid (such as the ASTM Oxalic Acid Etch Test) as the attack is more pronouced and the difference in surface level between adjacent bands is larger.

A study was made of this banding which is presumed due to segregation of some of the constituents of the steel during hot rolling. The main tools used were Electron Probe X-ray Microanalyser (EPMA) to investigate the elements involved, and the Scanning Electron Mircoscope (SEM) to study surface morphology of the bands and to correalate this with the EPMA.

5.1 Materials

One steel was studied: Cast B in the as received (works-softened) condition which had shown a high rate of inter-granular attack in the nitric acid test. This is an AISI 304L type steel.

5.2 Experimental

A specimen of the steel was cut by hand and mounted in conductive Bakelite to give an exposed surface area of 3 cm^2. This was ground using SiC papers and polished to a 1 μ finish on a diamond cloth. The specimen was mounted to ensure that the exposed face was parallel to the plane in which the steel had been rolled.

A line scan normal to the rolling direction was then performed on the surface of the polished steel using the EPMA. Four elements were chosen for analysis, Fe, Cr, Mo and Ni. The length of the scan was 0.80 mm.

The analysis volume of the EPMA is approximately 2.5 μ^3, with a width of $\sim$ 1.5 μ and penetrating to a depth of $\sim$ 1.5 μ. For quantitative analysis, full corrections for the Z, A, and F factors would have to be made, but a good indication of the qualitative situation can be obtained from the relative x-ray intensities obtained for each element by the crystal spectrometers of the EPMA. The results for each element were obtained as a graphical plot of x-ray intensity versus distance.

After the x-ray analyses had been obtained, the steel surface was etched electrolytically in a 10% solution of oxalic acid, at 4v at ambient temperature, the surface being the anode and a piece of AISI 316 being used as the cathode.

During the EPMA analysis the interaction of the electron beam and the specimen causes the breakdown of any hydrocarbons in the vicinity. This results in the build-up of a carbon deposit on the surface of the specimen where the electron beam has passed. The carbon deposit is quite adherent to the surface of the steel and thus the line of the analysis is distinctly marked.

During the oxalic acid etching the carbon deposit is removed at a much slower rate than dissolution of the steel surface itself, and it is possible to etch the surface to reveal clearly the banded structure of the steel while leaving the carbon deposit indicating the line of analysis relatively unaffected.

This enables the banded structure of the steel to be correlated to the EPMA line scan analysis.

After etching, the specimen was examined using an optical microscope and then a scanning electron microscope (SEM).

Photographs were taken of the area analysed and the photographs were blown-up to give the same degree of expansion for photograph/specimen as was obtained for analysis trace/specimen/ This was a linear scale expansion of 150X.

The surface morphology observed by optical and SEM methods was then compared directly with the line scan x-ray analysis. Because of its better depth of field, it was found the SEM gave better results. Examination of the etched surface was

made with the electron beam striking the specimen at a low angle of incidence (< 15°), as this accentuates surface relief. (Plates 31-34)

5.3 Results

The EPMA line scan gave a plot of x-ray intensity against distance for each of the four elements. For each element a mean intensity was calculated from twenty five regularly spaced points on the plot. The mean intensity for each element was taken to be equivalent to the bulk concentration of the element in the steel as measured by wet analysis. These concentrations were (per cent):-

Fe	-	67.9
Cr	-	18.06
Ni	-	11.8
Mo	-	0.1

The percentage variations in concentrations were then plotted as deviations from the mean. Cr and Ni were plotted on the same axis with a common mean.

The level of Mo in the steel was too low for measurement of such variations, but the other three elements all showed measureable variations. The nickel and chromium showed the largest variation from band to band. The band width, as measured by the variations in x-ray intensity, varied from 10 to 100 μ, at the mean concentration level. The variations in chromium level appeared to be related to the variations in nickel content with local maxima on the chromium x-ray

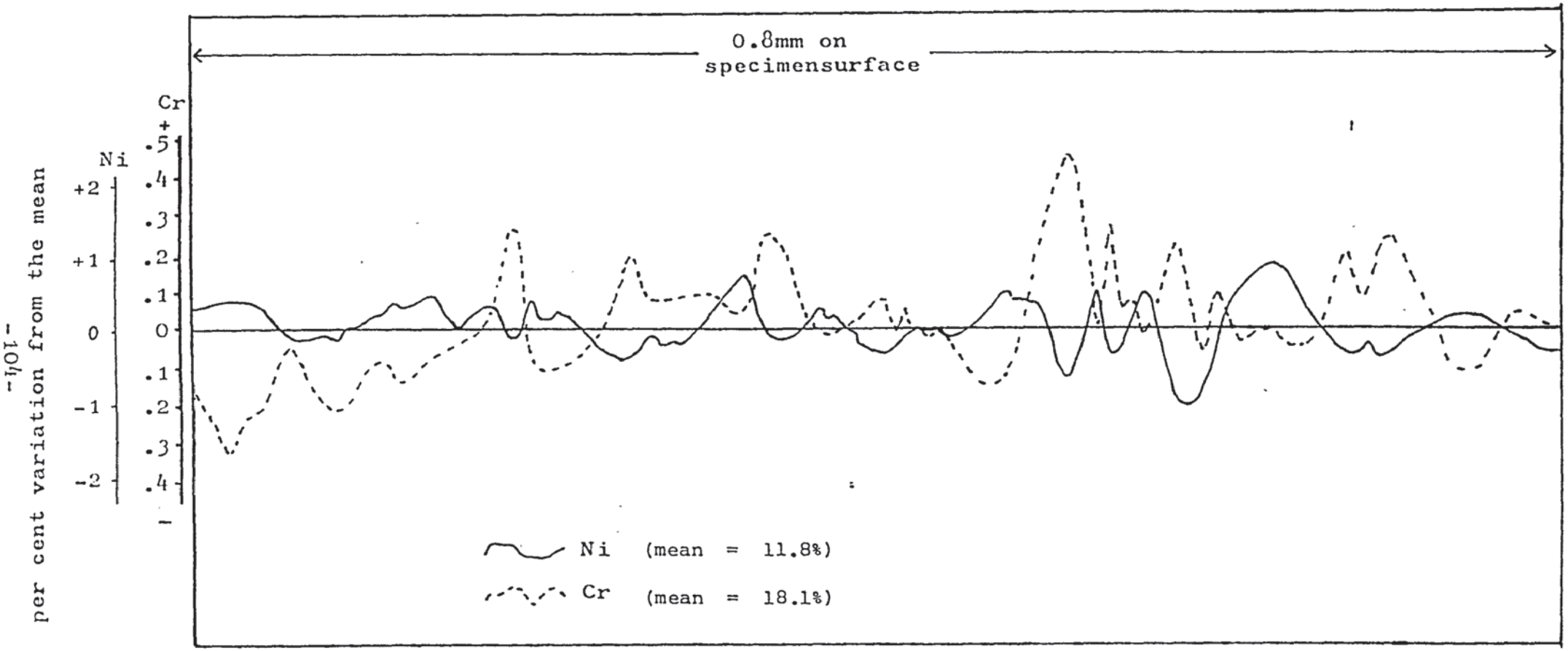

Fig. 19 Variations in composition across polished specimen surface of Cast B, determined using x-ray intensity measurements from electron probe microanalysis (EPMA).

intensity plot coinciding with local minima on the nickel x-ray intensity curve and vice versa. Of the 13 clearly identifiable maximum peaks in the nickel x-ray intensity curve, 11 are associated with minima in the chromium curve. Of the 14 clear chromium curve peak maxima, 12 are associated with nickel curve minima.

The variation in the iron x-ray intensity did not coincide with variations in Cr and Ni.

On the optical micrographs of the etched steel which had been made with the focal plane in differing positions to obtain the best contrast conditions, the area where a sudden change in contrast occurred were marked. These micrographs were then compared with the SEM micrographs to establish the position of various topographical features such as the ridges and valleys associated with banding.

There existed a definite coincidence between the valleys (removal of material during etching) on the metal surface and a higher than average chromium content, and a lower than average nickel content. This relation between the chromium and the valleys was especially pronounced for the deeper valleys.

5.4 Discussion

As the composition traces were made on a polished surface before the etching operation, the variations are due to compositional difference alone and not topographical effects

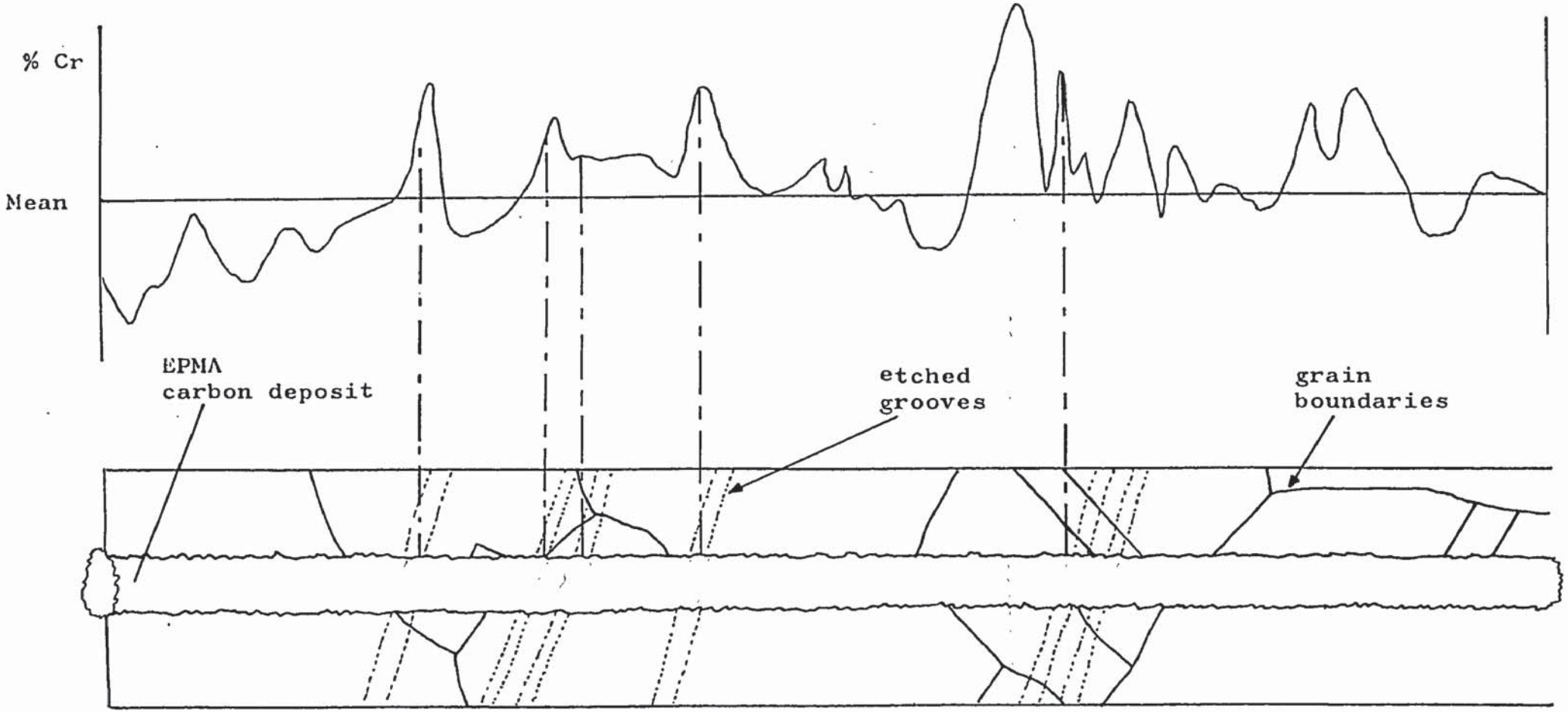

Fig. 20 Correlation between variation in bulk chromium content and the major grooves formed during electrolytic etching of 304L in 10% oxalic acid to reveal segregation banding.

of any kind.

The difference in composition between adjacent bands although marked, is quite small. The nickel content of the bands varied from approximately 10.6 to 12.6 per cent and the chromium content varied between 17.6 and 18.4 per cent indicating the nickel segregated to a greater extent than the chromium. These differences are insufficient to account for the significant variations in metal loss as a result of reduced resistance on its own.

As can be seen from the SEM photographs the banding consists of grooves where the metal has been removed at a greater rate than the surrounding material, rather than a series of ridges of more resistant metal.

In commercial alloys, banding will often arise as a result of the segregation that arises during the solidification of castings[107]. During subsequent heat treatment this segregation is not removed and processes such as hot rolling result in a banding structure.

The fact that the areas higher in chromium are removed during etching in preference to lower chromium regions is unexpected as higher chromium regions tend to show greater resistance to attack in strongly oxidising acids

It is most probably that there is a galvanic effect in action between the different regions.

Where pitting had occurred during etching it was found that these formed predominantly in the valleys of the etched surface. Many of these pits were quite large and were typical of the attack on an impurity inclusion. It is possible that segregation of unknown impurities may affect the segregation of nickel and chromium and may also reduce the corrosion resistance of these regions and affect the galvanic behaviour.

The pits and variable attack associated with the higher chromium regions may be due to either or both of two causes:-

(i) Foreign particles e.g. refractory material or slag which is insoluble and can get trapped in inter-dendritic regions during solidification.

(ii) Formation of a second phase such as delta ferrite which may be attacked directly [112]. An 18%Cr 8% Ni steel is border line with respect to fully austenitic structure and may contain a small amount of delta ferrite [110]. About 12% Nickel is necessary for a fully austenitic structure at solution temperatures of 1050°C. The nominal composition of the steel being investigated was 18.06% Cr, 11.8% Ni which should be sufficient to provide a full austenitic structure. However the variations of Cr and Ni indicated in the banded structure may be sufficient to allow delta ferrite to form in the high Cr, low Ni bands.

It has to be borne in mind that the banding investigated, although closely related, if not identical to nitric acid test banding was produced by impressed-current electrolytic etching in oxalic acid, and not by chemical attack in strongly oxidising nitric acid.

The oxalic acid etch accentuates the depth of banding, compared with exposure to boiling nitric acid. In steels exposed to boiling nitric acid the attack is most prominent where the acid has attacked and dissolved stringers, possibly of delta ferrite, lying within the bands of segregation.

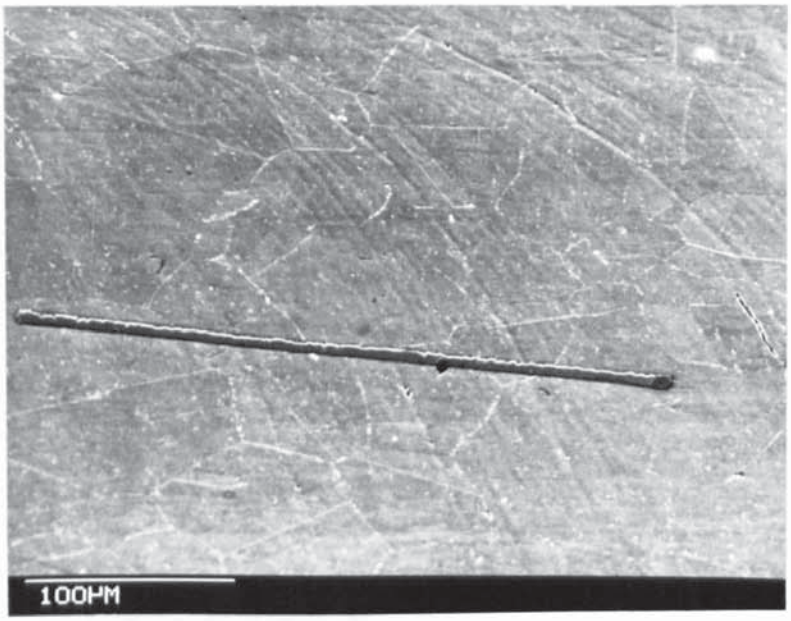

Plate 31 SEM photograph of the carbon deposit resulting from and electron probe analysis trace (2 passes). The surface has been etched electrolytically in oxalic acid for 10 seconds at 4V.

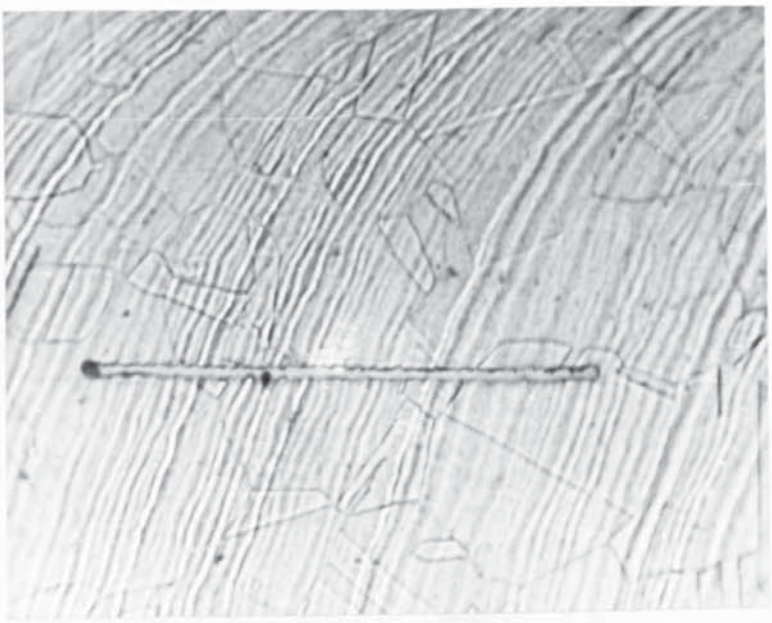

Plate 32 Optical micrograph of EPMA analysis trace on the surface of cast B in the as received condition. Grain boundaries and segregation banding revealed by a 10 second etch in oxalic acid (electrolytic).

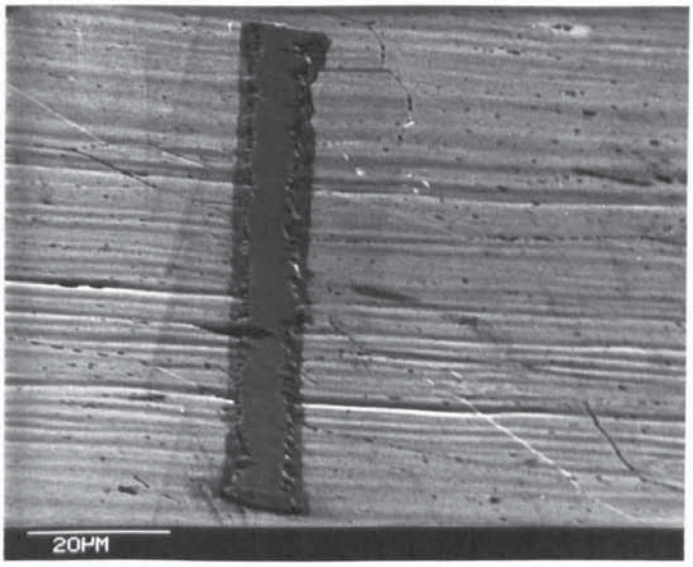

Plate 33 SEM micrograph of EPMA analysis trace on surface of cast B in the as received condition electrolytically etched in oxalic acid. A low angle of incidence between electrom beam and specimen was used to accentuate the relief of the segregation banding.

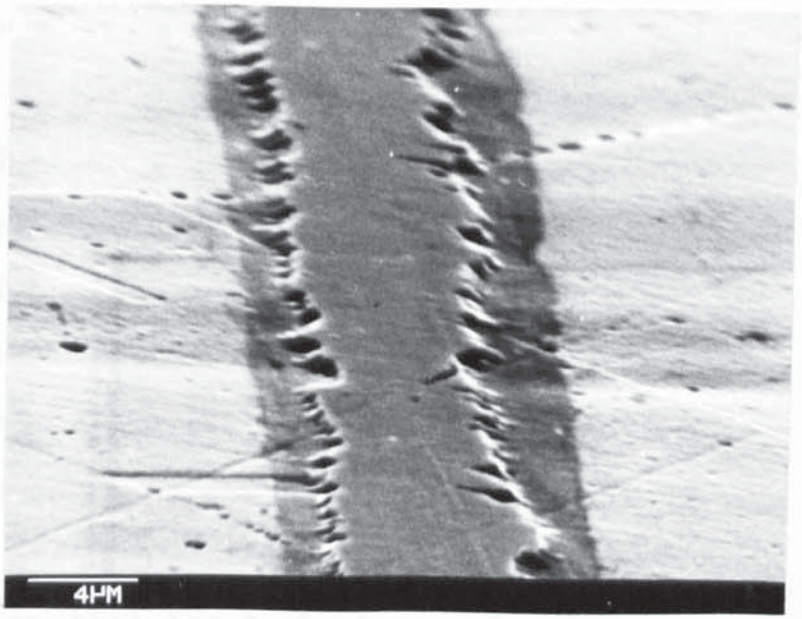

Plate 34 Detail of EPMA trace on etched surface. The etching process has resulted in the removal of some of the carbon deposit.

6. Solute Segregation

In polycrystalline metals containing solute impurity atoms, it is possible for the grain boundaries at act as sinks to which the solute atoms diffuse or segregate. The segregation can be either equilibrium (Gibbsian), where the process can be described thermodynamically by a redistribution of solute species in a way that minimises the total free energy of the system, or non-equilbrium due to preferential transformation, freezing and preferential diffusion, evaporation, dissolution or oxidation. It may also be caused by the preferential coupling between solute or solvent fluxes and point defect currents [61] such as those described by Williams et al [62] who showed that boron segregation in austenitic steels can be interpreted in terms of the migration of boron-vacancy complexes to grain boundaries.

Equilibrium segregation results from diffusion in the solid. McLean [63] considers that the driving force is the relief of lattice strain that occurs when a misfitting solute atom diffuses from the lattice to a grain boundary or free surface. The concentration effect due to equilibrium segregation probably is found only within a few atomic diameters of the boundary [64], in comparison with non-equilibrium segregation which can extend much greater distances [65].

Solute segregation has been observed and investigated in many metals although until recently most of the evidence has been indirect, such as hardening effects at grain boundaries of AISI 304 [21, 66], Ni [67], and Pb,Sn,Zb [68].

Other indirect observations have been made using diffusion, lattice parameter measurements, and background scattering of x-rays.

Solute segregation usually occurs without any change in the microstructure of the metal although mechanical properties such as fracture behaviour [69], and as we have seen electrochemical properties affecting corrosion [43], may alter.

Numerous researchers [16, 21, 39, 66, 70-76] have published work associating the intergranular corrosion of austenitic stainless steels with solute segregation when no microstructural constituent that could result in such behaviour was detectable. Fontana [77] states that the strain energy alone of grain boundaries free from impurities would not contribute to the reactivity of the boundary other than a small contribution that leads to grain boundary grooving. Solute segregation must therefore be considered with a high probability as having a large effect on intergranular corrosion.

The intensity of segregation is related to the solubility of the impurity elements in the matrix material with an impurity concentration at the grain boundaries of up to 10^4 greater than bulk concentration when the atomic solubility is low [78]. Coulomb et al [79] found that the grain boundary attack in iron varied from one type of boundary to another with least attack on coherent twin

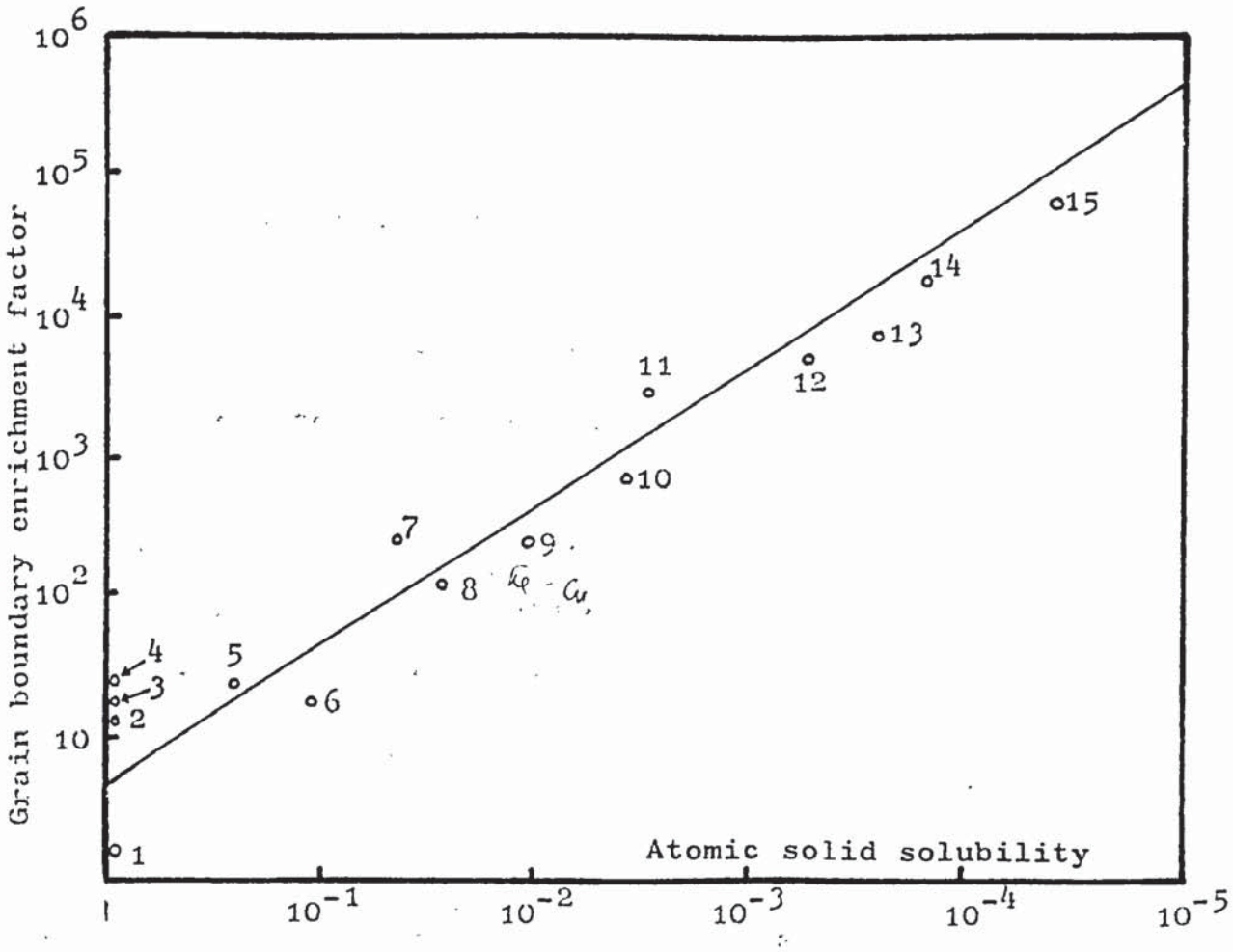

Fig. 21 Correlation of grain boundary enrichment factor with atomic solubility. 1. Fe-Ni-Cr 2. γFe-Ni 3. γFe-Mn 4. γFe-Cr 5. γFe-Si 6. δFe-Si 7. αFe-Sn 8. αFe-Sb 9. γFe-P 10. δFe-P 11. Fe-B 12. Ni-B 13. αFe-C 14. αFe-S 15. Cu-Bi (Ref. 48)

boundaries. When the pure iron was doped with sulphur the attack became more uniform. In general, boundaries with a higher degree of mismatch, and therefore a higher energy and larger strain field, should show a greater tendency to accommodate segregation than coherent or low angle boundaries with a small ($<15^{o}$) mismatch between adjacent grains.

Aust et al [68], while investigating solute induced hardening near grain boundaries, proposed a mechanism based on preferential solute-vacancy interactions, by which solute segregation to grain boundaries may occur. In certain pure metals, a soft region $\sim$ 30 μ wide was found adjacent to the grain boundary. This soft region arises due to the annihilation of defects such as vacancies by the grain boundary, which acts as a sink for these defects which would otherwise cause strengthening of the matrix. When the pure metals are doped with small amounts of solute it is found that some of the solute atoms result in excess hardening in the region of the grain boundaries. This was shown to be due to a positive binding energy between the solute atoms and vacancies. Thus during high temperature annealing, vacancies are generated and distributed evenly throughout the lattice. On cooling to lower temperatures the lattice becomes super-saturated with vacancies, some of which, when close enough to a grain boundary tend to migrate to that boundary where they are annihilated. Where there is a positive solute-vacancy binding energy, these migrating vacancies can transport the solute atoms through the lattice to the grain boundary where the vacancy is annihilated. This can result in a build-up of solute atoms at the grain boundary. The thermodynamic driving force for the diffusion of the solute atoms to the grain boundary is a decrease in lattice free energy associated with the annihilation of the vacancies. These researchers [68] consider that close to the boundary, interference will occur between adjacent solute-vacancy couples. This can

cause the release of one of the vacancies, with the result that a cluster of solute atoms begins to form. This cluster will be less mobile and consequently the size of the cluster of solute atoms can increase on interaction with other solute-vacancy couples.

Howard and Lidiard [80] indicated that the solute-vacancy interaction can result in two mechanisms of segregation:

(1) direct coupling where segregation occurs by vacancies dragging the solute atoms through the lattice; or
(2) contra-flow, in which vacancies move in one direction, and solute atoms in the opposite.

In direct coupling the solute atom(s) are bound to the vacancy with energy large compared with kT [81]. The excess of vacancies over the equilibrium concentration results in the diffusion of the vacancy-solute couples to the vacancy sinks in the grain boundary where the vacancies are annihilated. Steady state is reached when the solute atom flow resulting from vacancy drag is balanced by reverse solute flow due to the solute gradient produced.

Seah [82], in his work on grain boundary embrittlement, where he was considering equilibrium due to isothermal, or slow cooled, heat treatments, concluded that in most metal systems, most elements in solid solution segregate to grain boundaries and are located within one atom spacing of the boundary. He considered that at monolayer and submonolayer segregation levels in a multicomponent system, there will be no site competition between species, although at higher segregation levels there can be strong interactions,

In the determination of the segregation mechanism operating in a given alloy system, the effect of heat treatment on the corrosion rate can be used as an indirect method [81]. If equilibrium segregation is involved an increase in the annealing or quenching temperature should result in a decrease in segregation and intergranular corrosion. If non-equilibrium segregation were involved, an increase in the annealing temperature or an increase in cooling rate should result in increased segregation due to vacancy-solute interactions and increase corrosion.

Williams et al [62] in their autoradiographic studies of boron segregation in AISI type 316 suggested a similar mechanism to that proposed by Aust. The segregation increased with solution treatment temperature thus ruling out the binding of the boron atom to the grain boundary. If there was a binding energy E_s, then segregation varies as exp ($- E_s/kT$) in equilibrium giving the opposite trend with temperature. The segregation only occurred during a slow cool, and not during a quench and is therefore governed by diffusion kinetics on an atomic scale. As with Aust [68], the existence of solute-vacancy couples is proposed with an equilibrium between vacancies, couples and solute atoms existing at solution temperatures that alters on cooling, with the annihilation of vacancies at the grain boundary leading to build up of solute atoms at the boundary.

That solute segregation is associated with the intergranular corrosion of austenitic stainless steels is now

incontrovertible. However although several workers [43, 72] have produced direct evidence of such an association using Auger spectroscopy, there is very little indication as to why solute segregation should result in increased chemical attack at the grain boundaries. Evans [83] considers that when there are impurities in the form of solute atoms present at the grain boundary, it is possible for the region in the immediate vicinity of the grain boundary to differ from the centre of the grains in electrochemical behaviour. This difference is most notable where there is a small amount of impurity, just enough to saturate the accomodation sites in the grain boundary and leave the area of grain away from the boundaries relatively free from impurity. The boundary region could either become more or less noble than the grains around it. The most damaging situation is when the grain boundaries are anodic and the grains cathodic in a given electrolyte. There would then be an anodic current, caused by the difference in potential between the grains and the boundary, concentrated on the boundary region, resulting in the metal atoms passing into solution at the boundaries.

The effects of a passivating film on the surface of the metal may be important in the intergranular attack. If a passivating film forms on the surface of a metal in an electrolyte, the nature of the film formed over the grain boundary regions may be less perfect due to both the different substrate structure and the altered chemical composition of the segregated grain boundary region.

Braun et al [84] found that in aluminium, grain boundary diffusion could increase the impurity content of the oxide film. Vermilyea and Tedmon [85] suggested that the electrical conductivity of an oxide can be altered in the region of grain boundaries by any impurities that had segregated to these regions, resulting in increased corrosion locally. Once attack on the grain boundary region had started, it would progress rapidly due to the high local current density.

Any increase in solute atom concentration at the grain boundaries will necessarily result in a decrease in the concentration of the constituent atoms of the parent alloy. The preferential displacement of either nickel or chromium from the grain boundary region will alter its chemical nature and this could be sufficient to induce preferential corrosion.

Numerous techniques have been devised to try and establish the existence of solute segregation in austenitic stainless steels. Westbrook [86] and Inman and Tipler [65] have covered very adequately most of the earlier methods, which included mechanical and chemical sampling with wet analysis, selective etching of boundaries, use of radioactive tracers chemically and autoradiographically, chemical printing, electron microprobe analysis, x-ray lattice parameter measurements, and many others. None of these methods gave entirely satisfactory results in showing a segregated region. The main problem is that the segregation often exists only over a very small region and the resolution of the various methods has been insufficient to detect the very low concentrations of segregants that may exist.

In recent years several methods have been introduced which hold promise for the future. These are Auger electron spectroscopy, scanning transmission electron microscopy and electron energy loss spectroscopy.

Auger electron spectroscopy is very useful for analysing the composition of metal surfaces. The surface to be analysed is irradiated with an electron beam approximately 0.5 μm in diameter, the energy of the electrons being in the 2000-3000 eV range. Electrons are reflected, scattered and ejected from the metal surface in a wide range of energies. When excited electrons fall from a higher energy level to a lower energy level the energy differential may be made up by either the production of x-rays or the emission of an Auger electron. These electrons are emitted from a

surface layer 10-100 Å thick [87] and will have characteristic energies for a given material. By comparison of the energy of emitted Auger electrons, with a table of electron binding energies for different elements, it is possible to identify the elements present. The number density of the Auger electrons is proportional to the atomic concentration of the element at the surface. Normally the derivative of the Auger electron number density is plotted against energy and the peak to peak height is proportional to the atomic fraction. A normalised procedure based on empirical results from pure standards is required to arrive at an elemental composition. The main advantage of Auger spectroscopy is that it will only analyse a very thin surface layer, as the Auger electrons resulting from deeper in the specimen will be absorbed.

However the Auger method does have certain drawbacks. To obtain a good clean surface of a grain boundary for analysis, it is necessary to fracture the specimen in ultra high vacuum (UHV) in such a way that intergranular failure along the grain boundary occurs. This is relatively easy for specimens showing a ductile-brittle transition with temperature or where there is enough segregation material at the grain to produce inherent brittleness. Austenitic stainless steels do not transform from ductile fracture to brittle fracture at low temperature and even at temperatures of $< -150^{\circ}C$ their fracture behaviour is ductile. Joshi and Stein [43] and Abe and Ogawa [75] have obtained intergranular fractures of AISI type 304 stainless steel suitable for Auger spectroscopy. This has only been done with

severely sensitized steels [88] such as 600°C for 24 hour (Abe), or three days @ 580°C (Joshi). No such fracture or analysis has been achieved of non-sensitized or low carbon (304L) steels.

The other recently developed method of investigation that shows much promise for the analysis of solute segregation is scanning transmission electron microscopy (STEM) combined with an energy dispersive x-ray spectrometer.

6.1 X-ray analysis using STEM

This is one of the most useful methods of in situ analysis of electron microscopy specimens. The theory behind this method is very similar to that used in electron-probe microanalysis (EPMA), and the two methods are discussed and compared in detail in appendix 4.

STEM has a better resolution and can provide a clearer image of the area of interest than EPMA [89], which uses a bulk specimen, instead of the very thin specimen used in STEM. If a specimen is thin enough for conventional TEM work it will be thin enough for STEM.[90-93] STEM microanalysis utilises the characteristic x-rays produced by the interaction of specimen and electron beam to determine the elements present. A method of peak to peak ratios has been devised [94, 95] to determine elemental concentration from x-ray intensities. Although this method can be quite accurate, problems have arisen in practice from the production of unwanted x-rays [96-98] and difficulty in optimising spatial resolution [99-101].

6.2 Analysis of grain boundary regions using STEM in two casts of 304L

To try and determine if any particular solute segregate atom species was responsible for the increased intergranular corrosion observed in the two casts of AISI 304L several specimens were examined using STEM microanalysis. The specimens chosen for examination were those that had shown a high corrosion rate in the nitric acid test.

The specimens used were identical to the TEM specimens and the same preparation procedure was used (see Appendix). The microscopes used were a Jeol 100B and a Phillips 400* both with ancillary STEM attachments. With the Jeol a Kevex Si solid state detector was used in combination with Kevex 6000 subsystem electronics. The Philips microscope was used with an Edax Si solid state x-ray analysis system.

The first work was done on the Jeol and a new specimen rod was made to use in conjunction with a low background carbon specimen holder supplied by Jeol. The specimen could only be tilted about one axis, that of the specimen rod. This was also true of the Philips which utilised a beryllium low background holder supplied by the makers.

* Facility provided by Birmingham University

6.2.1 Effect of Angle

Using an AISI 316 specimen it was found that at low angles (< 20^{o} between beam axis and normal to specimen) the count rate or number of electrons reaching the detector dropped off dramatically, as the specimen was shielded by the holder. The count rate of x-rays was found to be a maximum between 35^{o} and 45^{o}. The most frequently encountered spurious x-ray lines were the Cu peaks, being present on all the spectra obtained during the tests. The ratio of peak counts Cu K_{α} to Fe K_{α} was a minimum in this region.

6.2.2 Effect of X-ray Detector Distance from Specimen

Keeping all other parameters constant, increasing the distance from detector to specimen resulted in decrease in count rate and an increase in the Cu K_{α}/Fe K_{α} ratio as fewer specimen originated x-rays and more spurious copper x-rays reached the detector. The detector was kept as close as possible for all tests.

6.2.3 Silver Plated Specimen Holder

Several trials with a silver plated specimen rod combined with a smaller low-background carbon insert to hold the specimen resulted in much lower Cu K_{α}/Fe K_{α} ratio with a 316 specimen. The hole count (no specimen) only had small FeK and CuK peaks arising from the interior of the specimen chamber. However this specimen holder was found to partially shield the specimen from the detector resulting in low count rates.

For analyses of grain boundary regions two spectra were recorded, one using a narrow electron beam on the feature of interest, the other a wide-beam spectrum from the centre of the grain away from the grain boundaries. For spectra comparisons either the integrated peak count of the Fe K_α peak was kept the same (usually 5000 or 10000 counts) or the count live-time was kept constant (e g 300 seconds) Dead time was kept in the region 20 - 30% on the Jeol. The smallest spot size was used for microanalysis. This resulted in a beam diameter of 0.025 μ.

6.3 Specimens examined using STEM microanalysis

The specimens examined were the two AISI 304L steels in the as-received condition, and after various heat treatments as shown in table [9] .

Table 9

Specimens examined using STEM with X-ray analysis

Specimen	Cast	Condition	Nitric acid corrosion
As received	A	Work softened	low
As received	B	"	very high
1	A	soltuion treated WQ	low
3	A	" " AC	moderate
13	B	sensitized 100 min 650°C	moderate
E3	B	sensitized 700 h 650°C	high

The analyses performed were qualitative or in some cases semi-quantitative, as lack of time and available machinery precluded full quantitative analysis. As previously discussed other workers have proposed P, Si, S and B as elements which may affect intergranular corrosion in nitric acid. Boron is of too low an atomic number to be detected by X-ray analysis and was excluded, but the other three elements were the main consideration when the spectra were examined. For each heat treatment, several different specimens were prepared, sometimes as many as fifteen, the exact number depending on the success during electropolishing which varied considerably. The area of the specimens used for analysis were under 250 nm thick, measured using the contamination spot method. Where intensity ratios were calculated, they were first background-corrected by removal of the part of the spectrum due to Bremstrahlung radiation.

6.4 Results

6.4.1 As received steels

In both steels A, B, there was little difference between the spectra obtained from a grain boundary region, and the spectra obtained from the grain centre. There were no detectable phosphorus or sulphur peaks, and although silicon was detected it was present in equal quantities. There were no unexpected peaks found in any of the grain boundary spectra.

6.4.2 Cast A Solution treated 1050°C Water quench

No difference was observed between grain boundary and centre grain spectra, and no unusual peaks were found in the spectra.

6.4.3 Cast A Solution treated 1050°C Air Cooled

This treatment resulted in a wider variation of spectra during analysis. There were slight differences in several characteristics peaks of lower intensity, while the peaks of the major elements Fe K_α, Cr K_α, Ni K_α remained at a similar ratio whether obtained from a grain or a grain boundary. On several specimens these differences were slight and could be attributed to variations in background noise and Bremstrahlung radiation. Two specimens showed a distinct difference in phosphorus level between grain and grain boundary. This can be seen from the x-ray count rates in counts per second for individual characterisitc x-ray peaks. The three readings were taken consecutively, the STEM beam ($\sim$ 100 Å diam) being moved from a grain boundary

triple point to the centre of the grain, then back to a region of the grain boundary away from the triple point. The x-ray count rates for the relevant peaks were:-

Table 10

X-ray peak	Energy KeV	x-ray counts/sec. grain	grain boundary	triple point
Si Kα	1.74	11.6	11.1	10.8 ± 0.1
P Kα	2.01	1.40	7.60	8.00 ± 0.05
S Kα	2.3	3.00	3.20	3.20 ± 0.05
Cr Kα	5.41	450	530	475 ± 5
Fe Kα	6.40	1145	1145	1465 ± 5
Ni Kα	7.47	230	230	225 ± 5
Peak ratios (Kα peaks)				
Cr/Fe		0.32	0.33	0.36 ± 0.02
Si/Fe		.007	.008	.007 ± .001
P /Fe		.0009	.0052	.0055 ± .0005
S /Fe		.0021	.0022	.0022 ± .0005

Similar results were found at all points analysed on this specimen, the grain boundaries showing higher phosphorus levels than the grains.

6.4.4 Cast B Sensitized 100 min @ 650°C

This specimen showed no significant difference between the spectra from grain and grain boundary regions.

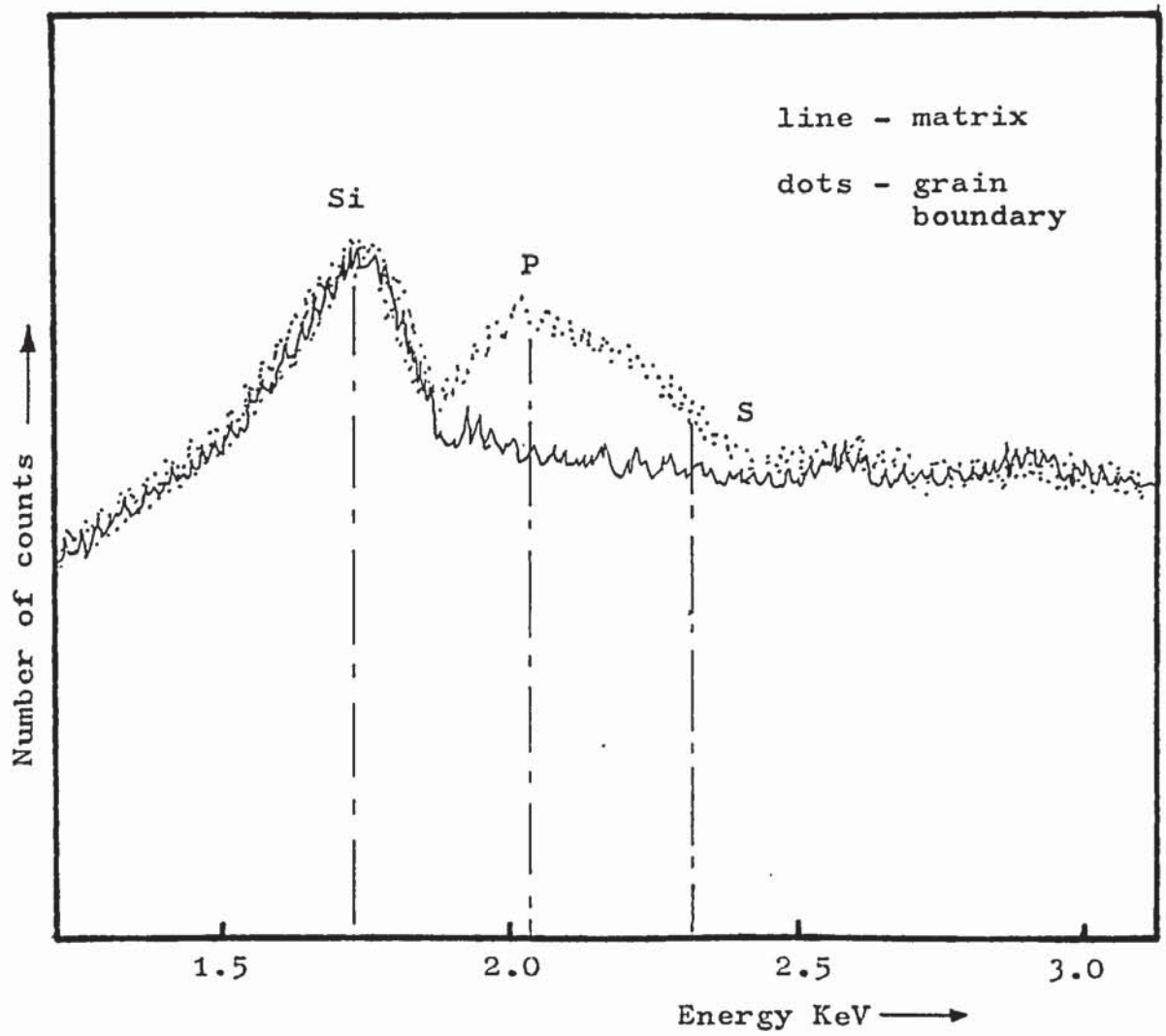

Fig. 22

Partial energy dispersive x-ray spectrum for air cooled specimen of cast A obtained by STEM.

Count live time - 221 sec.

Nominal beam diam. - 100 Å

Accelerating voltage - 100 KV

X-ray count rate - 3200 cps approx.

Channel width - 10 eV per channel

Counts full-scale - 1500

The graph shows a spectrum produced from a grain boundary region superimposed on one obtained from a matrix region in the centre of a grain. They show identical silicon and sulphur levels but the grain boundary spectrum has a distinct phosphorus peak not observed in the matrix spectrum.

6.4.5. Cast B sensitized 600 h 650°C

Of the analysis performed on these specimens two resulted in similar spectra from grain-broundaries and grain centres. One specimen resulted in a variation similar to that found in some of the solution treated air-cooled specimens, with a slightly higher number of phosphorus x-ray counts originating from the grain boundary region. Although there was a distinct difference observed between the two spectra, there was no pronouced phosphorus peak and the KeV energy band where the difference was found was slightly wider than expected. There did not appear to be any other distinct difference between the two spectra. The Cl peak is most probably due to the polishing solution used which contained perchloric acid (see appendix

6.5 Discussion

Although the different heat treatments on casts A and B resulted in widely varying corrosion rates, qualitative analysis of the steels using STEM with energy dispersive x-ray microanalysis did not show the irrefutable existence of solute segregation. Some evidence of higher phosphorus levels was found in the grain boundaries of two of the specimens that showed high corrosion rates but no such evidence was found in the as-received specimen of cast B which had the highest intergranular corrosion rate of all. The phosphorus enrichment was not found in all the samples of the two specimens which showed such attack. This may be due to the fact that only a small quantity of phosphorus is present at the boundaries. The most distinct difference

in x-ray spectra between grain and grain-boundary analyses was found when the grain boundary analysis was performed at a triple point. At such a point the atom spacing and lattice mismatch is greater and there would be more sites suitable for phosphorus atoms than would be found in an planar boundary.

Phosphorus was detected at some of the grain boundaries of a solution treated and air cooled specimen, and after sensitization for 600 hours at 650°C, but not in a solution treated and water quenched specimen or in one sensitized at 650°C for 100 min. This may be due to the effect temperature has on the diffusion and segregation of phosphorus, Devine et al [69] examining 316L using Auger spectroscopy, found negligible phosphorus segregation after ageing for 40 hours at 600°C, compared with considerable segregation at 675°C, and 700°C which showed the greatest segregation. The air cooled specimen would have passed through the range 1000 to 600°C in under a minute, but the diffusion and segregation would have been greater at the higher temperatures. Short sensitizing times at 650° may not result in phosphorus segregation while longer times at this temperature allow the level in the grain boundaries to rise above the minimum detection level.

The lack of any indicated grain boundary segregation of phosphorus in the as received material of cast B was unexpected, as it had a high intergranular corrosion rate. The mechanism operating may involve another species or combination of species, or the level of phosphorus at the grain

boundaries examined was below the detection limit. The number of specimens analysed was small and a more satisfactory conclusion could be reached from a larger number of analyses.

There will always be a problem when the concentration of the segregating species at the grain boundary is low. Very long counts are needed to give a good peak to background ratio and when the peaks are small, masking by other peaks can cause problems. The other main problem is that of resolution as the segregated species may only be a monolayer thick resulting in a large part of the signal coming from non-significant regions.

Phosphorus segregation could not be tied definitely to intergranular corrosion in these two steels. Although phosphorus was detected at the grain boundaries of some of the specimens that had a high corrosion rate, none was detected in the as-received material of cast B which had the highest rate of intergranular attack.

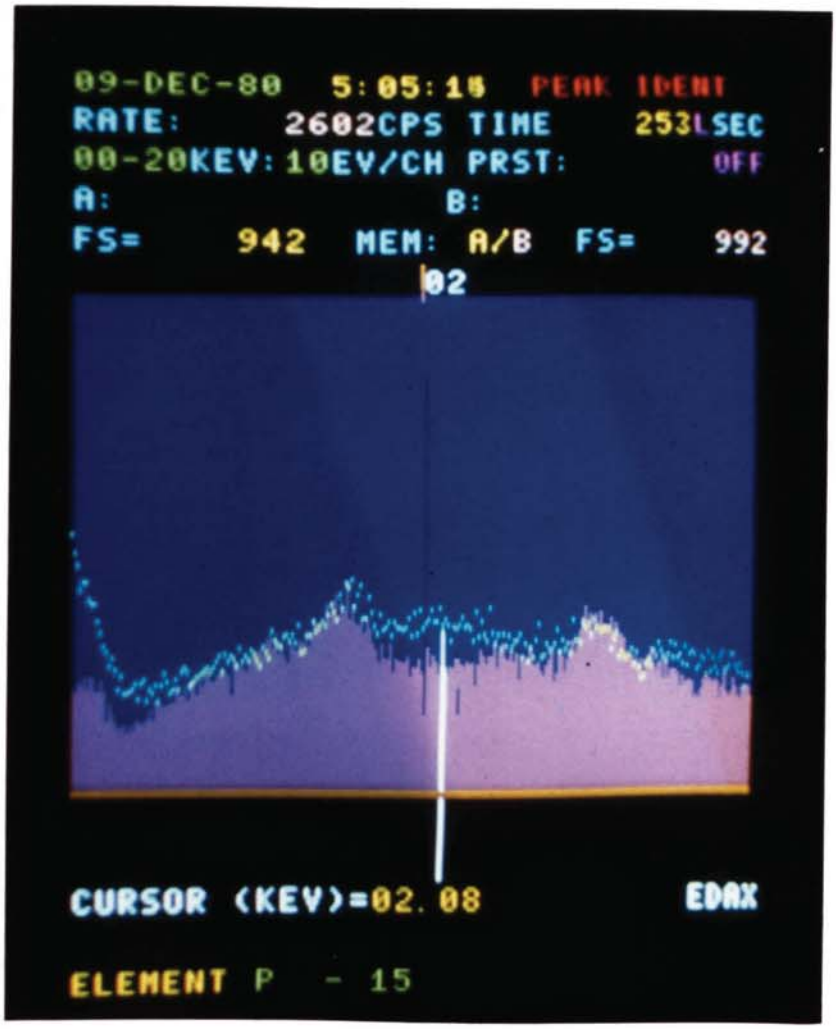

Partial STEM/EDAX energy dispersive x-ray spectra for cast A, solution treated 600 h @ 650^{o}C

White spots - grain boundary spot count

Pink bars - matrix area count

Graph covers range 0 - 4 KeV. Dark vertical line indicates position of phosphorus peak. In this case it is inconclusive as to whether phosphorus is present at the grain boundary.

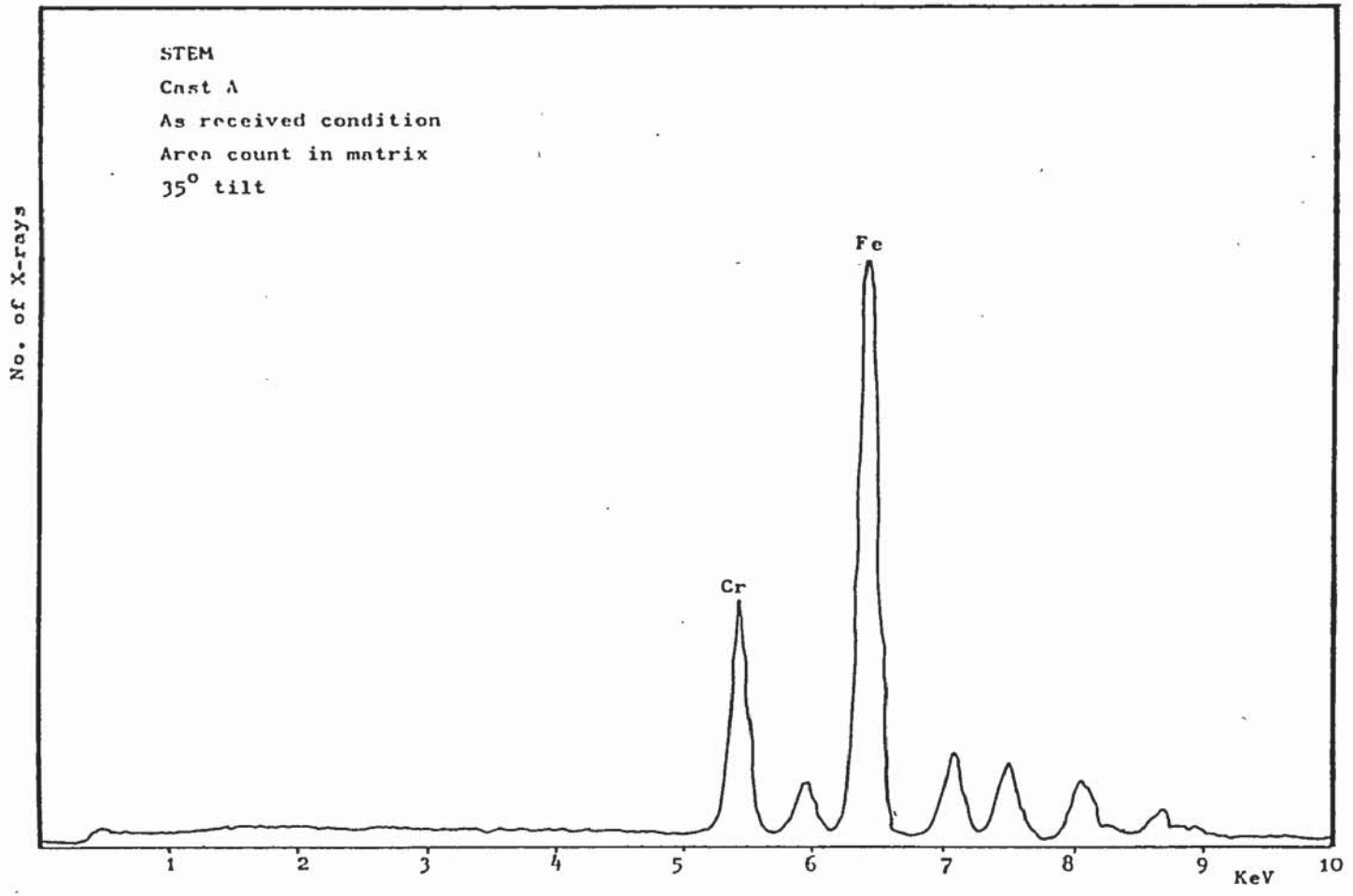

Fig.23 Energy dispersive x-ray spectrum, typical of AISI 304L matrix. A spurious Cu peak exists (8.1 KeV) due to use of a brass specimen rod.

7. Performance of 304L steels doped with Phosphorus and Boron in the nitric acid test

A link between phosphorus segregation and intergranular attack in nitric acid has been indicated in 304L in this work. This confirms the findings of the researchers working on austenitic steels mentioned earlier in this work. Other workers [12,23,24, 104,105] have shown that boron may affect the corrosion behaviour of stainless steel in acids deleteriously.

The effect of small additions of these elements to 304L type steel on its corrosion rate in the nitric acid test was studied to try and ascertain the manner in which these elements acted.

7.1 Materials

Two experimental casts of austenitic steel were used*, one cast having four different levels of boron additions the other set having four different levels of phosphorus The compositions of the steels were:

Cast	Cr	Ni	C	Si	Mn	Mo	B	P	Fe
803A	18.0	12.0	.011	.21	1.61	.09	.001	N/D	Bal.
803B	18.1	12.0	.010	.20	1.60	.09	.003	"	"
803C	17.9	11.9	.006	.21	1.58	.09	.0055	"	"
803D	17.9	12.0	.007	.21	1.57	.09	.0085	"	"

*Made and supplied by British Steel Corporation

Cast	Cr	Ni	C	Si	Mn	Mo	B	P	Fe
976A	17.2	9.2	.018	.12	1.47	.08	.001	.006	Bal.
976B	17.2	9.19	.019	.12	1.47	.08	.001	.014	"
976C	17.0	9.1	.020	.17	1.45	.08	.001	.021	"
976D	16.9	9.15	.018	.14	1.42	.08	.001	.028	"

The steels were produced from a Renko* Iron base melted in a HF furnace with the Ni. The melt was deoxidised with Si and low Carbon ferro-chrome was added with Mn metal. Phosphorus was added to 976 in the form of Fe/25%P and the 50 Kg cast was then split into 4 x 12.5 Kg casts with more phosphorus being added after each split. Cast 803 was treated similarly except that boron in the form of Fe/15%B was added instead of phosphorus. The casts were melted in a magnesite crucible and were top poured into ingots. These were then rolled to slab, surface dressed with a grinder, hot rölled to ½" thick, reheated to 1200°C and rolled to the finished size, (6mm x 150 mm)

* High purity, low residual iron.

7.2 Experimental

Prior to being subjected to the nitric acid test the steels were given a range of heat treatments designed to show differing cooling rates from the solution treatment temperature of 1050°C. The treatments were:

1.	S.T. 1050°C	30 min	Cooled in vermiculite
2.	"		Air cooled
3.	"		Forced air cooled
4.	"		Water quenced

The heat treatment* was performed in a furnace with an $N_2/H_2/CO$ (40/40/20) atmosphere. The vermiculite cooled specimen was transferred from the furnace to a box half-full of vermiculite and then covered with a thick layer of vermiculite and allowed to cool. The forced air cooled specimen was cooled on a thin gauge wide mesh grid, above a large fan giving a vertically upwards flowing stream of air at ambient temperature. Using a dummy specimen with a $\frac{1}{4}$" hole drilled out of the centre contained a Pt/Rh thermocouple, the cooling rate in each treatment was measured.

Time min	Vermiculite (V)	°C Air (A)	Forced Air (F)
0	1050	1050	1050
$\frac{1}{2}$	884	830	750
1	830	680	560
2	762	510	335
3	715	405	240
4	670	335	150
5	645	295	90
6	615	255	
7	590	225	
10	528		
15	452		
20	398		

Table 11 Cooling rates of 304L

*Facilities were provided by
BSC, Sheffield Laboratories, Rotherham

Over the first minute the average cooling rates ^{o}C/sec were:

Vermiculite Cooled	(V)	-	3.7
Air	(A)	-	6.2
Forced Air	(F)	-	8.2
Water Quench	(W)	-	Approximately 50 between 1050^{o}C and ambient temperature

During heat treatment, the specimens were painted with a proprietary compound to reduce oxidation. Oxidation was minimal, and after treatment the specimens were ground on wet SiC papers to a 180 mesh grit finish in preparation for the nitric acid test. The test used was the standard ASTM test, designated A-262-79, Practice C discussed earlier in this work. For most treatments two separate tests were performed, a third test sometimes being used where there was a wide disparity in the first two results. During testing care was taken to limit possible sources of contamination that could alter the test results.

After completion of the test, all specimens were examined by SEM to determine the nature and extent of the surface attack on the steel.

An optical metallographic examination was also made of the steels in the work softened condition and after the heat treatments. For this examination the steels were ground on SiC papers and polished to a 1μ finish using diamond paste. They were then given a light anodic etch

in 10% oxalic acid at ambient temperature for 30 secs. at 4v. The current density was 0.25 A/cm^2. This was found to reveal the metallographic structure better than the chemical etches investigated.

One specimen each of cast 976 and cast 803 was investigated using TEM/STEM in conjunction with energy dispersive x-ray analysis. These methods were used to search for evidence of grain boundary segregation and precipitation, arising as a result of the phosphorus and boron addition.

7.3 Results

There was found to be considerable variation in the nitric acid test results. These differences were even found between specimens that had been given the same heat treatment as well as between specimens given different treatments. The degree of general grain dropping over the whole surface, and the degree of localised attack were both assessed as being slight, moderate or heavy.

The localised attack on many specimens manifested itself as heavy grain dropping, occurring in narrow band-like regions that ran parallel to the rolling direction. It was possible for considerable grain dropping to occur in these regions of localised attack, while little or no grain dropping occurred elsewhere.

7.3.1 Nitric Acid Test corrosion rates and extent of intergranular attack

The results are displayed in tabular form to show the connection between corrosion rate and grain dropping and localised attack due to inclusions/inhomogeneity. The results are then displayed graphically to show the relation between corrosion rate and level of additive.

All specimens were held at 1050°C for 30 minutes prior to cooling.

Cast 976

1. Forced Air Cooled

Average cooling rate between 1050°C and 850°C = 12°C/sec.

	% P	Grain Dropping	Localised Attack	Corr.Rate mg/cm^2/48h	average
A(i)	.006	moderate	moderate	4.4	3.3 ± 1
(ii)		v.slight	v.slight	2.1	
B(i)	.014	slight	slight	1.6	1.4 ± 0.2
(ii)		v.slight	v.slight	1.2	
C(i)	.021	slight	slight	1.6	1.5 ± 0.1
(ii)		slight	slight	1.5	
D(i)	.028	slight	slight	1.6	1.8 ± 0.3
(ii)		slight	slight	2.1	

2. Air Cooled

Average cooling rate between 1050°C and 850°C = 8°C/sec

	% P	Grain Dropping	Localised Attack	Corr. Rate mg/cm^2/48h	average
A(i)	.006	slight	moderate	8.3	6.6 ± 1.7
(ii)		moderate	heavy	8.0	
(iii)		moderate	moderate	5.0	
B(i)	.014	moderate	moderate	5.9	4.5 ± 3.5
(ii)		slight	moderate	1.1	
(iii)		moderate	moderate	6.6	
C(i)	.021	moderate	moderate	6.6	4.6 ± 3.3
(ii)		slight	moderate	1.3	
(iii)		moderate	moderate	5.5	

2. Air Cooled (continued)

	% P	Grain Dropping	Localised Attack	Corr. Rate mg/cm^2/48h	average
D(i)	.028	slight	none	2.9	2.2 ± 0.4
(ii)		slight	slight	1.8	
(iii)		slight	slight	2.1	

3. Vermiculite cooled

Average cooling rate between 1050°C and 850°C = 15°C/sec

	% P	Grain Dropping	Localised Attack	Corr. Rate mg/cm^2/48h	average
A(i)	.006	none	slight	5.4	3.5 ± 1.9
(ii)		slight	slight	1.7	
B(i)	.014	none	v.slight	1.8	1.6 ± 0.2
(ii)		none	none	1.5	
C(i)	.021	slight	slight	2.0	1.8 ± 0.2
(ii)		slight	slight	1.7	
D(i)	.028	slight	slight	3.1	3.3 ± 0.2
(ii)		slight	slight	3.5	

4. Water Quenched

Average cooling rate between 1050°C and ambient temperature = 50°C sec.

	P %	Grain Dropping	Localised Attack	Corr.Rate mg/cm^2/48h	average
A(i)	.006	slight	slight	1.7	1.9 ± 0.3
(ii)		slight	slight	2.2	
B(i)	.014	slight	slight	3.2	3.7 ± 0.6
(ii)		moderate	moderate	4.3	

4. Water Quenched (continued)

	P %	Grain Dropping	Localised Attack	Corr. Rate $mg/cm^2/48h$	average
C(i)	.021	slight	slight	1.9	2.5 ± 0.6
(ii)		moderate	moderate	3.1	
D(i)	.028	slight	slight	3.0	2.7 ± 0.4
(ii)		slight	slight	2.3	

5. Effect of Solution Temperature

All specimens cooled in vermiculite

	Solution Temp ^oC	% P	Corr. Rate $mg/cm^2/48h$	average
A	900	.006	7.4	7.6 ± 0.2
			7.8	
	1050	.006	5.4	3.5 ± 1.8
			1.7	
	1100	.006	1.1	2.9 ± 0.9
			3.8	
D	900	.028	3.1	3.1
	1050	.028	3.1	3.3 ± 0.2
			3.4	
	1100	.028	1.7	5.3 ± 3.6
			8.9	

Cast 803

1. Forced Air Cooled

Average cooling rate between 1050°C and 850°C = 12°C/sec

	% B	Grain Dropping	Localised Attack	Corr. Rate mg/cm^2/48h	average
A(i)	.001	moderate	moderate	3.9	5.3 ± 1.4
(ii)		heavy	heavy	6.6	
B(i)	.003	slight	moderate	1.8	2.8 ± 1.0
(ii)		moderate	slight	3.9	
C(i)	.0055	slight	slight	4.6	4.8 ± 0.2
(ii)		moderate	slight	5.0	
D(i)	.0085	slight	slight	4.5	3.6 ± 0.9
(ii)		slight	slight	2.7	

2. Air Cooled

Average cooling rate 1050°C to 850°C = 7.8°C/sec

	% B	Grain Dropping	Localised Attack	Corr. Rate mg/cm^2/48h	average
A(i)	.001	heavy	heavy	6.1	6.1
(ii)		heavy	heavy	6.1	
B(i)	.003	heavy	heavy	14.6	12.8 ± 1.8
(ii)		heavy	heavy	11.1	
C(i)	.0055	slight	slight	2.7	6.5 ± 3.8
(ii)		v.heavy	v.heavy	10.2	
D(i)	.0085	none	slight	1.3	6.4 ± 6.6
(ii)		moderate	moderate	4.9	
(iii)		heavy	heavy	13.0	

3. Vermiculite Cooled

Average cooling rate between 1050°C and 850°C = 5°C/sec

	% B	Grain Dropping	Localised Attack	Corr. Rate mg/cm^2/48h	average
A(i)	.001	moderate	heavy	8.1	4.7 ± 3.4
(ii)		none	slight	1.4	
B(i)	.003	slight	slight	2.2	5.3 ± 3.1
(ii)		moderate	heavy	8.4	
C(i)	.0055	moderate	heavy	2.4	3.8 ± 1.5
(ii)		slight	slight	5.3	
D(i)	.0085	heavy	heavy	2.35	2.2 ± 0.3
(ii)		slight	slight	2.35	
(iii)		slight	slight	1.94	

4. Water Quenched

	% B	Grain Dropping	Localised Attack	Corr. Rate mg/cm^2/48h	average
A(i)	.001	slight	moderate	3.5	2.8 ± 0.7
(ii)		slight	slight	2.2	
B(i)	.003	slight	slight	3.3	2.8 ± 0.5
(ii)		slight	slight	2.3	
C(i)	.0055	moderate	v.heavy	13.9	8.5 ± 4.5
(ii)		slight	moderate	3.0	
D(i)	.0085	slight	slight	1.8	2.9 ± 1.1
(ii)		moderate	moderate	3.9	

5. Effect of Solution Treatment Temperature

	Solution Temp ^{o}C	% B	Corr. Rate $mg/cm^2/48h$	average
803A	900	.001	12.0	6.5 ± 5.6
			0.9	
	1050	.001	8.1	6.1 ± 2.0
			4.1	
	1100	.001	1.5	1.9 ± 0.4
			2.3	
803D	900	.0085	12.7	11.2 ± 1.6
			10.6	
	1050	.0085	2.3	2.1 ± 0.2
			1.9	
	1100	.0085	4.2	3.7 ± 0.6
			3.1	

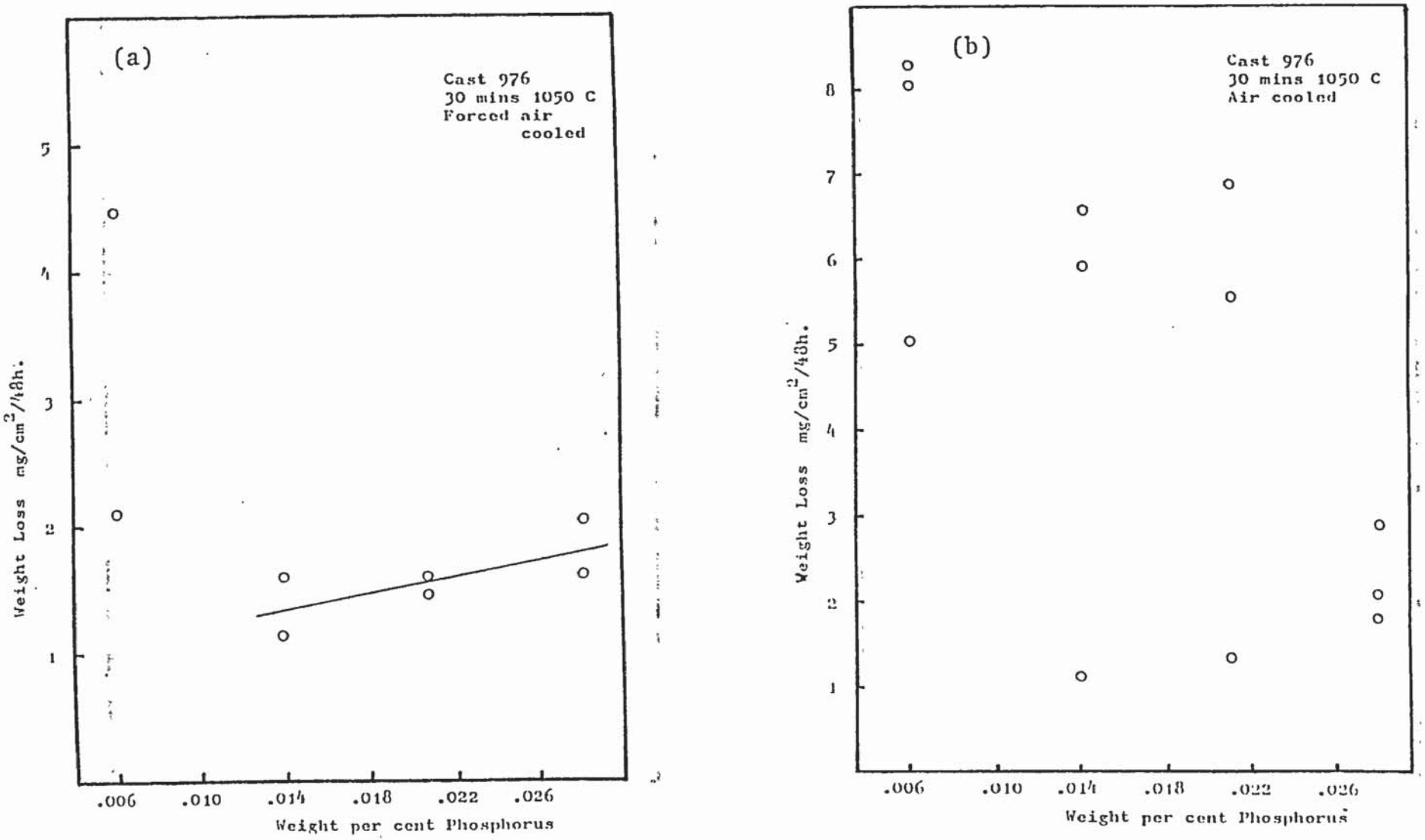

Fig 24 a,b Effect of Phosphorus Content on the Corrosion Rate of Cast 976 in the Boiling 65% Nitric Acid Test

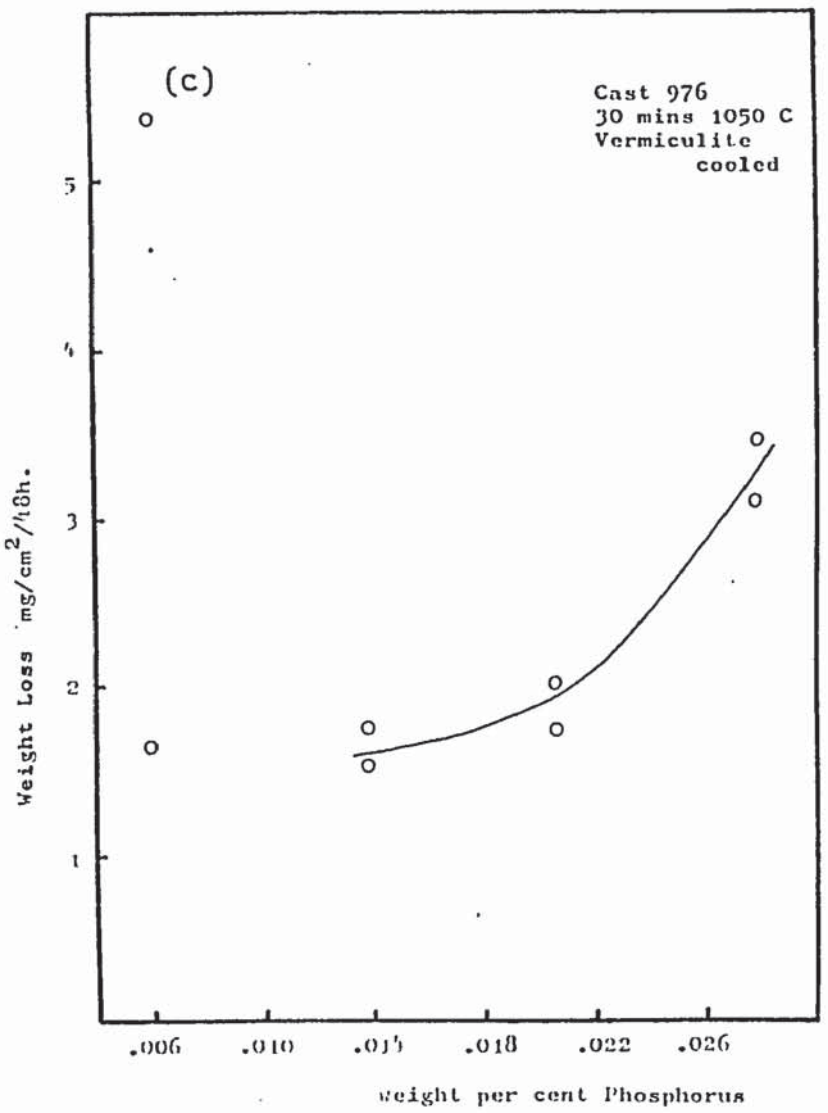

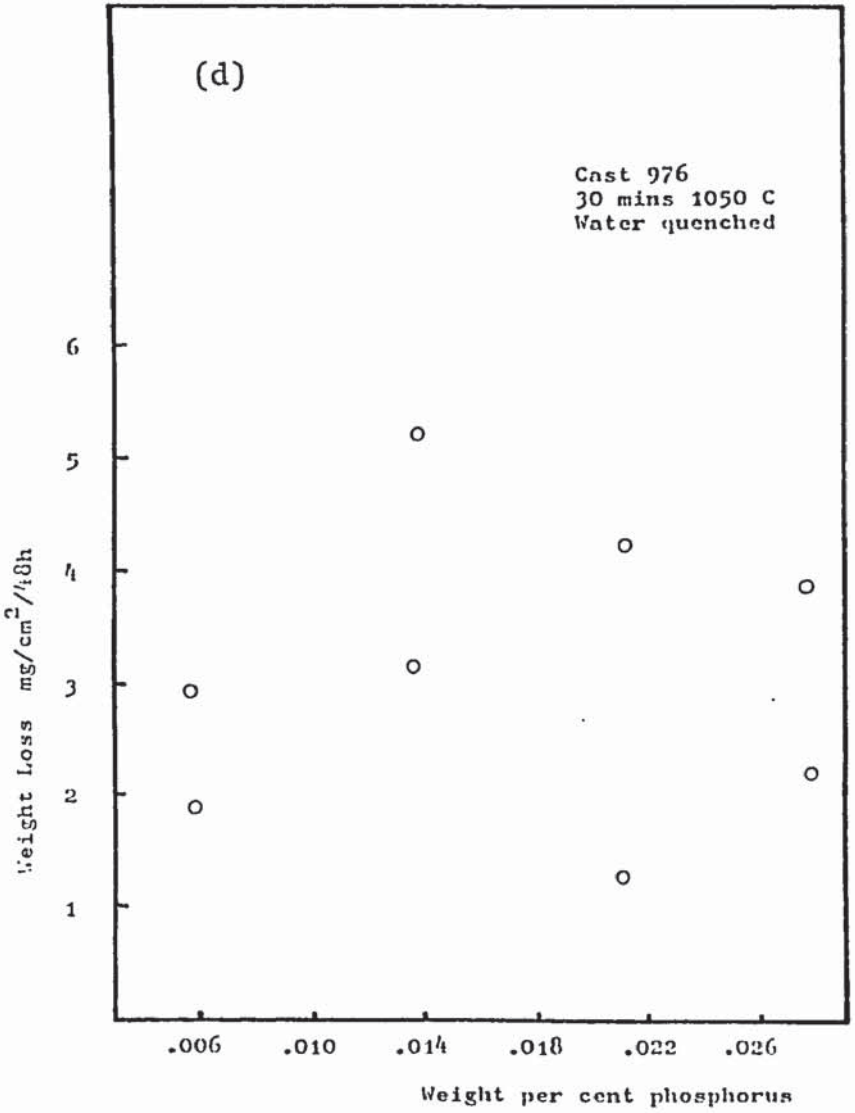

Fig 24 c,d Effect of Phosphorus on the Corrosion Rate of Cast 976 in the Boiling 65% Nitric Acid Test

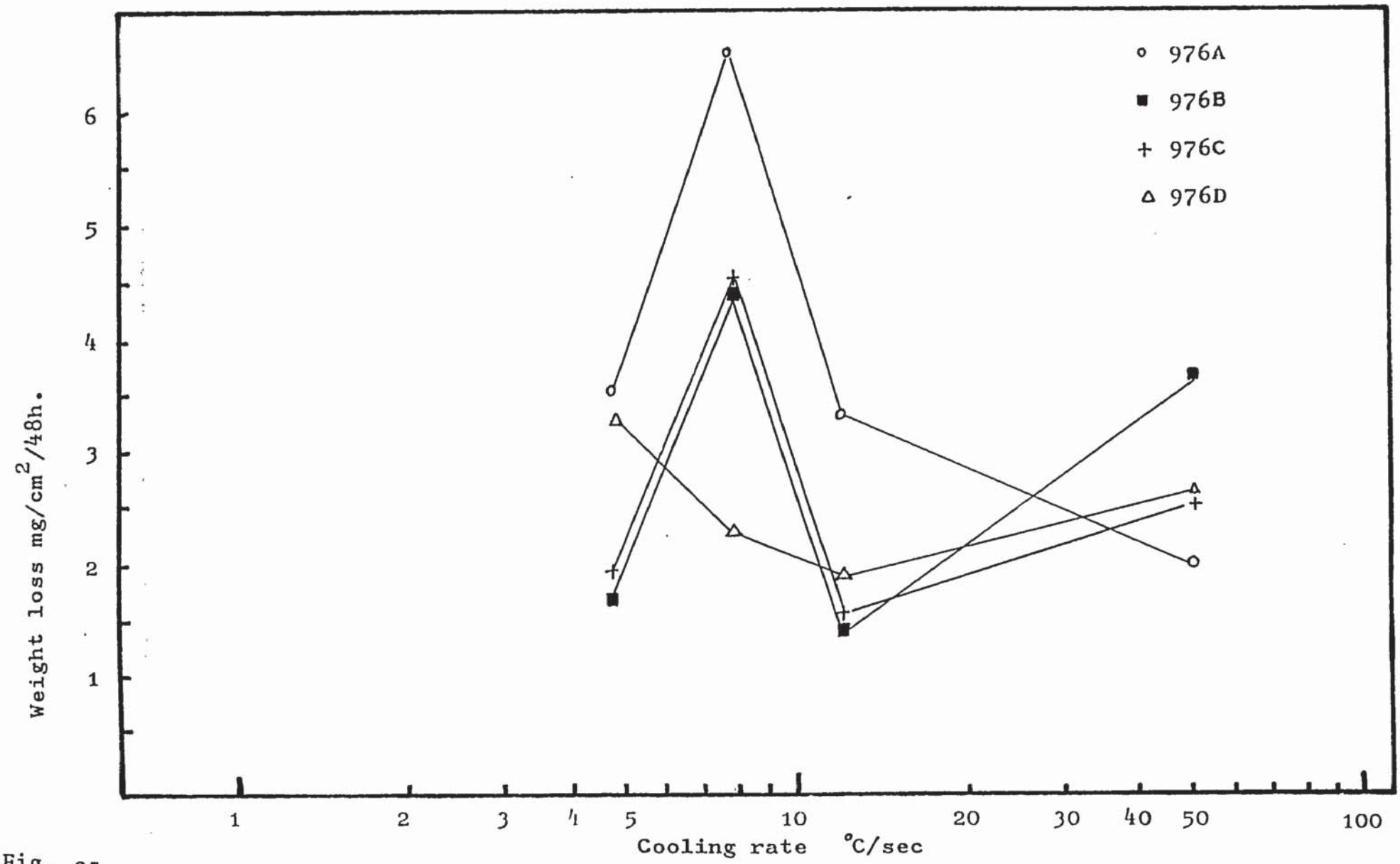

Fig. 25
Effect of cooling rate on the corrosion rate of Cast 976 in the Boiling 65% Nitric Acid Test

Effect of Different Solution Temperatures on the Corrosion Rate of Cast 976 in the Boiling 65% Nitric Acid Test

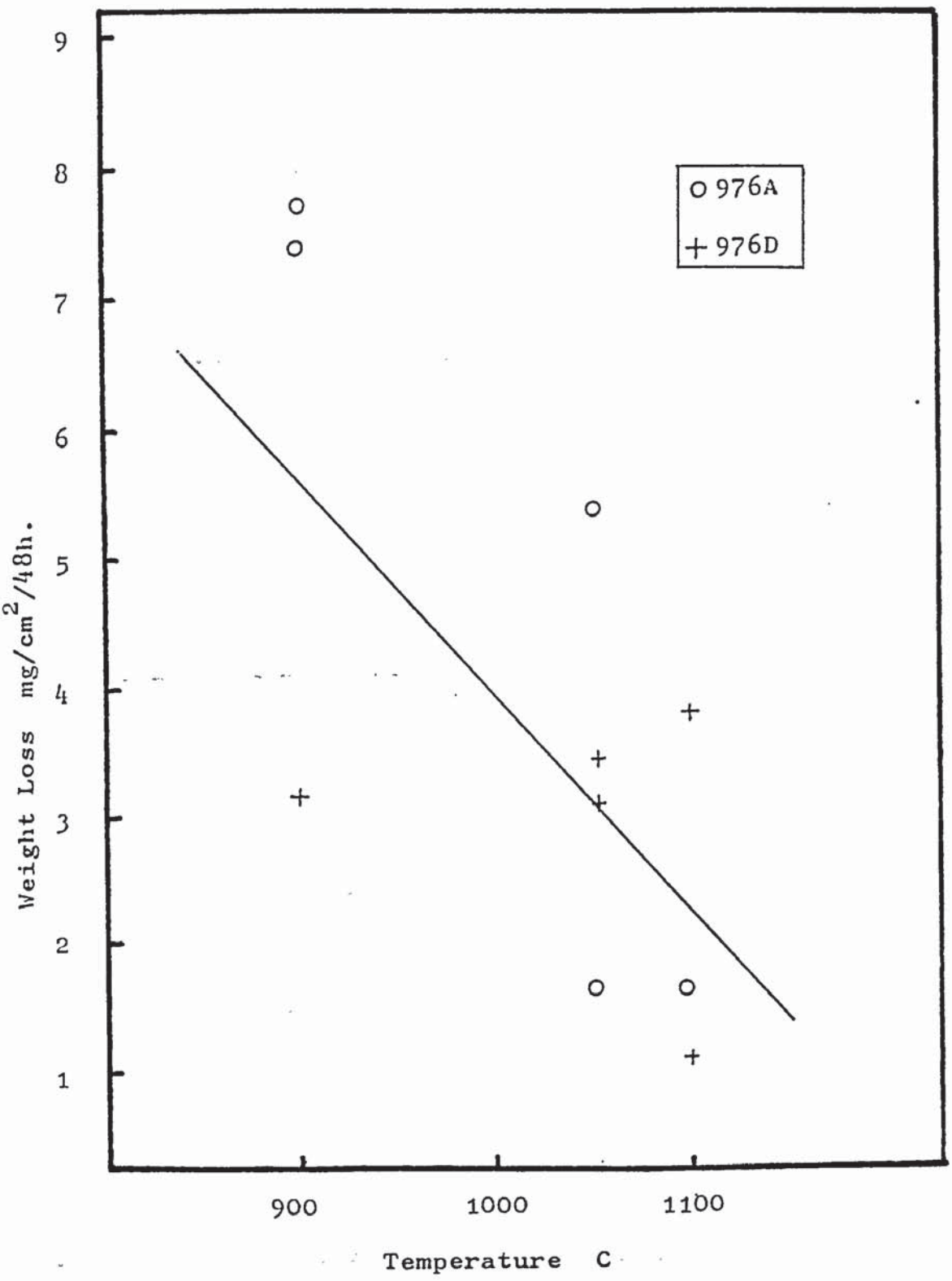

Fig. 26

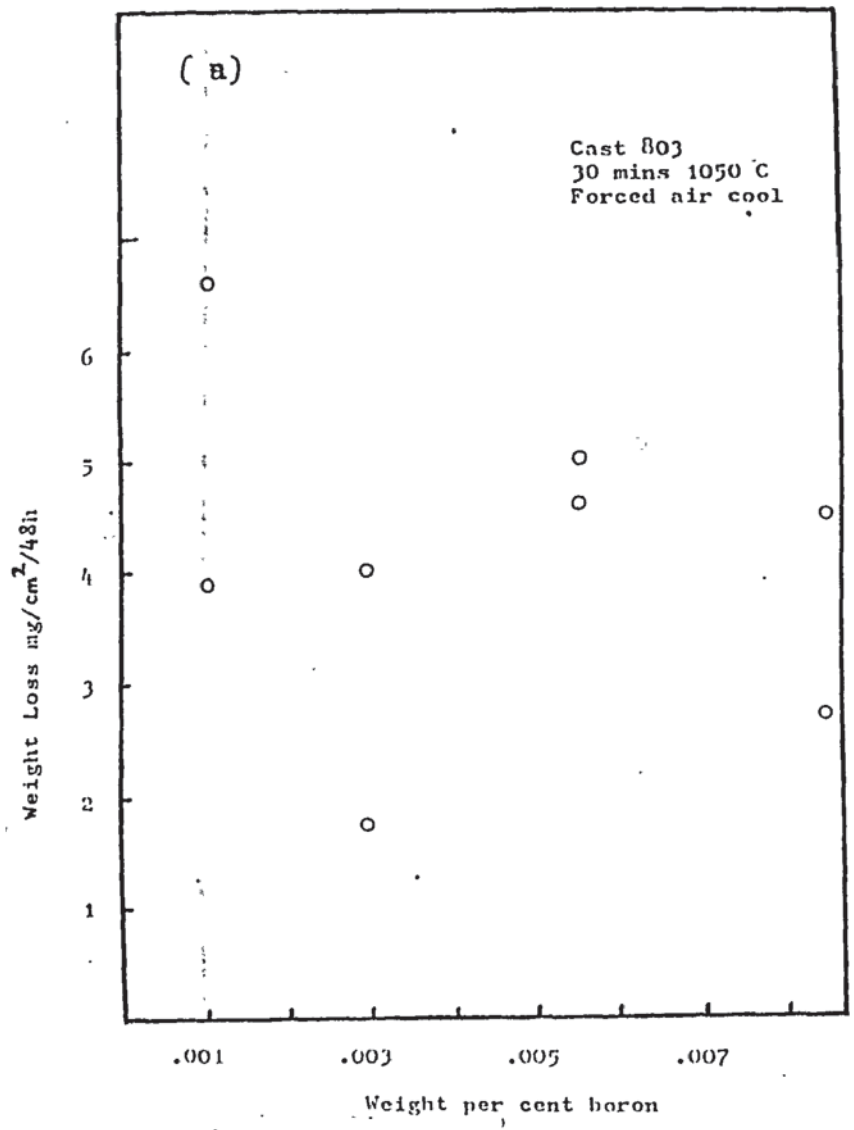

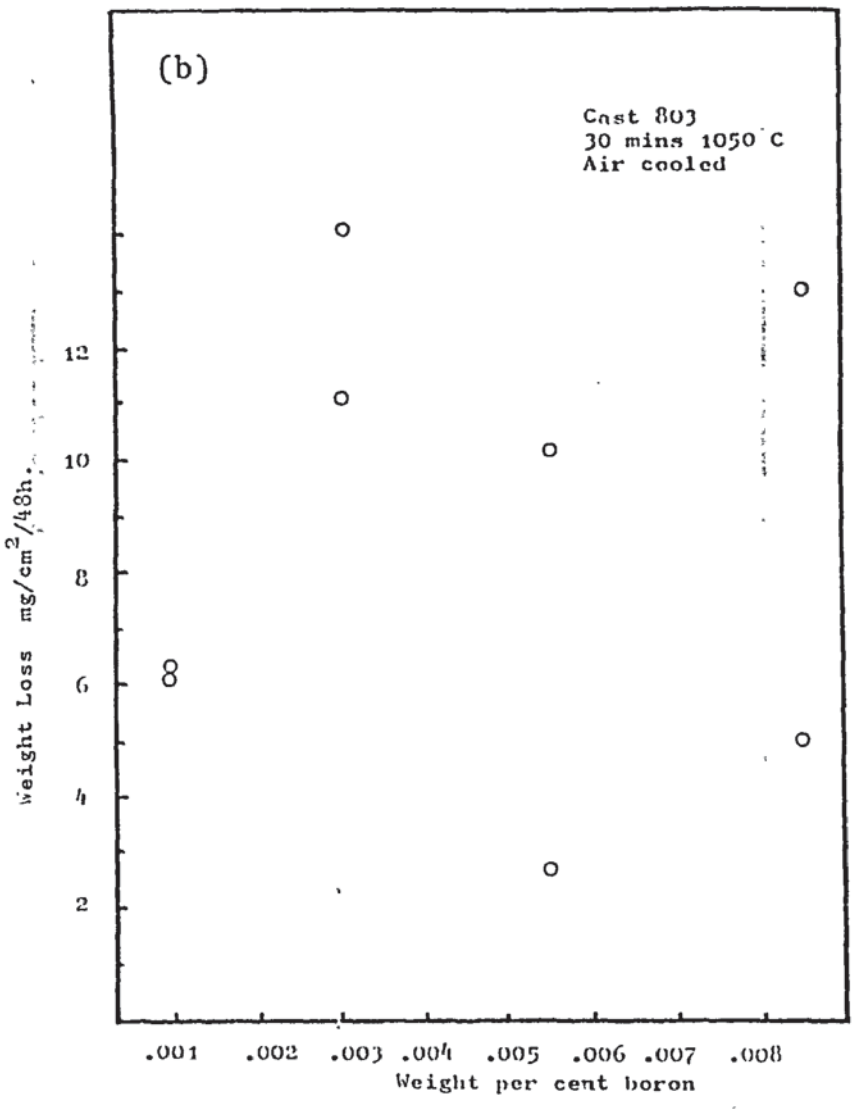

Fig. 27 a,b Effect of Boron Content on the Corrosion Rate of Cast 803 in the Boiling 65% Nitric Acid Test

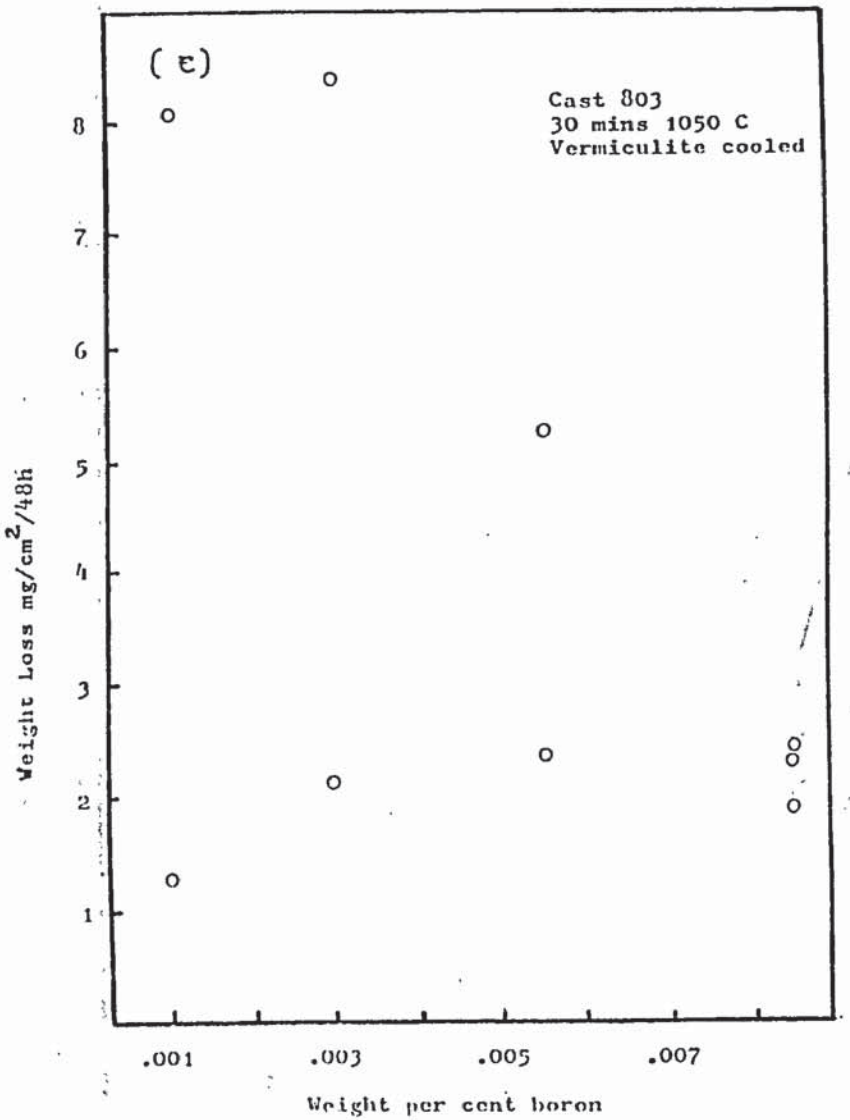

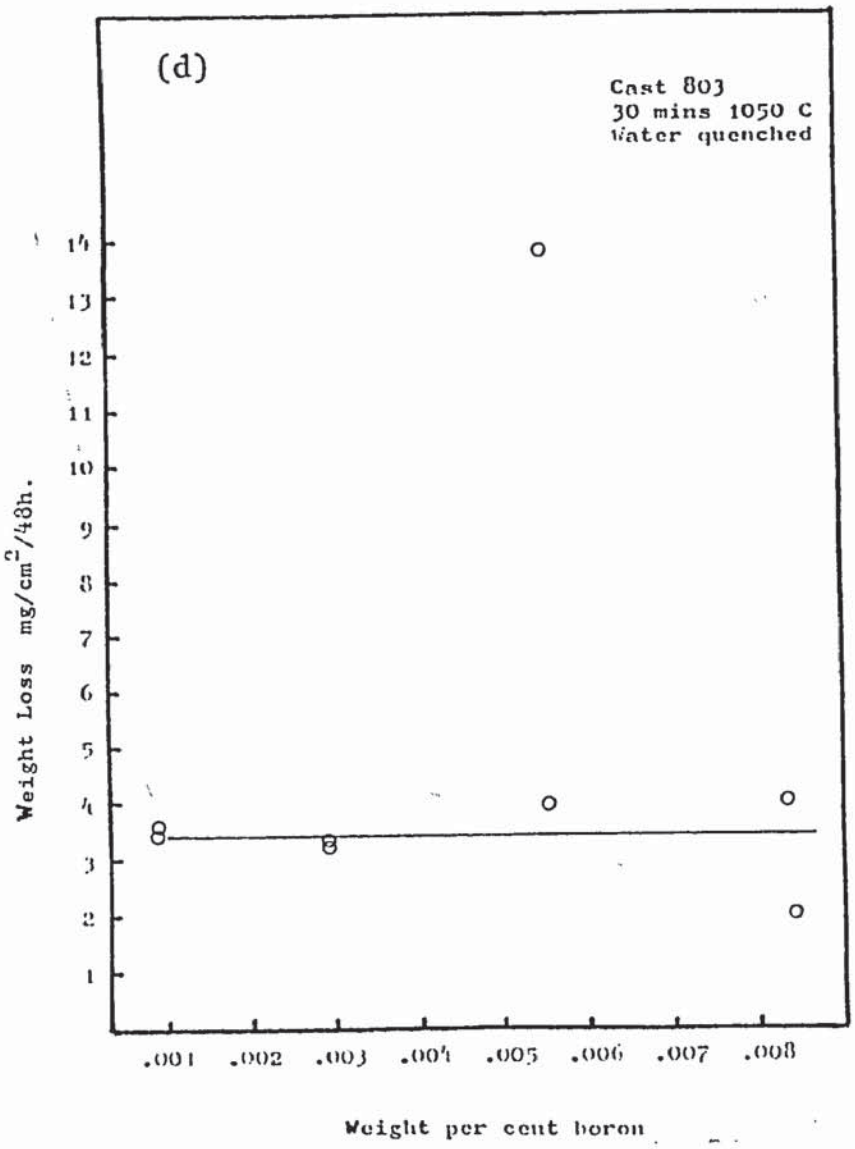

Fig. 27 c,d Effect of Boron on the Corrosion Rate of Cast 803 in the Boiling 65% Nitric Acid Test

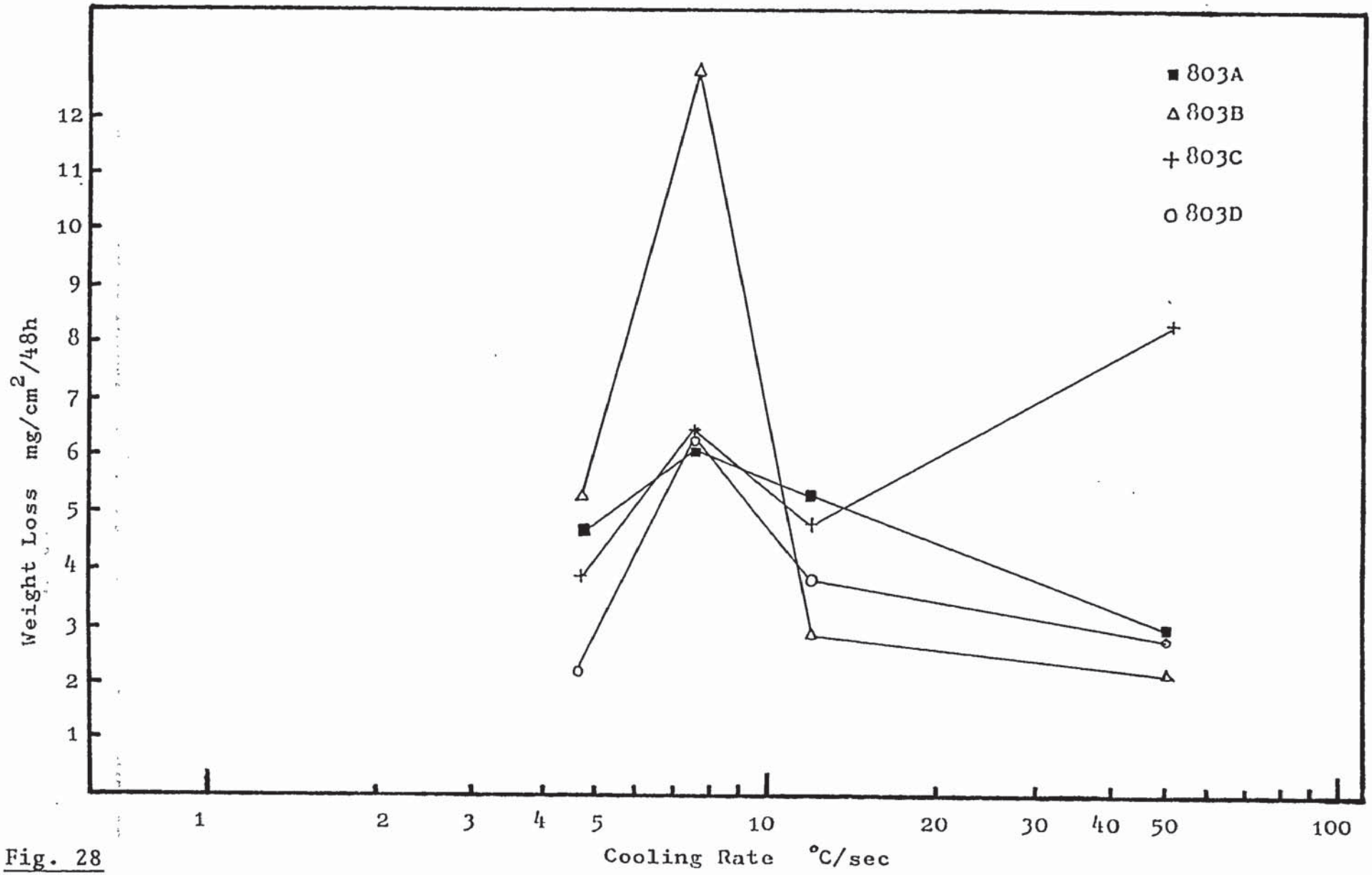

Fig. 28

Effect of Cooling Rate on the Corrosion Rate of Cast 803 in the Boiling 65% Nitric Acid Test

Effect of Different Solution Temperatures on the Corrosion Rate of Cast 803 in the Boiling 65% Nitric Acid Test

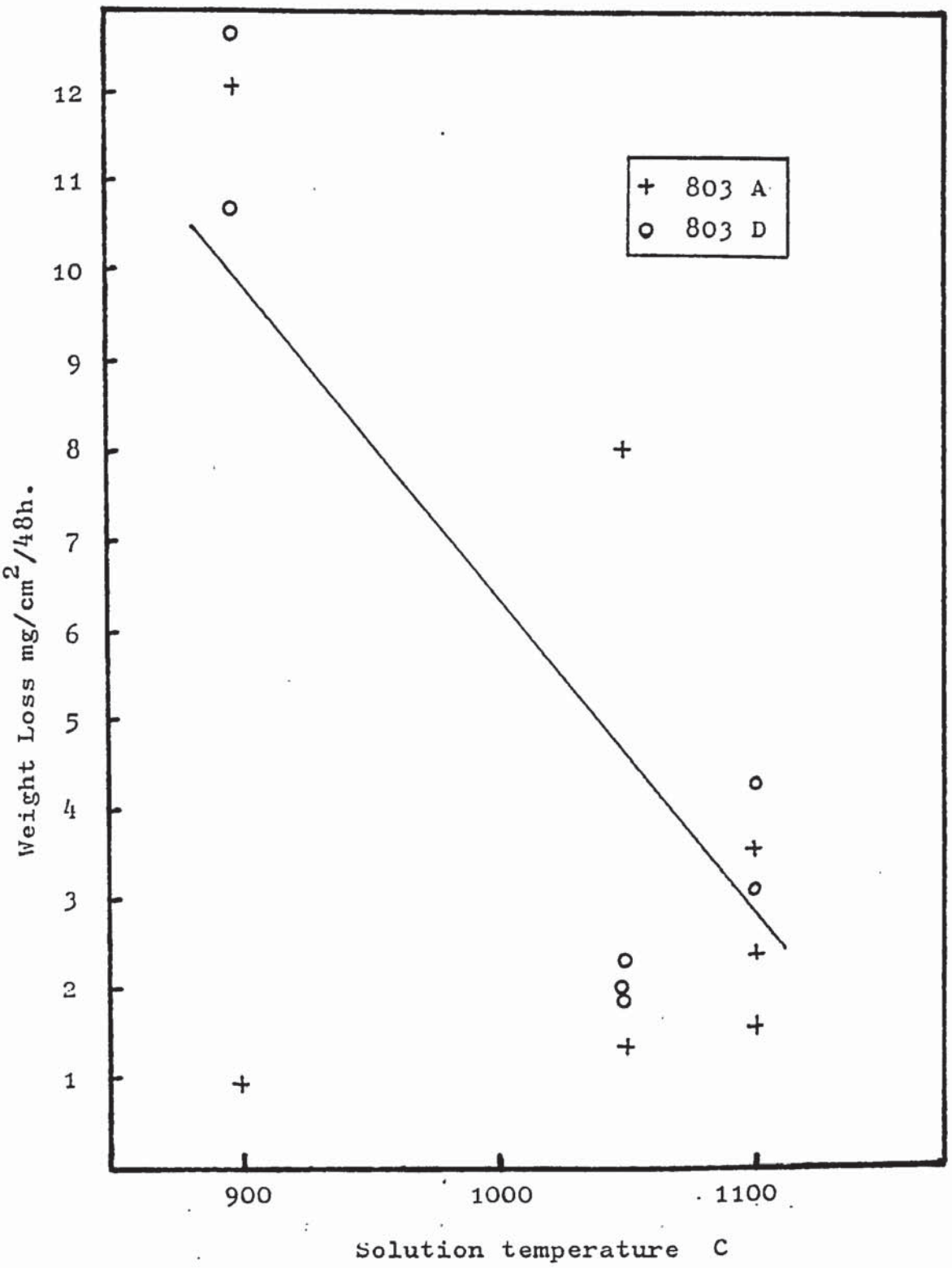

Fig. 29

7.4 Metallographic Examination of Casts 976 and 803

Optical examination of the steels in the work softened condition on a Reichart microscope after polishing, and an oxalic acid anodic etch, showed an equiaxed grain structure with a large number of annealing twins. There appeared to be only one phase, although dispersed through the steel were a number of inclusions that were often strung out in lines across several grains. Within the grains themselves were a large number of small round particles and inclusions. The distribution of the inclusions did not vary much across the specimens, and the directional inclusions always ran parallel to the rolling direction. There was also heavy banding across the the whole specimen in the same direction. It was noticeably heavier in some regions than others.

There appeared to be three types of inclusion morphology after the oxalic acid etch:

1. Clear grey, angular particles showing no attack
2. Particles showing dissolution at matrix/particle interface.
3. Pits showing no trace of a particle.

The individually dispersed particles showed a greater tendency to form pits than the directional inclusions, the pits were quite shallow and it was possible to focus on the bottom of the pits in most cases, with the optical microscope.

At a magnification of x400, this etch did not reveal any particles on the grain boundaries.

The metallographic structure of the steels after heat treatment did not differ to any great extent from that of the work softened condition. The same inclusions were evident after all the treatments. There was no precipitation visible to any great extent at the grain boundaries, even in the specimens with the slowest cooling rate, cooled in vermiculite. This constrasts markedly with the two commercial casts of 304L, A and B, which, after being cooled in vermiculite, showed very distinct grain boundary precipitates after an identical etch in oxalic acid.

(Plates 37,38,39)

The grain sizes of the as-received material in the works softened condition was:

	ASTM x 100
976A	5½
976B	6
976C	6
976D	6

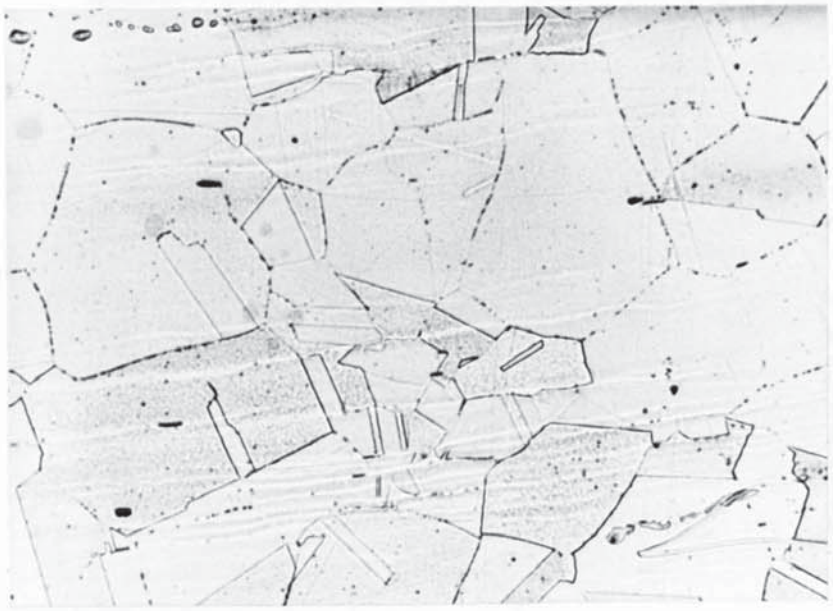

Plate 35 Cast 976, as received, works softened. Etched in 10% oxalic acid. Shows banding, inclusions and pitting on grain boundaries. x400

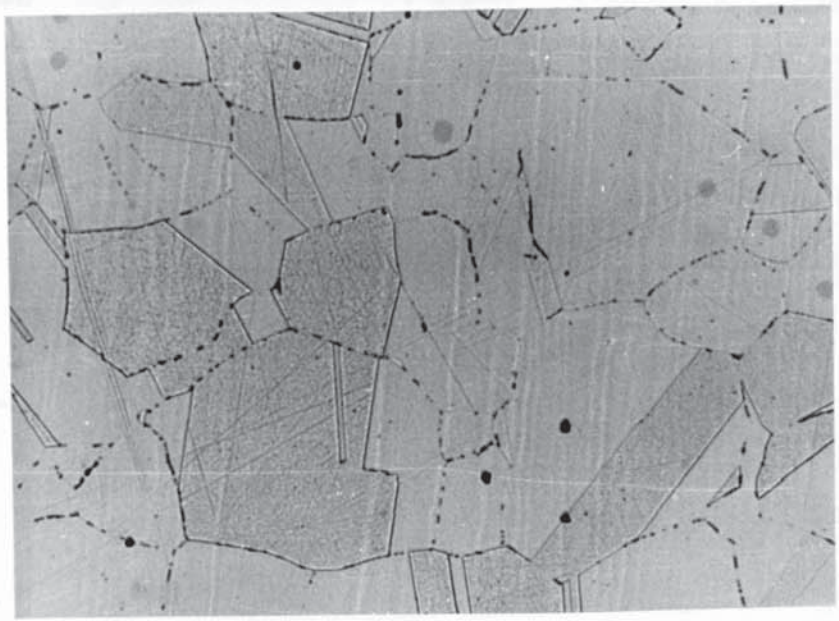

Plate 36 Cast 803, as received, works softened. Etched in 10% oxalic acid. x400

(37)

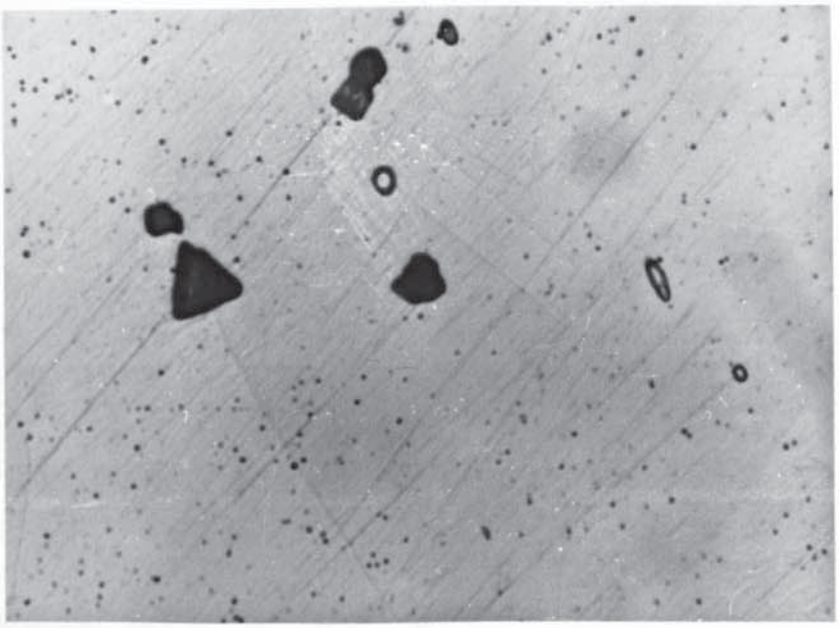

(38)

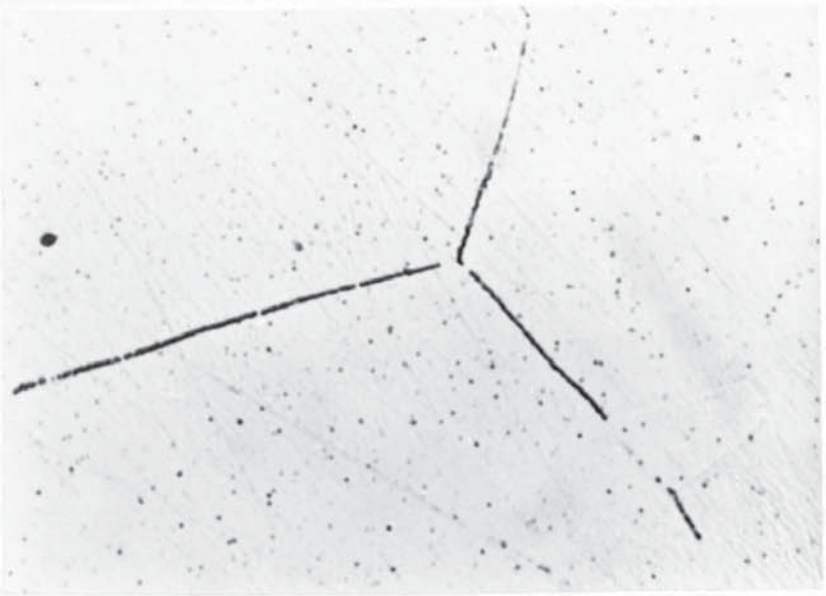

Plates 37, 38 Experimental cast 976D (37) shows no grain boundary precipitates, while commercial cast A(38) shows extensive precipitation. Both steels were solution treated for 30 mins at 1050°C, and cooled in vermiculite. Etched in 10% oxalic acid for 10 secs. at 4V.

X1125

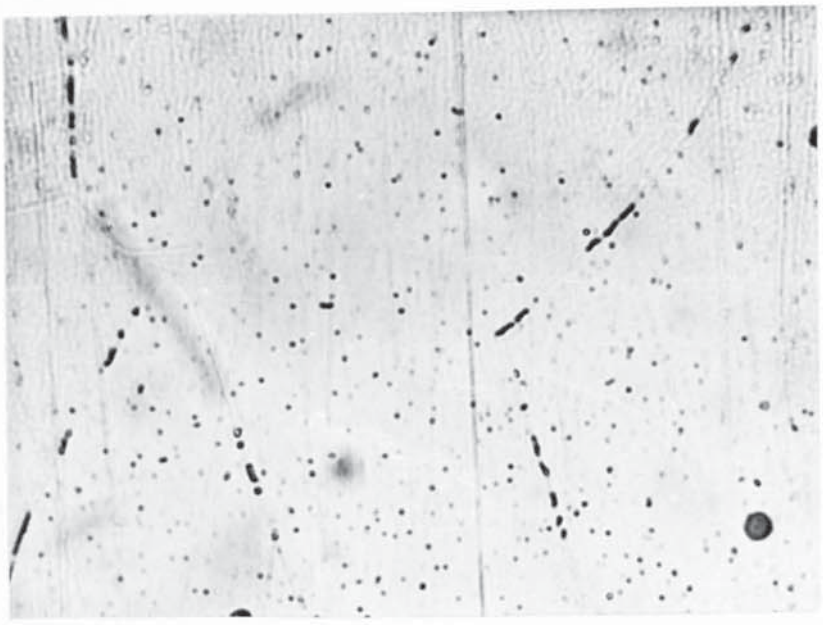

Plate 39 Cast B solution treated for 30 minutes 1050°C and cooled in vermiculite. Etched electrolytically in 10% oxalic acid for 10 seconds at 4V. Shows inclusion and precipitation on the grain boundaries.
x 1125

7.5 SEM Examination of Ground Specimen Surface prior to Nitric acid testing

On the ground surface of the specimens, very few features were seen except where grinding had revealed areas liable to localised attack. These had a rough appearance, and seemed to consist mainly of small nodules.

When a portion of the rough area, taking in a large number of the nodules was analysed using the Kevex equipment in conjunction with the SEM, it was found that it was rich in chromium. This can be seen by comparing the characteristic x-ray peak intensity ratios. Only Cr, Fe, Mn, and Ni were detected in significant quantities.

Ratio (Background Corrected)	Ordinary Ground Surface	Nodular Region
Cr K_α/Fe K_α	0.30	1.55
Mn K_α/Fe K_α	0.07	0.73
Ni K_α/Fe K_α	0.04	0.07

This type of flaw was common to both cast 976 and 803 although it did not arise in all specimens. It was not always present at the start of grinding, often appearing at later stages of grinding, indicating that it was not simply a surface defect.

7.6 SEM Examination of Specimens Subject to Nitric Acid Test

7.6.1 Cast 976 General observation

Several specimens showed a large area of the specimen surface being affected by grain dropping and localised attack, the specimens with the worst localised attack showing the most severe grain dropping. The localised attack varied from areas less then 50 μ in width, to areas more than 1 mm wide. These areas of heavy grain-dropping had a noticeable fibrous structure parallel to the rolling direction. In the areas of heavy attack no large inclusions were found, although this may be due to the initial inclusions having dropped from the surface. Within the grains however, were a large number of small angular inclusions. (Plates 41,42)

Using a 'Kevex' energy dispersive x-ray spectrometer and analysis equipment, a spot analysis was performed on a wide selection of the angular inclusions.

Most of the larger (∿ 5 μ diam.) particles analysed had a high chromium content. There was also manganese and possibly iron present but it is more difficult to assess the presence of these elements as the manganese K_α peak is masked by the chromium K_β peak and the iron K_α peak is masked by the manganese K_β peak. The background - corrected intensity ratios for these peaks were:-

Cr K_α/Fe K_α	13.87
Mn K_α/Fe K_α	7.04

No other elements were detected in any significant quantity, and although the particles varied in size and shape the intensity ratios did not alter much. A typical triangular particle had sides of 3.5 μ and dissolution had occurred at the particle/matrix interface. Some smaller particles were also present. These tended to be round or oval. Two such particles analysed using the Kevex equipment gave the following characteristic x-ray intensity ratios (background corrected)

Particle 1	0.5μ x 0.5μ	
	Cr K_α/Fe K_α	0.51
	Mn K_α/Fe K_α	0.77
	S /Fe K_α	0.65
Particle 2	0.1μ x 0.5μ	
	Cr K_α/Fe K_α	0.44
	Mn K_α/Fe K_α	0.36
	S /Fe K_α	0.32

No other significant elements present.

Some of the Fe and Cr x-rays may have come from the bulk material. It is most probable that these inclusions were manganese sulphides.

The interfacial dissolution was less noticeable on the manganese sulphides but was a common feature of the high chromium inclusions in cast 976. The various heat treatments made little or no difference to these inclusions.

The amount of localised attack was independent of phosphorus levels in the steel. However, in most heat treatments it was found that 976A, with the lowest phosphorus, had the highest localised attack, and more general grain dropping, than the other three phosphorus levels.

7.6.2 Water Quenched

Most of the water quenched specimens of cast 976 showed only a small degree of intergranular attack although the measured weight losses were higher than expected. After 48 hours (one period) in the nitric acid there was a clear relationship between phosphorus level and surface appearance and weight loss.

Table 14

Weight loss and degree of intergranular attack of Cast 976 after 48 hours in the nitric acid test.

Cast	Phosphorus wt. %	Weight loss mg/cm^2	Intergranular attack
976A	.006	1.31	none
976B	.014	1.65	slight grooving
976C	.021	1.79	40% ditch
976D	.028	3.3	80% ditch

The definite pattern was not maintained in the subsequent 4 periods and the weight loss figures increased in each period, except in cast 976D which showed a decrease and then remained steady.

None of the four parts of cast 976 water quenched showed massive grain dropping except where there was heavy localised attack. A common feature of the water quenched specimens was a sub-surface end-grain type attack that resulted in removal of considerable amounts of metal without any appreciable surface attack. This attack was not evenly distributed over the end-grain surface that was exposed to the acid, but was

limited to a layer 0.5 - 2 mm below the rolled surface.

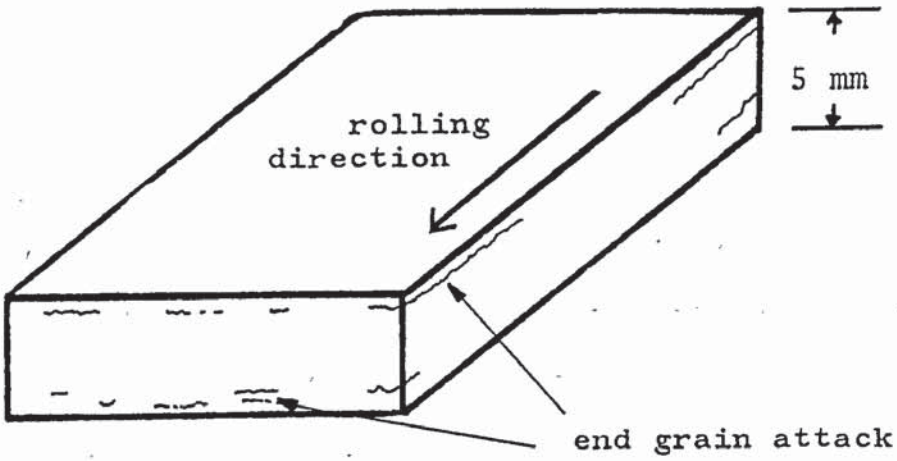

Fig. 30

End grain attack on water quenched cast 976 after exposure to the nitric acid test

The end grain attack often penetrated to a considerable depth (> 5mm).

7.6.3 Forced Air Cooled

Only one specimen showed grain dropping evenly over the whole surface, but several showed the localised dropping of grains due to inclusion attack. In nearly all cases the original grinding marks could still be seen. At higher magnifications it was observed that the grain-centres of some grains had suffered attack related to the crystal structure. This resulted in a honeycomb type structure on the grain surface. There was no clear trend of surface attack against level of phosphorus.

7.6.4 Air Cooled

The air cooled specimen with the highest phosphorus level had the lowest intergranular attack but this coincided with the lowest localised attack. The specimens showed a very wide range of intergranular attack, one specimen of 976A (.006 P) showing virtually no intergranular attack, with another showing heavy attack with widespread grain dropping due to massive intergranular penetration. The nature of the attack was similar to the forced-air cooled specimens but overall there was more grain dropping and more localised attack.

7.6.5 Vermiculite Cooled

These slow cooled steels resulted in the lowest level of intergranular attack and grain dropping, and the lowest degree of localised attack of the three cooling rates. In all cases the marks remaining from the original surface could be clearly seen. The intergranular attack, such as it was, generally increased with increasing phosphorus level. Several of the specimens which showed very little intergranular attack showed the centre grain attack that resulted in the honeycomb structure found in some of the forced-air cooled specimens. This kind of attack was absent in the specimens where large amounts of grain boundary material had been removed by the action of the nitric acid.

7.6.6 Vermiculite cooled from different solution-treated temperatures

Of the three solution-treatment temperatures 900, 1050, 1100°C, the amount of intergranular attack and grain-dropping was worst in the specimen that was cooled from 900°C and least in that cooled from 1100°C. The morphology of the corroded surface was similar to that of the specimens vermiculite-cooled from 1050°C, but the honeycomb-type grain-centre attack was absent in the specimens that showed a low level of intergranular attack. The specimen with the higher level of phosphorus had in general more severe intergranular penetration and grain dropping.

7.6.7 Cast 803 General Observations

Cast 803 showed the same localised attack on many specimens that was observed in Cast 976. This localised attack coincided with the worst cases of grain dropping. The grain dropping was very variable.

The inclusions found were mostly similar to cast 976 but in some of the narrow regions of localised attack, some slab-like inclusions were observed. These were found in several specimens after the nitric acid test. The presence of these inclusions, as with the other much smaller high chromium content inclusions was independent of boron additions to the steel. (Plates 43,44)

The slab-like inclusions were analysed using energy dispersive x-ray analysis. They were found to be

mainly silicon with small amounts of chromium, manganese, titanium and iron, decreasing in that order. This analysis was typical of the inclusion analysed and although the ratios of the different elements varied slightly, the major element was always silicon. Typical intensity ratios (background corrected) for slab-like inclusions were:-

Cr K_α/Fe K_α	=	8.09 ± 0.5
Mn K_α/Fe K_α	=	5.89 ± 0.5
Si K_α/Fe K_α	=	54.18 ± 2
Ti K_α/Fe K_α	=	0.92 ± 0.05

Due to the wide spread of the electron beam in a bulk specimen, a very small percentage of these counts may have originated from the bulk material and not from the inclusion. Oxygen cannot be detected by this analysis method, but it is most probably that these inclusions are silicates with small amounts of chromium and manganese.

7.6.8 Water Quenched

All the specimens of 803 that had been water quenched showed similar corrosion behaviour except 803C which had a very high level of localised attack, with massive silicate inclusions that could be seen plainly with the naked eye. There was very little grain dropping in any of the specimens except in the immediate vicinity of the localised attack. Ditching had occurred at most of the grain boundaries.

7.6.9 Forced Air Cooled

Several specimens showed some grain dropping. In the worst case approximately 40% of the original surface grains had dropped from the surface. In the case of least attack this figure was less than 10%, and appeared still less, as the first grains to drop were always very small (<30 μ) compared with an average 60 - 80 μ. Localised attack was found in several specimens always coinciding with heavy grain dropping. The amount and severity of general intergranular and localised attack tended to decrease with increasing boron content.

Grain-centre attack occurred in most of the specimens in some cases quite extensively. It affected the larger grains more and usually left a region at the periphery of the grain that was unaffected. This region was found in nearly all specimens that showed grain-centre attack.

7.6.10 Air-Cooled

The general intergranular, and localised attack were more severe after air cooling than forced air cooling. Grain dropping and localised attack were found in all specimens except one of 803D with the highest boron content, which, although having extensive grain boundary attack, dropped only a few grains. It had a smaller grain size than the specimens showing extensive grain dropping.

There was no noticeable trend of intergranular attack with level of boron addition.

7.6.11 Vermiculite Cooled

With only two exceptions these specimens showed considerably less intergranular attack and grain dropping than the air cooled specimens. The variations in boron level had no effect on the severity of intergranular attack.

None of these slow cooled specimens showed the grain-centre attack that was found in the forced-air and air cooled specimens. There was generally very little attack on the grain surfaces except some round clearly-defined pits.

Although there was some attack of twin boundaries, some such boundaries showed no attack whatsoever. Incoherent twin boundaries were more readily attacked than coherent ones.

7.6.12 Vermiculite Cooled from Different Solution Treatment Temperature

The steels treated at 900°C showed far more intergranular attack and massive grain-dropping compared with those treated at higher temperatures. As with the other Cast 803 specimens that had been cooled in vermiculite, none showed the honeycomb type grain-centre attack at any stage. The different boron levels of the two steels investigated 803A and 803D made no difference to the morphology of the corroded surface or the severity of intergranular attack.

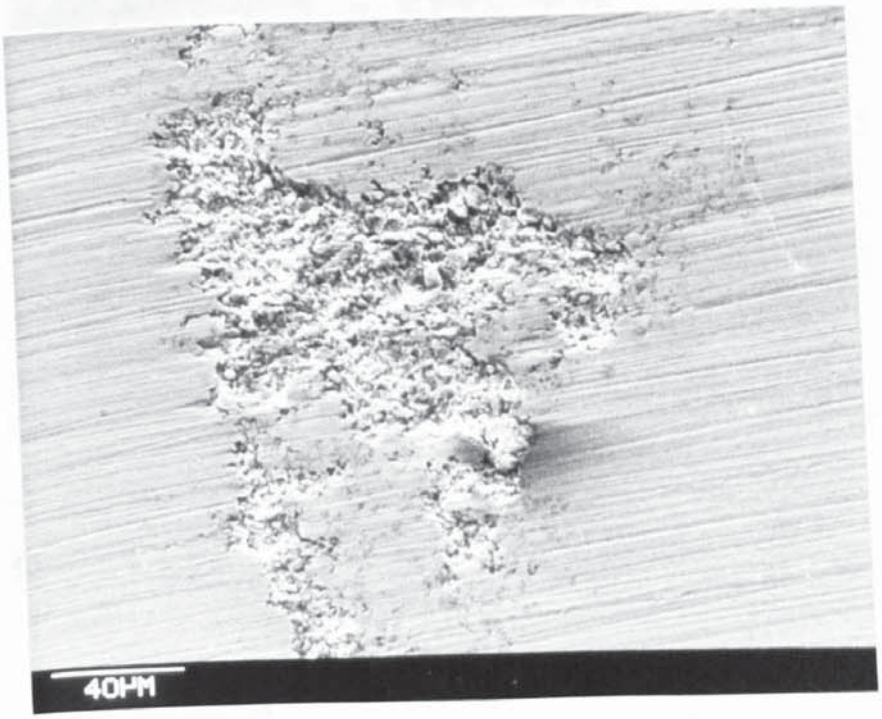

Plate 40 SEM micrograph of ground surface of specimen prior to the nitric acid test showing defect that appeared after several minutes grinding. Analysis showed this area to have a higher Cr/Fe ratio than normal.

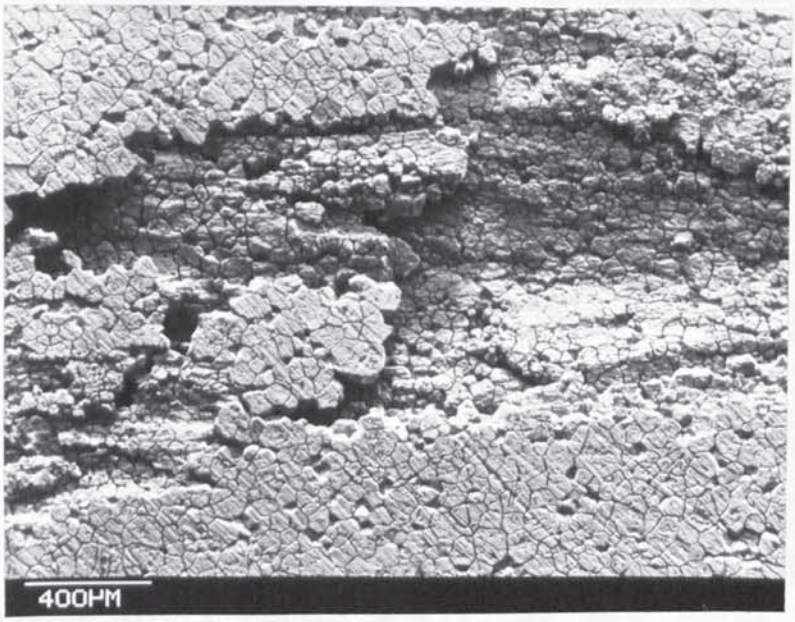

Plate 41 Cast 803 solution treated 30 minutes 1050°C and cooled in forced-air draught. Shows massive grain dropping on surface after nitric acid test with fibrous structure of grains revealed underneath.

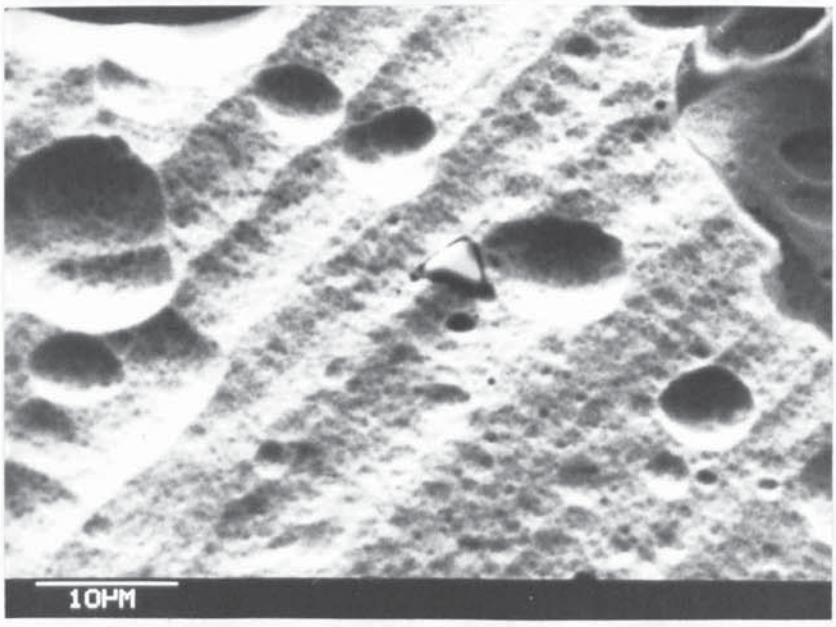

Plate 42 Cast 976 D solution treated 1050°C for 30 minutes and cooled in vermiculite. Shows high chromium particle in grain surface after the nitric acid test.

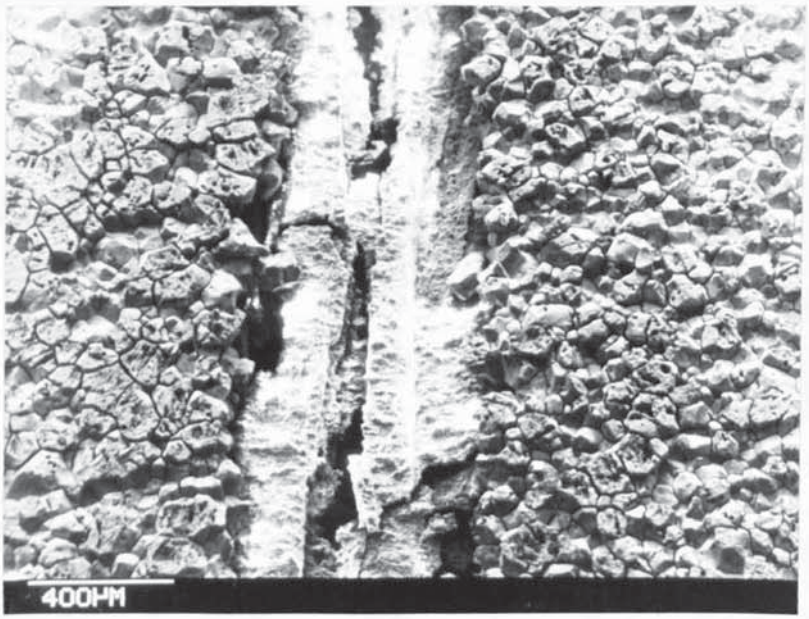

Plate 43 Cast 803 A soltuion treated 30 minutes 1050°C and cooled in air. Shows specimen surface after acid test with massive grain dropping and large silicate inclusions.

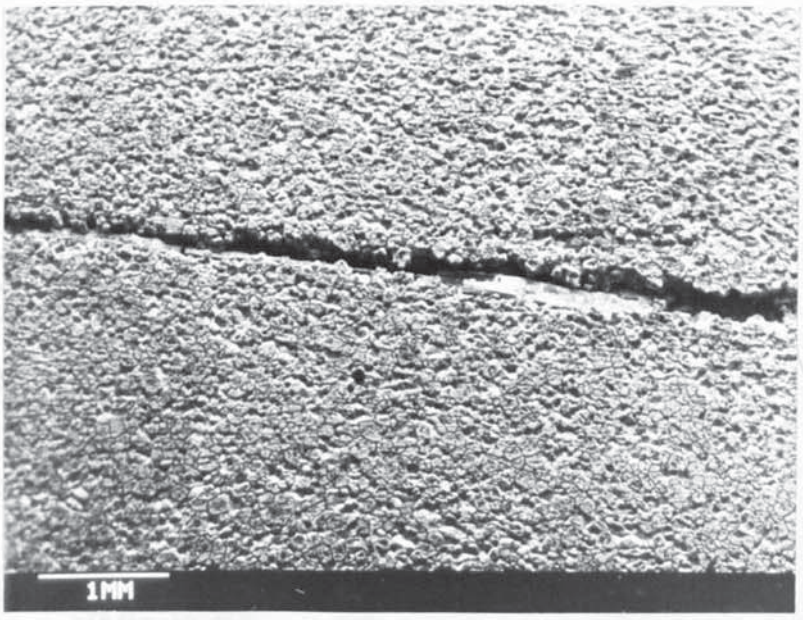

Plate 44 Cast 803 C solution treated 30 minutes 1050°C and cooled in air. Shows large slab-like silicate inclusion and severe attack and grain dropping on the specimen surface after nitric acid test.

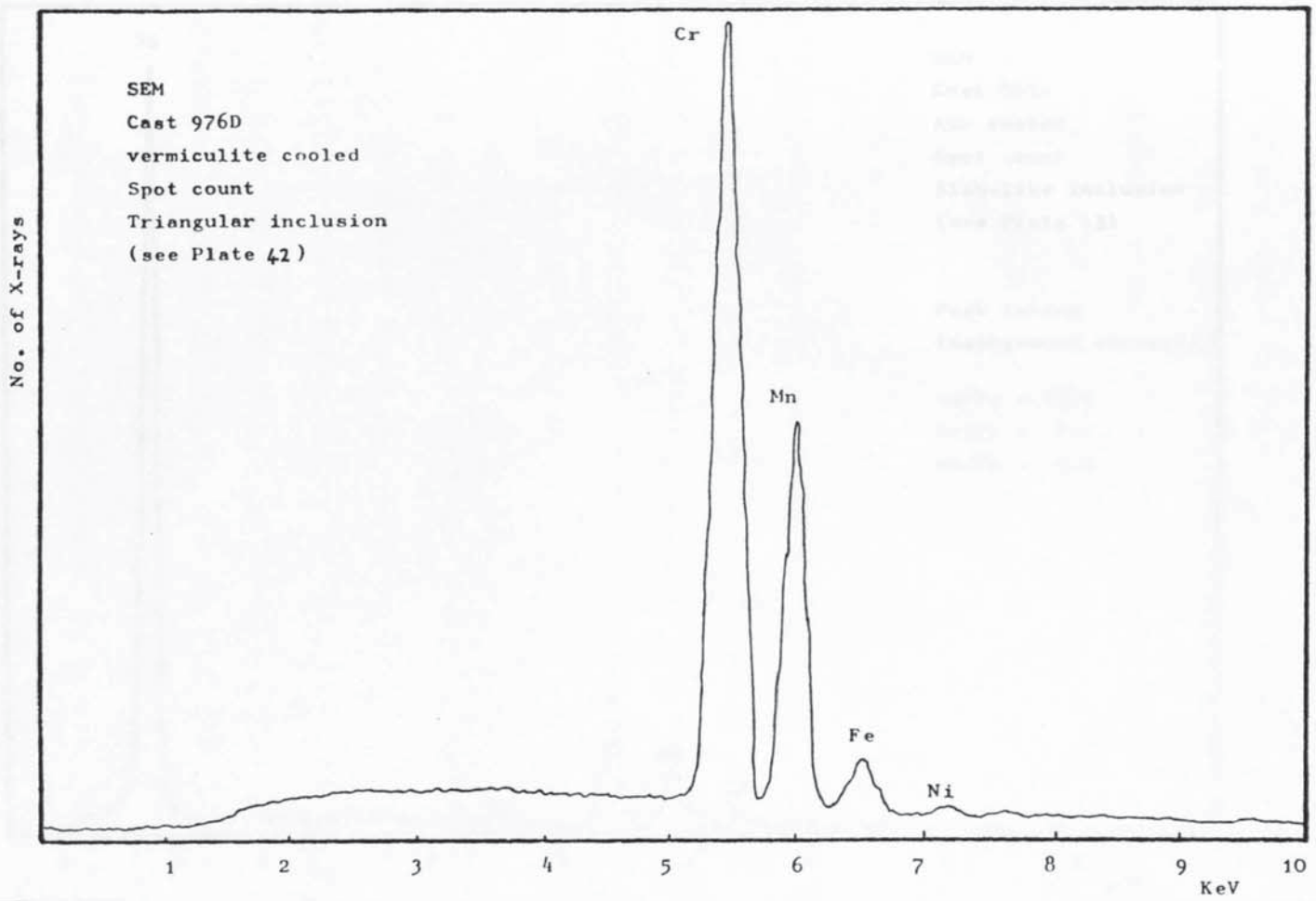

Fig. 30 Energy dispersive x-ray spectrum showing high level of chromium and manganese in triangular inclusion

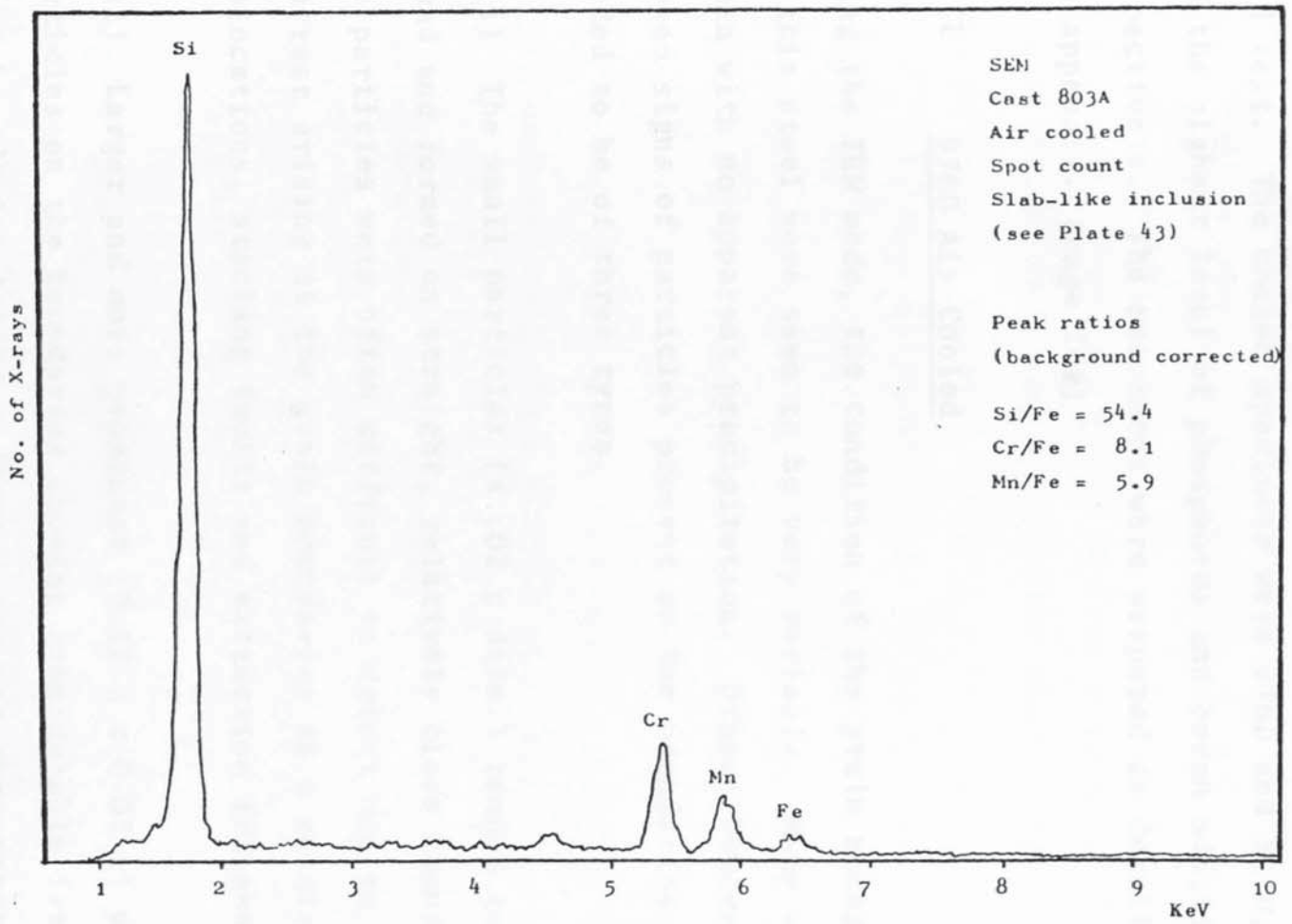

Fig. 31 Energy dispersive x-ray spectrum, showing high level of silicon in large slab-like inclusion, probably silicate.

7.7 TEM/STEM Examination of Casts 976 and 803

Due to the limitation of time only one treatment from each of cast 976 and cast 803 was examined. The specimens that had been air cooled were chosen for examination as these had shown the highest intergranular attack in the nitric acid test. The chosen specimens were 976D and 803D, which had the highest level of phosphorus and boron additions respectively. The specimens were prepared as detailed in the appendix. (page 208)

7.7.1 976D Air Cooled

Using the TEM mode, the condition of the grain boundaries of this steel were seen to be very variable. Many were clean with no apparent precipitation. Others however, showed signs of particles present on the boundaries and tended to be of three types.

(i) The small particles (< .02 μ diam.) tended to be round and formed on straight, relatively clean boundaries. The particles were often difficult to detect due to the contrast arising at the grain boundaries as a result of dislocations, stacking faults and extinction fringes.

(ii) Larger and more prominent (0.12 μ x 0.03 μ) were the particles on the boundaries showing considerable irregularity. These boundaries tended to have a zig-zag appearance with the particles forming on the boundary in one direction only, The particles were quite closely spaced along the boundary.

(iii) The largest particles were approximately 0.04 μ wide and tended to be more continuous along the boundary than the other particles, so forming a distinct boundary phase. Several of these particles had a high stacking fault density indicating the possibility of Cr_7C_3. However the extent of these particles was quite limited, being found on only a few boundaries.

The specimen discs were found to have perforated frequently where particles had dropped from the foil, and the holes were often in straight lines. One such hole still contained a particle although dissolution of the matrix round the particle had occurred. When analysed using the energy dispersive x-ray analysis it was found to be high in chromium, and also contained some molybdenum.

STEM examination showed some very small particles on the grain boundary, only just visible at a magnification of 25K. When a spot analysis was performed on a particle in the grain boundary, there was very little difference between that spectrum and one obtained from the centre of the grain. In the STEM mode numerous analyses of the grain boundary region detected no segregation whatsoever.

7.7.2 803D Air Cooled

This treatment resulted in cleaner grain boundaries than were found in cast 976. The polishing resulted in quite a few small holes in the specimen disc. Most of these holes were associated with grain boundaries. However, no

particles were observed on adjacent boundaries, and they appeared to be caused by etching during the electropolishing.

Boron cannot be detected by energy dispersive x-ray analysis and no other segregants were detected at the grain boundaries when they were analysed by spot analysis, using the Kevex in the STEM mode.

There were holes in the foil in the centre of the grain as well as those on the boundaries. These appeared to be where particles had dropped from the foil. One hole had not completely perforated and still contained a particle. Qualitative energy dispersive analysis showed the particle to be high in chromium.

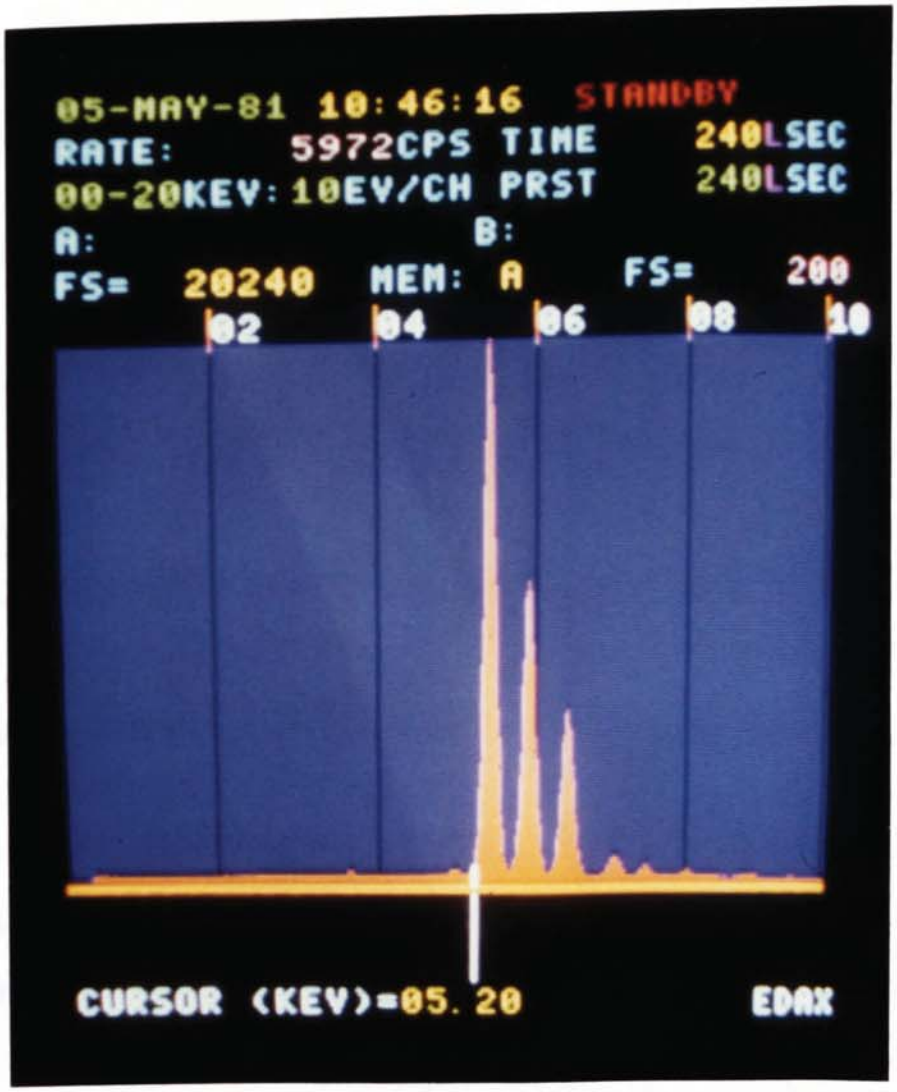

Energy dispersive x-ray spectrum, produced by STEM, of high chromium/manganese particle, in a solution treated and air cooled specimen of cast 976D. The three major peaks are:

Cr (Kα)	5.4	KeV
Mn (Kα)	5.9	KeV
Fe (Kα)	6.4	KeV

The spectrum is a histogram and the horizontal axis shows the x-ray energies in KeV on a scale from 0 to 10 KeV. The vertical axis indicates number of x-rays for a given energy with a full scale of 20240 counts. The horizontal axis channel width is 10eV. The counting time was preset for a live-time count of 240 seconds.

7.8 Auger Spectroscopy

Previous workers have achieved, with heavily sensitized 304 steel, the intergranular fracture necessary for Auger spectroscopic analysis. However this has not been achieved with 304L.

Using the steels in this study (304L) from cast 976 with the highest intergranular corrosion rates, and therefore the greatest tendency to fracture intergranularly, several Auger specimens were made in hope of studying the grain boundary chemistry. Even after cooling in liquid nitrogen, all specimens were found to fracture trans-granularly. This is expected where there is no distinct grain boundary weakness, as austenitic steels do not show a brittle-ductile type transformation, and normally show ductile fracture even at very low temperatures.

Examination of the fracture surfaces revealed the lack of grain facets which indicate intergranular fracture in all specimens.

7.9 Discussion

As with the nitric acid tests on cast A and B, the results obtained with cast 976 (17/9 Cr/Ni) and cast 803 (18/12 Cr/Ni) were found to be very variable. 976 and 803 were both small (50 kg) experimental casts which showed a large amount of differential surface attack on certain specimens, with some localised areas showing massive grain dropping whilst adjacent areas showed none. This type of attack was not found in the commercial casts A and B.

In the nitric acid test investigations of 976 and 803 there was intergranular attack in all specimens, even in those that had been solution treated and water quenched and they showed considerably more intergranular attack than the commercial casts A and B showed after similar solution treatments. There was however, no catastrophic intergranular failures, with grain dropping occurring on over 90 per cent of specimen surface area, as was found in some of the sensitised commercial steels.

The poorer performance of the experimental steels in the nitric acid test when in the solution treated condition, and the wide variability in results in this test can almost certainly be attributed to the high level of impurities in the form of inclusions in this steel. The impurities can result in disastrous localised attack in the nitric acid test.

When the localised type of attack occurred in 976 and 803, the grains could be removed to a depth of more than 1 mm

in the affected area, which was often quite extensive. The affected area on several specimens was as much as 10 per cent of the total specimen surface area. This affects the weight loss result in two ways. The dropped grains themselves can weigh considerably more than the mass of metal that is removed by the dissolving action of the acid, thus producing a misleading result. Also, once the grains have dropped from the metal surface into the acid, the total metal surface area exposed is greatly increased, and this increases the metal dissolution rates. The higher levels of dissolved chromium then lead to a more vigorous corrosive attack on the steel due to the effect of hexavalent chromium in solution in nitric acid, discussed earlier in this work.

Prior to the nitric acid test, after the surface of the specimens had been ground to a 180 mesh grit finish, very slight dull marks were observed on some of the specimens. The marks were variable in length and width, and ran parallel to the rolling direction. They could not be entirely removed by grinding, as new marks appeared as others were ground away. It was these marks that eventually showed the high localised rate of grain dropping in the nitric acid test. SEM examination and qualitative x-ray analysis indicated that these areas were mainly chromium, with some manganese, the surface topography being nodular in appearance. Neither carbon nor oxygen can be detected by this x-ray analysis method but from the morphology it is most likely that these are chromium oxides

(Cr_2O_3) that have been rolled into the metal during hot rolling.

This is similar to the kind of attack on oxidised stainless steel found by Szummer [108] who attributed the surface intergranular corrosion of oxidised 304L to chromium depletion of the grain boundaries caused by formation of chromium rich scale.

Also present in the experimental casts were the slab-like inclusions, high in silicon that ran parallel to the rolling direction. The steel surface in the vicinity showed heavy attack in the nitric acid test and in many cases the variations in the weight-loss figure resulting from the test depended more on the oxide and silicate inclusions than the controlled addition of boron or phosphorus.

In cast 976, in all three heat treatments, but not in the solution treated specimens, it was 967A, with the lowest level of phosphorus (0.006 %) that showed the highest corrosion rates in the nitric acid tests and the highest level of localised attack. This probably is due to the fact that cast 976 was split into four, and 976A, being the first of the four to be poured off out of the laddle, would have a higher proportion of slag, dross and other low-density impurities than the later portions of the cast. These would result in enhanced attack in nitric acid.

In the forced air cooled specimens, apart from specimen 976A there was a slight increase in nitric acid test corrosion rates with increasing phosphorus level.

The vermiculite cooled specimens showed similar results with a high corrosion rate for 976A and lower corrosion rates, increasing with increasing level of phosphorus for 976B, C and D.

The corrosion rates for the air cooled specimens however, were greatest, showed considerably variability, and produced no distinct trend with level of phosphorus. It is possible that this lack of correlation, and high rate of attack is due to another mechanism, in addition to segregation of phosphorus, affecting the behaviour of the steel in the nitric acid test.

The susceptibility to intergranular attack that has arisen in these steels during continuous cooling sensitization (CCS) has resulted from cooling through the sensitization range. Solomon [102] found that degree of sensitization during CCS is strongly dependent on the temperature from which the steel is cooled. For a 304 steel, he found sensitization occurred more readily when cooled from 800 or 900°C, than if it is cooled from 700°C or 1000°C. This work agreed with these results to a certain extent with specimens slow cooled from 900°C showing the most severe intergranular attack, while those cooled from 1050°C and 1100°C showed decreasing amounts of attack.

For the steels with phosphorus additions it appears that the cooling rate has a significant effect, the highest corrosion rates occuring in the air cooled specimens. Increasing the cooling rate (forced air, water-quench)

decreased intergranular attack, as did decreasing the cooling rate (vermiculite cool).

The existence of a critical cooling rate can be explained in terms of the mechanism of a continuous grain boundary path, proposed by Aust et al. Cooling at the critical rate results in a continuous grain boundary path for intergranular attack due to the presence of segregants or carbides, or both. Faster cooling (e.g. quench) does not allow time at temperature for segregation or precipitation to occur at the grain boundaries. Slower cooling, e.g. vermiculite cool, will allow some segregation and precipitation to occur but a continuous grain boundary path will not be formed. The formation of isolated grain-boundary carbides during vermiculite cooling may provide sites where solute impurities can be incorporated, removing them from the grain boundary region. During the air cooling there is insufficient time for this 'mopping-up' operation to occur. It is known [113] that phosphorus is readily dissolved substitutionally in the carbide $M_{23}C_6$.

Brown [108] states that solute segregation cannot be detected by any of the tests designed for carbide precipitation (such as the nitric acid test). This work does show a connection between the phosphorus level of 304L after certain heat treatments and performance in the nitric acid test. The air cooled steel had the higher corrosion rate and contained only a few grain boundary precipitates and showed no trend with phosphorus. However the corrosion rates of the water quenched and forced-air cooled specimens

which had virtually no precipitates, and the vermiculite cooled steels which had the highest level of precipitates, were both lower, and were linked to phosphorus level. This lends support to the notion that in the air-cooled condition another mechanism in addition to segregation of phosphorus is operative as the air cooled steels showed no trend of intergranular attack with level of phosphorus. In addition, the same behaviour of high corrosion rate in the air cooled steels, with lower corrosion rates in the other treatments was observed in the boron doped steels Cast 803 which had a low phosphorus content.

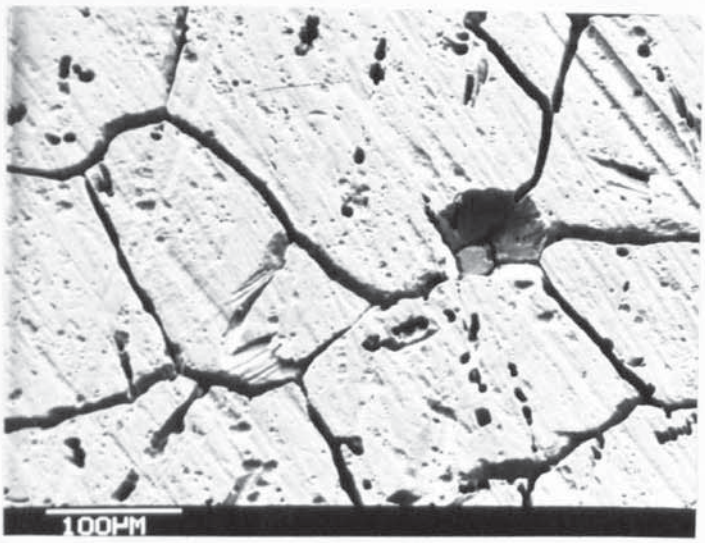

(a)

1100° C

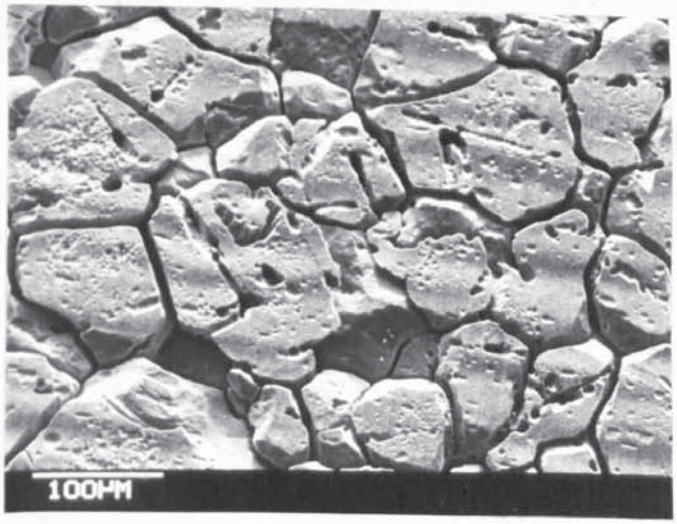

(b)

1050° C

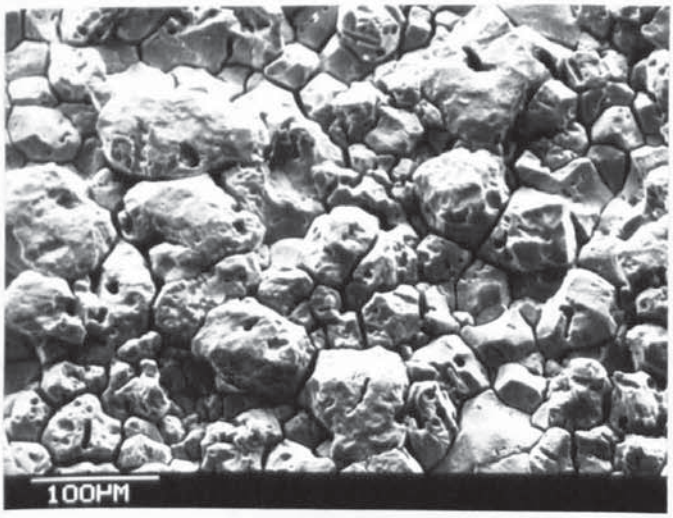

(c)

900° C

Plates 45 a,b,c, Cast 803 D. Nitric acid test specimen surfaces resulting after solution treatment at three different temperatures. All specimens treated for 30 minutes and cooled in vermiculite.

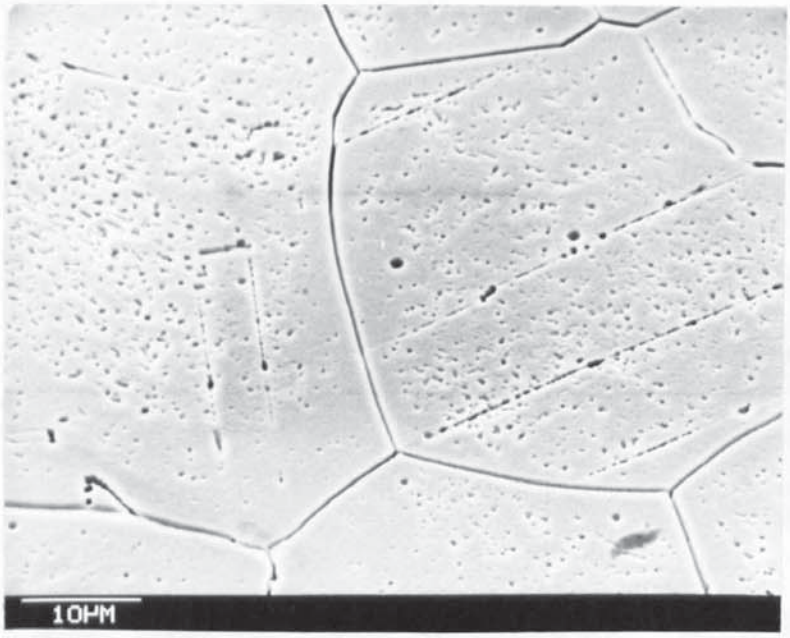

Plate 46 Cast A solution treated, water quenched. Nitric acid test surface. Pit free zone adjacent to boundary. In this zone coherent twin boundaries are unattacked. Coherent twin boundaries generally show less attack that incoherent twin boundaries.

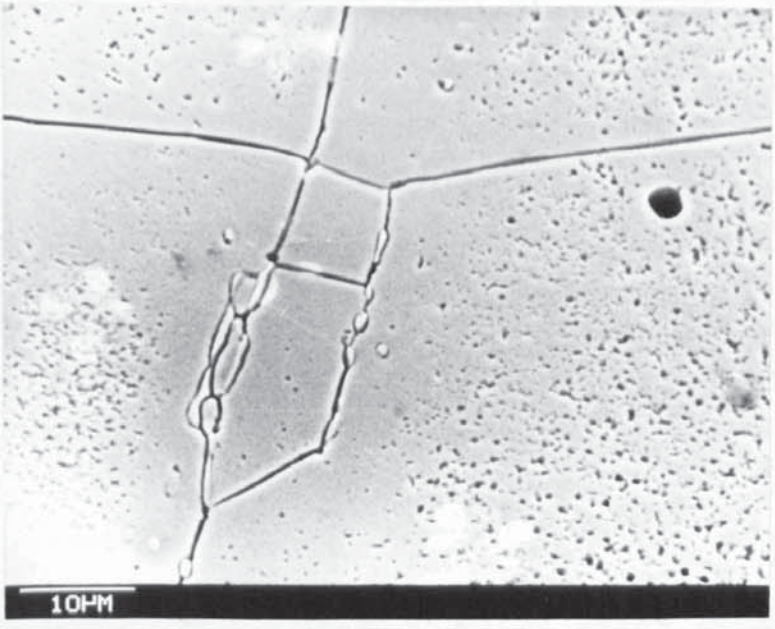

Plate 47 Cast A solution treated, water quenched. Presence of delta ferrite islands in grain boundary. Note also pit free zone adjacent to boundary. Nitric acid test surface.

Plate 48 Cast 976C, solution treated, water quenched. Shows low level of intergranular attack, after nitric acid test.

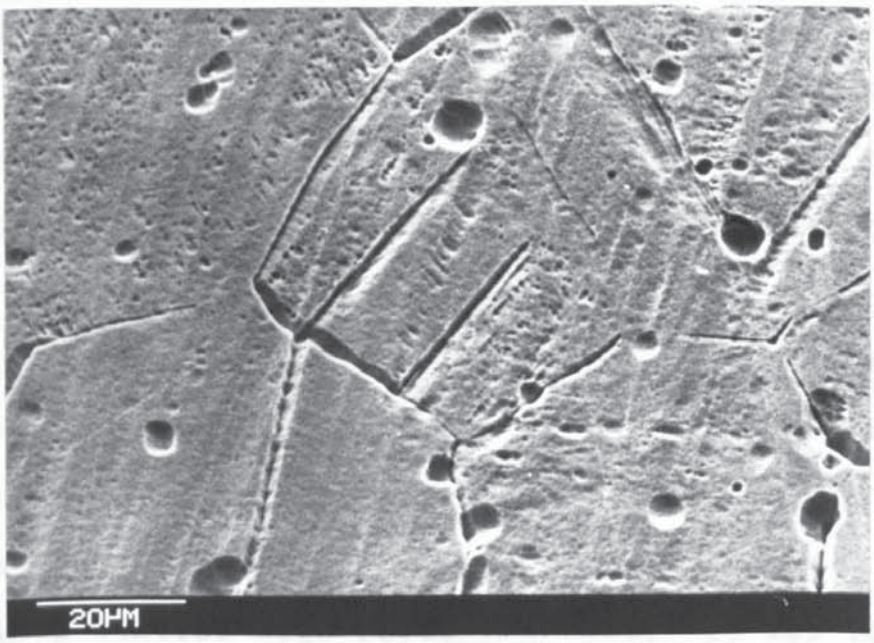

Plate 49 Cast 976B, solution treated water quenched. Nitric acid test surface showing some grain boundaries with heavy attack while others show no attack. Shows differential attack on grain surface where twinning has occured.

8. General Discussion

This section discusses the work as a whole in context with the general problem of intergranular corrosion and draws together the individual discussion sections placed earlier in this thesis after each section of experimental work.

Intergranular corrosion of AISI 304L in boiling nitric acid was seen to occur in one commercially produced cast of steel (Cast B) while another cast (Cast A) with similar composition was found to be resistant to such attack. The large difference in behaviour of the two steels was only found in the as-received condition. Although the condition which made Cast B susceptible to attack may have arisen during a faulty production process sequence, the root cause must be an inherent component of the steel. The condition was sufficiently transient as to be removed by a short heat treatment (10 minutes @ 650°C). This treatment reduced the corrosion rate in the nitric acid test to a level similar to that of the unaffected steel. This is unusual in that treatment of type 300 series steels at this temperature usually increases susceptibility to attack (sensitization). None of the heat treatments applied to these steels, except one for an extended period (168 hours) resulted in a similar high corrosion rate. It was found that air cooling produced higher corrosion rates in the nitric acid test than either a water quench or an isothermal treatment at the sensitizing temperature (650°C).

With these steels A,B, and throughout the work detailed earlier, the results for the corrosion rates in the ASTM standard nitric acid test were found to be very variable with individual treatments giving large differences between identically treated specimens. This test was found to have considerable drawbacks in this study. The time (10 days for each test) and expense (a specimen of surface area 12 cm^2 requires 1.2 ℓ of high purity nitric acid per test) precluded a large number of repeat testings. This greatly reduces the statistical accuracy of the results. As the specimens used in the test have a very small size compared with a bulk steel cast, the results are far more prone to the effect of inhomogeneity in the steel. A small change in microstructure of a specimen can result in quite large changes in weight loss in the nitric acid test. A homogeneous steel would give reproducible results as all other parameters in the test should be constant.

The intergranular attack that occurs during the test was sufficient to cause extensive grain dropping in some specimens of the commercial steels. These steels had a low carbon content to reduce precipitation of carbides at the grain boundaries but TEM examination showed some small carbides to be present in the as-received steels. The size of the particles increased after air cooling from 1050°C, but they remained quite widely dispersed, and there appeared to be insufficient carbides for a continuous grain boundary corrosion path to form. Such a path may be present as a result of solute segregation to the grain boundaries. Evidence for such segregation was found in only two specimens of the heat treated commercial steels, one that had been air

cooled from 1050°C and one that had been held for 600 hours at 650°C. In these specimens the level of phosphorus at the grain boundaries was considerably higher than at the grain centre when measured using x-ray analysis with STEM.

The intergranular attack is however due not only to the presence of phosphorus. Despite an extensive examination no segregation of phosphorus was detected in the as-received cast B which had shown a very high corrosion rate in the nitric acid test. No evidence was found to directly connect segregation of any particular ion species with this kind of attack. Although small carbides were present on the grain boundary of the commercial steel with the high corrosion rate, it is probable that these carbides do not directly result in the intergranular attack. The same carbides were found in the commercial steel with the low corrosion rate.

When the intergranular attack was examined on a microscopic scale by studying TEM specimens of the commercial steel that had been exposed to boiling nitric acid, a considerable difference in behaviour was found between an air cooled steel and a water quenched steel. The air cooled steel suffered grain boundary penetration on numerous boundaries at various thicknesses of metal, penetration occurring at regular, closely spaced intervals along the boundaries. This resulted in small, regular, round holes. In the water quenched steel fewer boundaries perforated, and these were only in the thinner areas of the TEM specimen. The boundary tended to perforate in long lengths instead of the small regularly spaced points in the air cooled steel.

This would occur if, in the air cooled steel, a deleterious ion species segregated to the grain boundary region and formed small clusters along the boundary, instead of forming a uniform boundary layer, while in the water quenched steel such segregation would fail to occur due to rapid cooling.

The oxalic acid etch test, using impressed current on bulk specimens, which dissolves stainless steel more rapidly than the nitric acid test, showed the different modes of attack very clearly. The water quenched steel showed uniform dissolution along the grain boundaries, with differential dissolution between the grains resulting in a "step" structure. The air cooled steel etched preferentially at the grain boundaries in a non-uniform manner with series of pits forming along each boundary. Although the separation of the oxalic acid pits was several orders of magnitude greater than the perforation of the air cooled TEM specimen in the nitric acid test, the same principle of attack starting at discrete points along the boundary was involved. Although some workers [39, 60] consider the oxalic acid test will show the presence or absence of grain boundary carbides, the pattern and distribution of attack and dissolution of the grain boundaries did not conform with the distribution of carbides visible in TEM specimens.

One factor of intergranular attack that was marked in the oxalic acid test and was also prominent during the early stages of exposure to the nitric acid test was the variation in severity of attack from boundary to boundary. In both

tests it was possible for ditching to occur at one boundary while the adjacent boundary showed no attack whatsoever. The variation was most visible on twin boundaries and in general it was the coherent twin boundaries which showed the least attack although this was not always the case. The attack of the grain boundary depends on the orientation of the grains on either side of the boundary, the worst attack occurring on the boundaries that show the greatest atomic mismatch. Incoherent twin boundaries have a greater degree of mismatch than coherent boundaries.

It is known that high purity stainless shows no intergranular attack in nitric acid [18], and that the inherent boundary energy resulting from variations in mismatch only contribute in a small degree to intergranular corrosion [77]. The preferential attack of certain boundaries may therefore be due to the increased probability of segregation of deleterious ion species occurring at the boundaries that exhibit the largest degree of mismatch.

One observation that supported this idea was seen clearly in some of the specimens that exhibited attack on the grain face as well as the grain boundary. Often attack occurred on the grain faces of specimens subjected to the nitric acid test, resulting in widespread pitting over the face. These pits were frequently found in linear arrays that appeared to be crystallographic in nature. It is probable that the attack is associated with the formation of small groups of atoms at line defects such as dislocations, which are found in linear arrays within the crystal. In

many specimens there was found to be a pit-free zone adjacent to the grain boundary that surrounded each grain. This pit-free zone may have arisen from:

1. Annihilation of dislocations by the boundary, acting as a sink, preventing any precipitation on these dislocations.

2. Removal of deleterious ion species, again by the boundary acting as a sink.

3. Formation of a cathodically protected zone adjacent to the boundary with the boundary acting as a "sacrificial anode".

It was observed that where a twin boundary (in most cases coherent) existed within a grain, it was attacked preferentially in the centre of the grain. It was often completely unattacked where it traversed the pit-free region of the grain and intersected the grain boundary. This indicates that in the pit free region either no segregated species were present on the twin boundary or that this region was protected from attack. The former appears the most likely explanation, as localised corrosion cells such as resulted in the pitting attack in the centre of the grain, can still be active in a cathodically protected surface. This means that segregated ion species may render a boundary more liable to attack and that the grain boundary can act as a sink for these ion species removing them from the matrix region adjacent to the boundary.

It is known that phosphorus [43], and also boron [104], segregate to the grain boundaries in stainless steel, and they may play an active role in the mechanism of intergranular corrosion in strong acids. For this reason a study was made of two series of casts of AISI type 304L, one with varying levels of phosphorus (976) and the other with varying levels of boron (803). The assessment of corrosion resistance was again by the standard ASTM nitric acid test, and because of the small size (50 Kg) of these experimental casts the test results were seriously affected by in-homogeneity of the test specimens. The experimental steels contained more gross inclusions such as silicate stingers and oxide particles, than the commercial steels. Performance of the experimental steel specimens in the nitric acid test was related to the heat treatment received, the level of inclusion in the particular specimen and the level of added material. The time and temperature of solution treatment also affects the result but this was constant in most tests as were other parameters that could have altered the results.

Fast cooling (quench) and slow cooling (in vermiculite) from 1050°C both seemed to decrease the corrosion rate of cast 976 and 803 compared with an intermediate air cool. This agrees to an extent with the commercial steels which also showed a higher corrosion rate after an air cool than after a quench or a short isothermal sensitizing treatment at 650°C.

In cast 803 with different boron levels, all of the heat treatments resulted in corrosion rates which indicated that the levels of added boron used in these experiments had no direct effect on the behaviour of those steels in the nitric acid test. Boron is a normal additive in 304L to aid hot workability and at these levels, < 0.085 per cent, it was found to have little or no influence on intergranular corrosion in the nitric acid test.

Phosphorus on the other hand is a residual element from the iron ore and it can be quite difficult to remove from the melt. In this study of the effect of cooling rates on nitric acid corrosion, two of the cooling rates indicated a trend of increasing corrosion rate with increasing phosphorus level. The two other cooling rates investigated showed no distinct trend of corrosion rate with phosphorus level.

The phosphorus level did not appear to be the major factor in governing the corrosion rates of specimens given a particular heat treatment. The spread of corrosion rates within a series of specimens with identical phosphorus levels and heat treatments was often greater than the spread between specimens with different phosphorus levels. The effect of phosphorus may have been masked by the effect of gross impurities in the steel, or another unknown species may have been active at the grain boundaries.

The nitric acid test results for the experimental steels showed considerably more weight loss generally than the

commercial steels except in one or two individual cases. In the commercial steels the weight losses tended to be in the range 0.5 to 1 mg/cm^2/48 hrs. compared with an approximate range of 1 to 5 mg/cm^3/48 hrs. for the experimental steels, probably as a result of impurity levels.

Both the commercial and experimental steels had similar, low, carbon levels (approximately .019 per cent), to reduce the likelihood of carbide precipitation at the grain boundaries. Metallographic examination of specimens that had been solution treated at 1050^{o}C and then slow cooled in vermiculite to ambient temperature, showed that precipitation of small carbides had occurred extensively along the grain boundaries of the commercial steel, while no such precipitation occurred in the similarly treated experimental steels. This was true for cast 976 (a 17/9 steel) and cast 803 (a 20/12 steel). The main variations in chemical composition between the commercial and experimental steels that may account for this difference in carbide precipitation were as follows (per cent):

	Commercial	Experimental
C	.019	.019
Si	.25	.14
P	.023	.006 → .028
B	.002	.001
Mo	.10	.08

The other elements analysed in both steels were present at similar levels. It is possible that the presence or lack of certain elements at the grain boundary affects the precipitation kinetics of carbides.

The most likely element to be responsible for such an effect would appear to be boron or silicon. From the STEM x-ray analysis work silicon segregation to the grain boundaries was not found in any specimen investigated, but the involvement of boron in grain boundaries mechanisms has been noted.

Other workers disagree as to whether boron reduces or increases resistance to intergranular attack. In AISI 304 Robinson [24] found that boron at the level of .005% retarded carbide precipitation while Costello [25] found that boron levels > .002 % intensified such precipitation.

However, without more experimental results it is not possible to say for certain what caused the difference in carbide precipitation between the commercial and experimental steels. It is also difficult to say to what extent this difference contributes to the difference in intergranular corrosion.

The solution temperature of the experimental steels was found to have considerable effect of the intergranular corrosion in the nitric acid test. The highest solution temperature 1100^{o}C followed by slow cooling, resulted in lower corrosion rates with minimal grain dropped while a solution treatment at 900^{o}C and slow cooled, resulted in

massive grain dropping over the whole surface. Treatment at 1100°C will result in more of the deleterious material passing into solution than a treatment at 900°C.

The solution heat treatment also affects the grain size of the material as follows:

Solution temperature °C	Grain Size (microns)
1100	125
1050	65
900	40

This will affect the intergranular attack to a certain extent as was indicated by Tupholme and Bouchier [59], but it is doubtful that grain size alone could result in the large difference in corrosion that existed. The slow cooling in vermiculite from 900°C resulted in quite castastrophic intergranular attack and resulted in weight losses comparable with those found in the air cooled specimens. In 304 with a higher level of carbon the higher initial solution treatment temperature result in larger grain size and more continuous coverage of grain boundaries by $M_{23}C_6$ on subsequent 650° sensitization [115]. Vermiculite cooled specimens would pass through the sensitizing range 800 - 500°C in about 10 minutes which is sufficient for carbide formation to occur on the boundaries of commercial 304L.

The segregation that results in intergranular corrosion arises mainly as a result of heat treatment history of the specimens. The EPMA study of segregation banding showed

that in the commercial steels, in the as-received condition, there was considerable variation in Ni and Cr levels across the whole grain that had arisen as a result of the thermo-mechanical treatments received during the first stages of the production process. This segregation existed in a series of quite small bands with a separation of 10 - 15 μm, and was unaffected by a solution treatment at 1050°C for 100 minutes with a water quench, a treatment that effectively prevented intergranular corrosion in the nitric acid test.

The results of the nitric acid tests were affected by two main factors. The general level of inclusions and inhomogeneity of the steel, and the degree of sensitization caused by segregation at the grain boundaries.

It would appear from this work that the nitric acid test can be unreliable as an indicator of resistance to intergranular corrosion in experimental studies.

9. Conclusions

1. The high nitric acid test corrosion rate that was found in one case of as-received commercial 304L but not in another, was due to a condition that arose during production. The condition was sufficiently transient to be removed by a short heat treatment (10 mins @ 650°C) and did not appear to be connected to precipitate distribution on grain boundaries.

2. The corrosion rate of the affected steel was reduced by all heat treatments investigated (including sensitizing treatments). In this case sensitization reduced susceptibility to intergranular attack, as opposed to the more usual increase.

3. Long sensitizing treatments resulted in higher nitric acid test corrosion rates, and this was associated with increased carbide precipitation.

4. After long heat treatment (e.g. 700h at 650°C) carbide precipitation was detected on dislocations associated with low angle boundaries.

5. In a TEM specimen of commercial 304L that had been solution treated at 1050°C and then air cooled, exposure to boiling nitric acid for 10 seconds resulted in the formation of small (.015 μ diam.) perforations, regularly spaced (.04 μ separation) along the grain boundaries. A solution treated and water quenched specimen showed no such attack and perforation of

of longer lengths of boundary ($\sim$ 0.1 μ) occurred only after 5 minutes exposure to boiling nitric acid. Using TEM, no precipitates were detected on the perforated boundaries.

6. The oxalic acid tests differentiated more clearly the relative corrosion resistance of the two commercial casts of 304L after heat treatment, than the nitric acid test. The nitric acid test gave similar, mixed results for both casts, while the oxalic acid test showed cast A to be consistently more resistance to intergranular attack that cast B.

7. Banding attack parallel to the rolling direction was found in most nitric acid test and oxalic acid test specimens. Using EPMA this was found to result from micro-segregation of nickel and chromium, that probably occurred during hot working processes. Higher chromium regions were also lower nickel regions and these areas dissolved preferentially. This segregation banding was unaffected by a solution treatment of 100 minutes at 1050^{o}C.

8. Using x-ray analysis in conjunction with STEM the segregation of phosphorus to the grain boundaries was detected in a specimen of commercial 304L, solution treated at 1050^{o}C and air cooled. The same segregation was observed in a similar steel sensitized for 600 hours at 650^{o}C.

9. The nitric acid test corrosion rate of two experimental casts of 304L was dependent on rate of cooling after solution treatment. Four cooling rates were used.

1. Vermiculite (slowest)
2. Air cooling
3. Forced air cooling
4. Water quenching (fastest)

and air cooling resulted in a higher corrosion rate than the other three.

10. Increasing the level of phosphorus in experimental 304L in the range .006 to .028 per cent tended to increase corrosion rate in the nitric acid test. This was most noticeable after either vermiculite cooling or forced air cooling following a solution treatment.

11. 304L with phosphorus additions, that had been water quenched after solution treatment, showed a distinct trend of increasing nitric acid test corrosion rate with increasing phosphorus level (in the range .006% to .028%) after the first period (48 hours) of the test. This trend was not maintained after the third period (total 144 hours) of the test.

12. The level of boron addition from .001 to .0085 per cent in experimental 304L was found to have no affect on the corrosion rate in the nitric acid test. This was true after all the cooling rates investigated.

13. Between solution temperatures of 1100°C and 900°C the nitric acid test corrosion rates of experimental 304L cooled in vermiculite, was found to increase with decreasing solution treatment temperature. This may be due to smaller grain size as well as increased segregation at the lower solution temperature.

14. Even in 304L sensitized for long times (600h at 650°C) Auger spectroscopy was not practicable due to the failure to produce a fracture surface containing grain facets. All specimens failed by fracture in the ductile mode, even at very low temperatures.

15. The corrosion rate of experimental 304L in the nitric acid test was significantly affected by inhomogeneity of the specimen in several forms

(i) Solute segregation at the grain boundaries

(ii) Large slab-shaped, slag-like inclusions analysed by x-ray to be high in silicon, probably in the form of silicates.

(iii) Variation in composition over quite large distances (5mm) that resulted in some areas showing massive grain dropping while adjacent areas showed very little. The cause of the compositional variation is unknown and no change in microstructure was detected.

(iv) In some specimens high corrosion coincided with increased grain boundary precipitates ($M_{23}C_6$) although this was not always the case.

(v) Areas high in chromium, probably in the form of oxide that had been rolled into the metal, showed preferential attack.

(vi) Numerous stringers parallel to the rolling direction existed, and resulted in end-grain attack. Some of these appeared to be delta ferrite.

16. The initial attack on the grain boundaries of 304L in the nitric acid test varied from boundary to boundary and appeared to be connected to misorientation. Incoherent twin boundaries consistently showed more attack than coherent twin boundaries.

Suggestions for Further Work

The factor responsible for high intergranular attack in cast B of as-received AISI 304L was unidentified. The use of electron energy loss spectroscopy (which is sensitive to light elements), for analysis of the grain boundaries may enable the presence of such elements to be established.

The initial attack on the grain boundaries of 304L in the boiling nitric acid, and oxalic acid tests appeared to be heavily dependent on boundary type and orientation. With a large enough grain size (100 μ) and a sufficiently thin specimen (100 μ), electron channelling patterns in the SEM could be used to easily determine which type of boundaries show the highest attack in the early stage of exposure.

The results of the standard nitric acid tests on phos phorus and boron showed considerable scatter, mainly due to inhomogeneity of the specimens, and presence of inclusions. The use of high purity steels with similar additions of phosphorus and boron in the nitric acid test, in conjunction with grain boundary microanalysis, should reveal more clearly the action of these elements in intergranular corrosion mechanisms.

A study of the potential/time and potentiostatic polarisation behaviour in nitric acid of the boron and phosphorus doped steels used in this study, may contribute

to the understanding of the effect these elements have on the corrosion of the steels.

Appendix 1

Specimen Preparation for TEM work

From the steel to be examined a thin slice approximately 1 mm thick was cut using a diamond slow saw. This ensured that there was minimal deformation and heating during the cutting operation which may have affected the metallographic structure of the steel. The slice was then thinned down further to approximately 0.5 mm thick using a special grinding jig and wet SiC grinding papers. From this thinned piece of metal several small 3 mm diameter discs were cut. This was done by spark-machining using a brass tube with an internal diameter of 3 mm as the cutting tool. The cutting tool was fed vertically down on to the flat surface of the steel, immersed in a suitable fluid, and a high voltage applied across the two. This resulted in spark erosion of a small ring of metal leaving a 3 mm diameter disc. Using a special specimen holder, this disc was further mechanically thinned using wet SiC grinding papers of 600 mesh grit down to a thickness of between 0.125 mm and 0.3 mm. This disc then had to be electropolished at the centre to give a region that was electron optically transparent. The largest such region could be achieved with the thinnest possible initial starting thickness (0.125 mm). Although this could result in specimens with very large electron-optically thin areas, these specimens were far more liable to deformation effects and mechanical damage during handling, and transport became a problem. The optimum thickness prior to electropolishing was found in most cases to be 0.175 mm. Final electrothinning

was achieved using a Tenupol electropolisher supplied by Struers. This is a commercially developed version of the widely used jet-polishing technique for preparing thinned discs. The disc is placed in a special holder and immersed in an electrolyte of 5 per cent perchloric acid in 2-Butoxy-ethanol. The specimen holder is arranged so that jets of flowing electrolyte approximately 1 mm in diameter are played onto either side of the disc. The flow rate of the two jets is adjustable. The electrolyte is maintained at a temperature between -10^{o} and $0^{o}C$. The specimen disc is made the anode and there is a circular platinum wire cathode on each side of the specimen. When there is a voltage (usually between 50 and 60 volts) applied between anode and cathode, current flows and the anodic specimen polishes and dissolves electrolytically. The jets of electrolyte ensure that the rate of dissolution during polishing is greatest at the centre of the disc so that when perforation occurs, a hole appears at the centre of the disc, dishing having occurred on both sides of the disc. If the polishing is stopped as soon as perforation occurs then there should be an electron-optically transparent region round the hole. This is not always the case, because if the steel has a high concentration of particles and inclusions, perforation can occur by one of these particles dropping out of the specimen leaving a hole right through the disc, while the rest of the steel is still electron-optically opaque. In the Tenupol equipment a light beam and photo-electric cell are so arranged that at the moment of perforation, the light beam shines through the hole in the specimen, triggers the

photo-electric cell, which then cuts the circuits to the electrolyte pump and the anode/cathode cell, thus stopping instantly any more specimen dissolution. During polishing the electrolyte flow rate was kept at the lowest setting attainable without the pump actually stopping. High flow rates were found to result in flow patterns on the polished specimen and a reduced thin area due to high dissolution rates.

Appendix 2

Etching Reagents for Stainless Steel

1. Oxalic Acid Electrolytic Etch

10% oxalic acid (w/v) in water. Specimen anode. 6v for 0.5 to 20 secs.

Results in good clean surface. Presence of carbides at boundaries result in intergranular attack and dissolution of carbides. Lack of carbides results in step-type structure with differential dissolution of grains. Delta ferrite dissolved.

2. 50 volumes H_2O, 0.2 vol. HF (50%), 10 HNO_3 (70%)

Immersed 5-10 minutes.

Generally clean appearance, directional segregation clearly revealed. Grain boundaries not clear revealed at first. Slight pitting.

3. Vilella's Reagent 5 ml HCL, 1 ml picric acid, 100 ml ethanol

Immersed 2-3 minutes.

Not very clear. Misty film covered surface. No distinct grain boundaries revealed. Segregation banding clearly exposed.

4. Marble's Reagent (4g $CuSO_4$, 20 ml HCe, 20 ml H_2O)

Immersed 2-10 seconds.

Good clean etch, revealing grain boundaries, twin boundaries, and segregation banding. Some general attack of surface.

5. 720 cm^3 H_2O, 180 cm^3 HCl (conc), 60g $FeCl_3$

Immersed 1-3 min

Poor etched structure, with grey film deposit on surface, not easily removed. Some grain boundaries and segregation banding revealed.

Appendix 3

Nitric Acid used for Nitric Acid Test

The nitric acid used in the tests was Analar grade acid supplied by BDH Ltd. This was then diluted with deionised water to give a 65 per cent solution. The manufacturers quoted levels of impurity for this acid are:-

Non-volatile matter	0.001%
Chloride	0.00005%
Phosphate and silicate (SiO_2)	0.0001%
Sulphate (SO_4)	0.0002%
Arsenic	0.000001%
Copper	0.00001%
Iron	0.00002%
Lead	0.00001%
Manganese	0.00004%

Appendix 4

X-ray microanalysis using EPMA and STEM

Both of these methods are widely used for the chemical analysis of metallurgical specimens. EPMA uses a bulk specimen of the order of 2 mm thick while STEM utilises a standard TEM specimen (foil or disc), which must be of the order of 500 Å thick in the area of interest. EPMA usually uses crystal spectrometers to calculate the wavelength of the x-rays produced from their diffraction behaviour. STEM on the other hand usually uses a solid state silicon detector to analyse and count the x-rays by their characteristic energies.

When an incident electron beam, such as that in SEM, strikes a bulk metal specimen, some of the electrons will interact strongly with the charged nucleii of the atoms and will emerge as back scattered electrons. Other incident electrons will lose energy to electrons within the specimen displacing them from their atoms. These electrons can escape if generated near the surface of the specimen. If however they are ejected from core positions, the transference of electrons from one energy shell to vacancies in a lower level shell will result in the production of X-rays. As the energy difference between the shells depends on the atom species, the x-rays thus generated will be characteristic of the atom species present. In a bulk specimen the x-rays are generated from a onion-shaped volume of material.

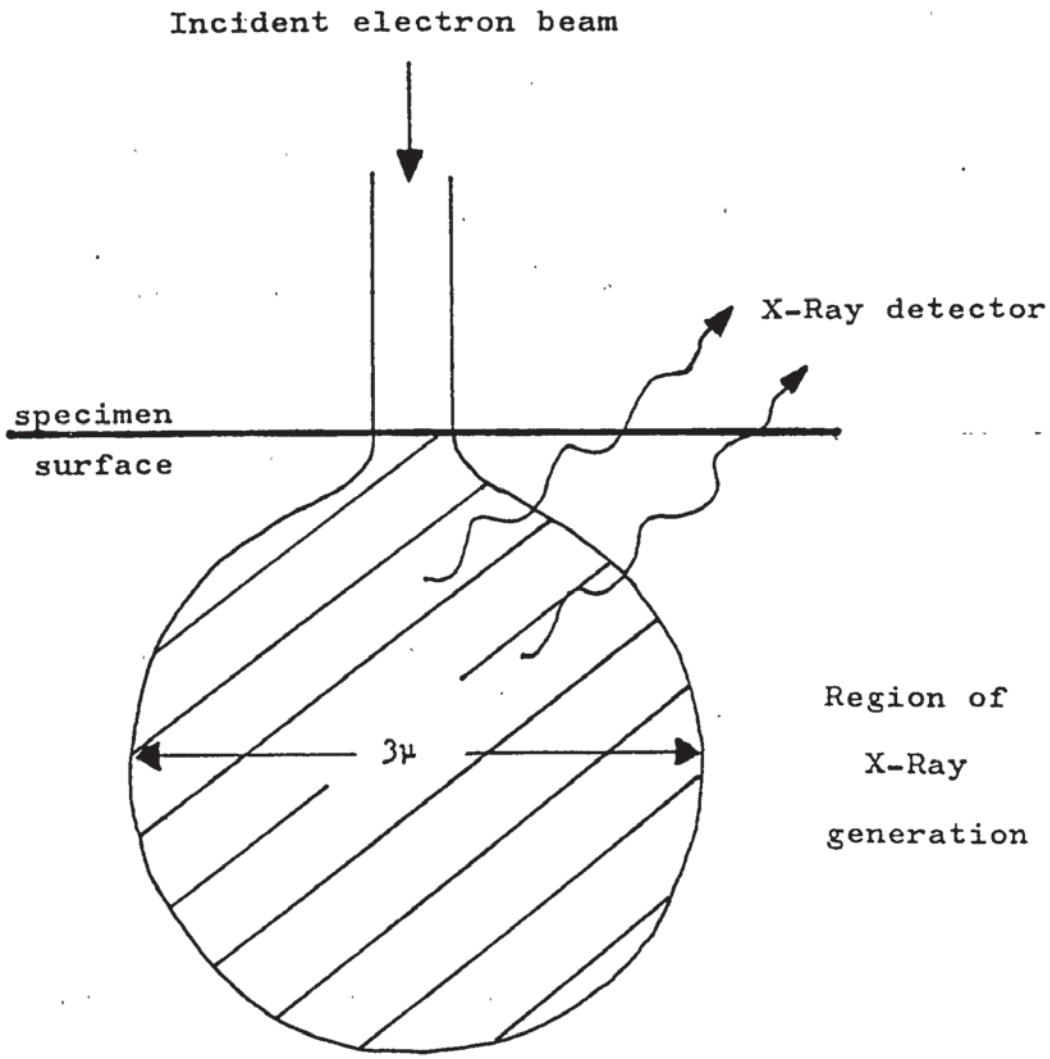

Fig. 32 Diagram showing region from which x-rays are generated during analysis of a bulk specimen in EPMA.

The main use of this method has been in EPMA (Electron Probe Microanalysis) in which the characteristic x-rays resulting from the incidence of a fine electron beam are collected in crystal spectrometers which can measure and count wavelength or energy spectra. EPMA however has rather a poor spatial resolution of 1000 nm on bulk specimens and can only count one energy at a time. The EPMA is also restricted in that the image provided is of rather poor quality and topographical examination at the same time as microanalysis is relatively difficult [89]. The poor spatial resolution is a result of the beam spreading that will occur in bulk specimens.

The multiple scattering of the electrons results in x-rays being generated from a volume of material many times wider than the beam itself. The raw x-ray data from a bulk specimen have to be corrected for three effects that arise as a result of beam spreading.

(i) The "atomic number effect" arises because the volume of material excited and the proportion of electrons that are backscattered depends on Z. A high Z specimen will have a larger excited volume and higher proportion of back-scattered electrons.

(ii) The "absorption effect" is due to the fact that the x-ray path length and absorption coefficient of specimen will differ to that of the standard causing a difference in attenuation of the emerging x-rays.

(iii) The third effect is the fluorescence effect which can result in the introduction of a secondary contribution to the generation of a given characteristic x-ray due to the fluorescence excitation by x-radiation from another element. Many extremely complicated methods have been devised to correct the Z, A and F effects, but use of these usually requires considerable software.

STEM microanalysis uses a much higher intensity electron probe than EPMA in conjunction with an extremely thin

specimen, of the order of 300 nm, prepared specially. The very thin sections used mean that below a certain thickness the effects of absorption and fluorescence are minimal and in some cases can be neglected.

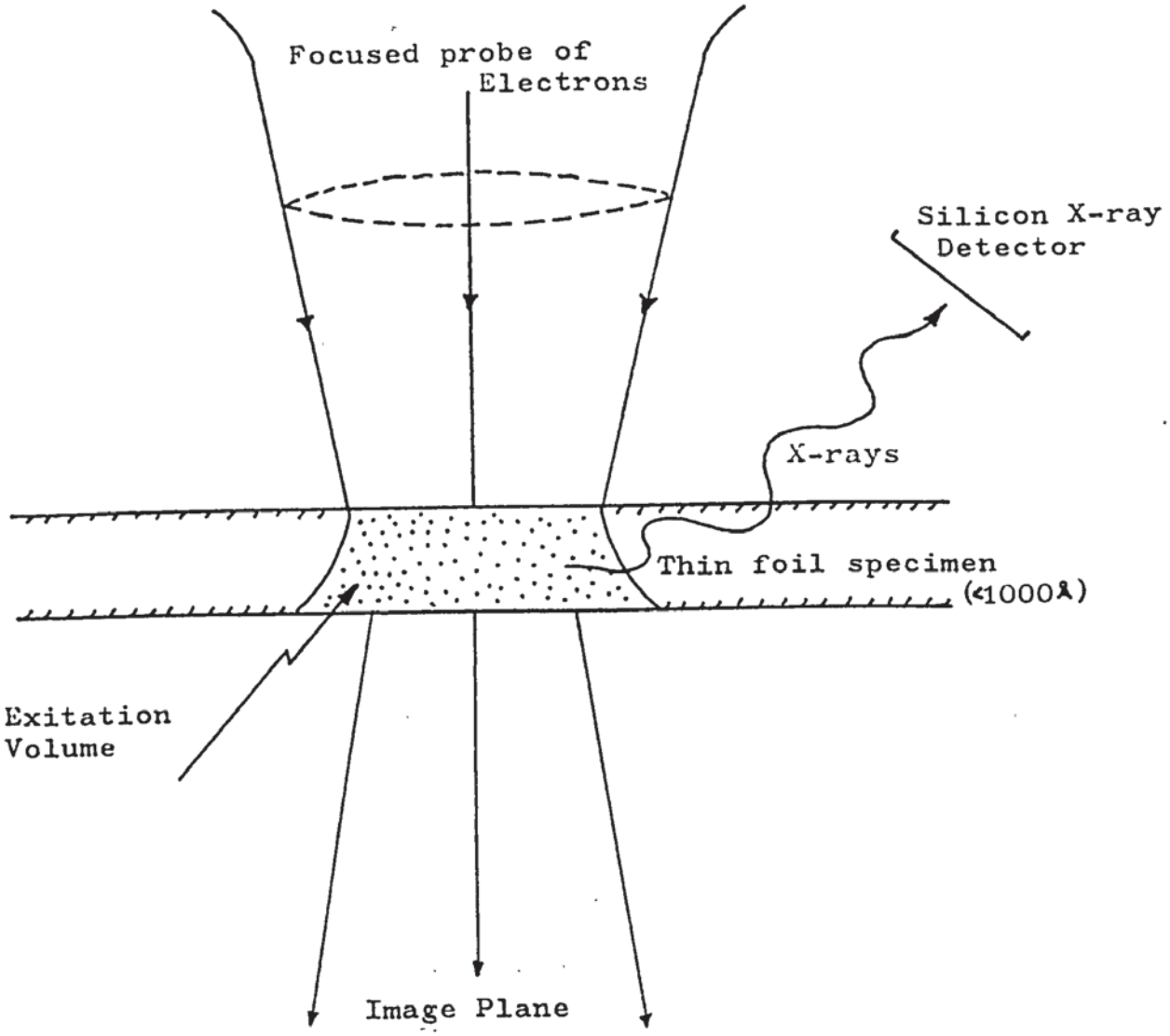

Fig. 33 Schematic diagram showing production of x-rays from thin specimen (Ref. 89).

The method of analysis of the x-rays collected while using STEM can be either wavelength or energy dispersive, the latter being the most popular. Energy dispersive analysis systems can count all emitted energies simultaneously thus shortening the analysis time considerably. The resolution of wavelength dispersive systems is slightly

better but they are on the whole more cumbersome to use.

In energy dispersive systems the x-rays emitted by the specimen are collected, sorted and counted, and a multichannel analyser produces a histogram of number of x-rays versus energy. Thus when the STEM electron beam is placed on a particular microstructural feature and the x-rays collected, the peaks on the N(E) v E histogram will be characteristic of the elements in that feature. As we shall see the x-ray spectrum is made up of other components as well as the characteristic x-rays.

When STEM is used in conjunction with an energy dispersive x-ray analyser such as Kevex or Edax, it is possible to carry out semi-quantitative or quantitative analysis of thin foils using a ratio technique developed by Cliff and Lorimer [90].

In a sufficiently thin specimen only a small amount of scattering takes place. In general if a specimen is thin enough for conventional electron microscopy (CTEM) at 100 kV then it will be thin enough for STEM.[90, 91, 92, 93] If it satisfies these conditions then the A and F corrections are small and the ratio of characteristic x-ray intensities of any two elements is independent of the specimen thickness and is related by an experimentally determined constant to the chemical weight fraction of the two elements. Thus Cliff and Lorimer [90] have shown that

$$\frac{I_A}{I_B} = K_{AB} \frac{C_A}{C_B}$$

where I_A, I_B are the measured intensities of the characteristic x-rays of elements A, B, while C_A, C_B are the corresponding concentrations of A, B in the volume of specimen analysed, and K is a constant determined experimentally and which is independent of thickness and composition. Lorimer et al [94] found that experimental values of K agreed satisfactorily with the calculated values of K obtained by the equation proposed by Goldstein et al, [95] except at values of Z < Si. Except at such values it would thus appear to be sufficient to determine K for a given detector and accelerating voltage. However certain considerations and precautions must be undertaken.

In addition to the characteristic x-ray peaks in the spectrum it has another component which spreads broadly across the whole spectrum in varying intensity, the Bremsstrahlung. Its intensity varies with atomic number of the specimen and the energy of the electron beam. In any quantitative analysis of the chracteristic x-ray peaks, the Bremstrahlung continuum background must be deducted from the spectrum prior to counting. Most commercially produced analysis equipment now have built-in procedures to enable the background to be deducted easily and rapidly.

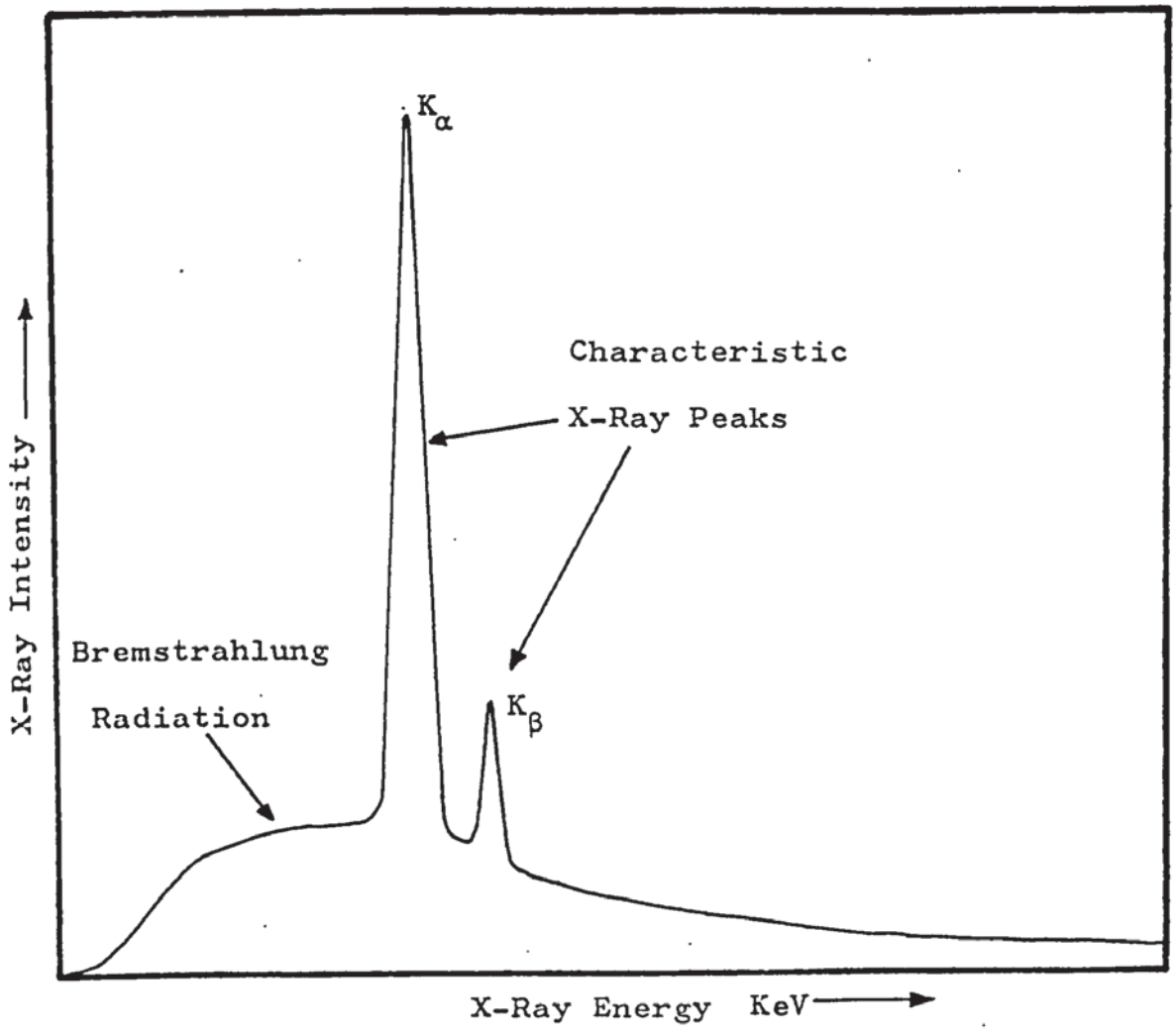

Fig. 34 Schematic diagram showing distribution of x-ray intensity when an electron beam interacts with a copper specimen.

Goldstein and Williams [96] indicated the problem that many workers using STEM had with the recorded spectrum containing spurious x-rays which had not been generated in the area of interest.

The spurious x-rays can be produced by either unwanted x-rays or electrons striking the 3 mm diameter specimen.

Unwanted electrons can strike the specimen outside the area of interest if they are scattered by the final collimating aperture in the electron optical system. The final objective lens will focus these electrons onto the

specimen but not at the point of interest, and also onto the specimen holder itself resulting in spurious x-rays. It is also possible that some incident electrons may be back-scattered from the specimen so as to strike adjacent parts of the microscope such as the final pole piece.

Unwanted x-rays arising from the interaction between the main electron beam and the final C_2 aperature can fluoresce the whole of the 3 mm specimen thus producing spurious x-rays from the specimen. This will occur if the aperture is too thin to absorb all the x-rays produced when the main electron beam strikes its upper surface.

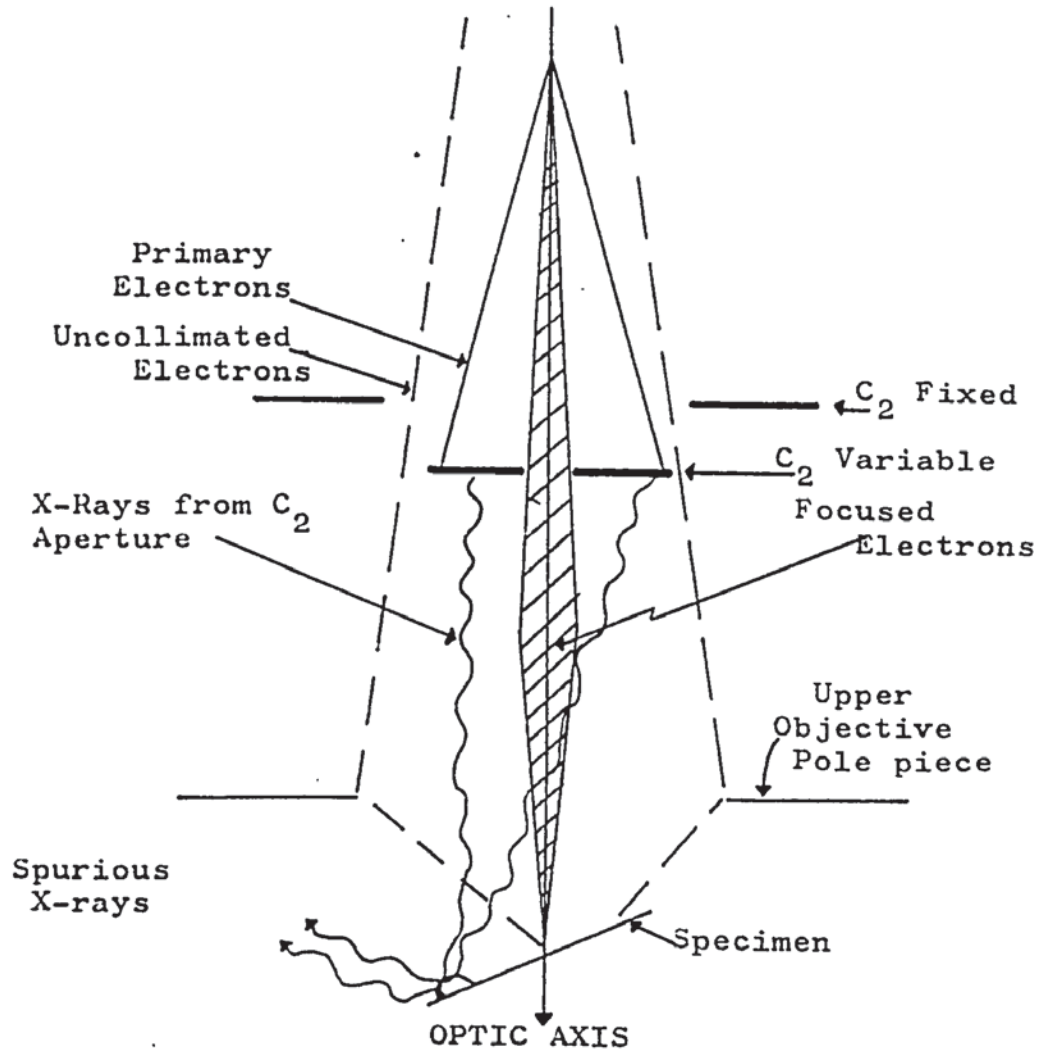

Fig. 35 Diagram of electron optical column showing the two principal sources of spurious X-rays. (after ref. 96)

Goldstein et al [96] consider that self supporting discs such as used in this work are more prone to production of spurious x-rays due to the larger area, and that characteristic x-ray production is proportional to specimen thickness.

Other workers [90, 97] have commented on the production of spurious x-rays, Nicholson et al [98] investigated the main sources of these x-rays and attempted to reduce their effect. The main interferences he found were Cu K and L series lines from the grid bar and specimen rod, Mo K and L lines from the objective aperture, Au L and M lines from the anti-contaminator and Fe K lines from the objective lens pole piece. Normally during microanalysis the objective aperture would be withdrawn. By use of carbon and brass discs above the specimen and in the top of the anti-contaminator respectively and a shortening of the aperature slide,Nicholson found he could significantly reduce spurious x-ray counts in the spectra.

The presence of spurious x-rays can be demonstrated by performing a hole count. That is, allowing the main electron beam to pass through a hole in the specimen without striking any of the specimen and then counting the x-rays collected at the detector as a result of unwanted interactions.

It is difficult to reduce the spurious x-rays without sophisticated and time consuming alterations being made to the microscope. Significant improvements can be made

by using a low background specimen holder made either of beryllium or carbon, both of which are commercially available.

Goldstein and Williams [96] do not consider that deducting the spurious spectrum from the collected spectrum, as proposed by Kenik and Bentley [99], will necessarily result in the correct spectrum. They suggest that where quantitative measurements are being made and there is a large (of the order of 50%) contribution of spurious x-rays to a spectral peak, the only solution is to eliminate as far as possible uncollimated electrons, and C_z aperture-induced high energy continuum x-rays.

For microanalysis it is critical that the spatial resolution be maximised to avoid signals from outside the area of interest. Faulkner at al [100] consider four factors have to be optimised.

1. Beam diameter at specimen must be minimised.
2. Specimen thickness must be minimised.
3. Accelerating voltage must be maximised.
4. Beam drift must be minimised.

Spatial resolution will always be limited by the beam spreading within the specimen. Monte Carlo calculations by Kyser and Geiss [101] showed that at 100 kV in a Cu foil 100 nm thick with a 10 nm beam, 90% of the x-rays come from a cylinder 50 nm diameter. With a zero width beam the cylinder will be 16 nm diameter. Beam spreading worsens at higher atomic numbers.

Goldstein describes a simple model to demonstrate the extent of beam spreading which correalates beam spreading (b) with specimen thickness (t) in the equation

$$b = k \, {}^{Z}/_{E_o} \, {}^{p}/_{A}^{\frac{1}{2}} \, t^{\frac{3}{2}}$$

where k is a constant, Z and A are sample atomic number and weight respectively, p is sample density and Eo is the beam energy in KeV.

The time of analysis at one given spot with an electron beam is limited primarily by the beam-induced contamination of the specimen. The most common form of these is the build-up of two conical piles of contamination on the sample surface, one where the beam enters the sample and the other where it leaves on the other side. These conical piles can cuase deflection of the beam should charging occur, and they increase the effective thickness of the specimen, decreasing spatial resolution. To overcome contamination it is essential to have a working pressure as low as possible in the specimen chamger i.e. better than 10^{-8} Torr. Most modern TEM/STEM machines have a liquid nitrogen cooled anti-contaminator.

Contamination spots can be usefully utilised in the measurement of specimen thickness. If the beam passes through the specimen while normal to it and contamination spots are allowed to form, then when the specimen is tilted through an angle θ, the spots will have a separation s such that the thickness of the specimen t, is given by:- $t = s/\sin \theta$

Acknowledgements

I would like to thank Dr D J Arrowsmith for his help and guidance throughout the period this work was undertaken, and would also like to thank the technical staff of the Department of Metallurgy and Materials Engineering, University of Aston in Birmingham, for their assistance.

Financial assistance from the Science and Engineering Research Council and the British Steel Corporation who also supplied some of the laboratory facilities is gratefully acknowledged. The help of staff of the Department of Physics, University of Warwick and staff of UKAEA (Risley) was invaluable and greatly appreciated.

Some of the electron microscopy facilities were provided by the Department of Metallurgy and Materials, University of Birmingham, whose staff were particuarly helpful.

Miss K A Monson-Davies assisted with the drawings and the thesis was typed with patience by Miss Gillian Davies.

1. Sedriks, A.J. "Corrosion of Stainless Steels" publ. J. Wiley and Sons (N.Y.) 1979.

2. Colombier, L. Hochmann J., "Stainless and Heat-resisting Steels", 143 ff, publ. E. Arnold 1967.

3. Bain, E.C., Aborn, R.H., Rutherford, J.J.B., Trans. Am. Soc. Steel Treat., 21, 481, 1933.

4. Kinzel, A.B., J. Met. Trans. AIME, 194, 469 - 488, May 1952.

5. Tedmon, C.S., Vermilyea, D.A., Rosolowski, J.H., J. Electrochem. Soc. 118, 192, 1971.

6. Cihal, V. Prot. Met. Vol 4, No 6, 563, 1968.

7. Binder, W.O., Brown, C.M., Franks, R., ASM Trans. Vol. 41, 1301, 1949.

8. Heger, J.J., Hamilton, J.L., Corrosion 11, 6, 1955.

9. Warren, D., Corrosion 15, 5, 221-232t, May 1959.

10. Warren, D., Corrosion 15,4,213-220t, April 1959.

11. Schwaab, P., Schwenk, W., Ternes, H. Werkstoffe u. Korrosion 16, 844, 1965.

12. Cihal, V., Kasova, I., Kubelka, J., Metaux Corros. 44, No 529, 281, September 1969.

13. Scharfstein, L.R., Effects of Residual Elements on the Properties of Stainless Steels, ASTM STP 418, p. 90, 1967.

14. Rosenberg, S.J., Darr, J.H., Trans. Am. Soc. Met. 41, 1261-1288, 1949.

15. Dillon, C.P., Corrosion 16, 433t, 1960.

16. Franks, R., Corrosion Handbook, publ. J. Wiley (N.Y.) p. 160, 1948.

17. Brown, M.H., DeLong, W.B., Meyers, W.R., Evaluation Tests for Stainless Steels, ASTM STP 93, p.103, 1950.

18. Armijo, J.S., Corrosion 24, 24, 1968.

19. Briant, C.L., Corrosion NACE, 36, 9, 497-509, 1980.

20. Joshi, A., Interfacial Segregation, publ. ASM, 46, 1979.

21. Aust, K.T., Trans. AIME, 245, 2117, 1969.

22. Voeltzel, J., Henry, G., Plateau J., Crussard C. Memoires Scientifique, Rev. Metall. 60, 879, 1963.

23. Farrell, J.W., Rosenthal, P.C., Metal Prog. 77, 101, 1960.

24. Robinson, F.P A. and Scurr, W.G., Corrosion 33, 11, 408, 1977.

25. Costello, T.M., Pinnow, K.E., Moskowitz, A., Mat. Prot, 8, 15, Nov. 1969.

26. Williams, T.M., Harries, D.R., Furnival, J., J1S1 210, 351, 1972.

27. Williams, T.M., Stoneham, A.M., Harries, D.R., Metal. Sci, 10,14, Jan. 1976.

28. Brown, A., Garnish, J.D., Honeycombe, R.W.K., Metal. Sci. 8, 317-324, 1974.

29. Levitin, V.V., Syreishchikova, V.I., Fiz Metal, Metalloved 7, 2, 1959.

30. Sumner, W.B., Materials Perf. 18, (9), 39, 1979.

31. Stickler, R., Vinckier, A., Trans ASM, 54, 362, 1961.

32. Chaudron, G., EURAEC -976 Quart. Rept. 6, Oct-Dec, 1963.

33. Henthorne, M., ASTM STP 516, 66-119, American Society for Testing and Materials, 1972.

34. Alm, S., Kiessling, R., JIM, 91, 5, 190, 1962-63.

35. Fleetwood, S., JIM, 90, 429, 1961-62.

36. Weaver, C.V., JIM, 90, 404, 1961-62.

37. Osozawa, K., Bohnenkamp, K., Engell, J.H., Corros. Sci. 6, 421, 1966.

38. Stickler, R., Vinckier, A., Corros. Sci. 3, 1-8, 1963.

39. Streicher, M.A., J. Electrochem Soc., 106, 161, 1959.

40. Coriou, H., Hure, J., Plante, G., Electrochim. Acta, 5, 105, 1961.

41. Blom, U., Kvarnback, B., Materials Perf. 14, 42-46 July 1975.

42. Hooper, R.A.E., Honess, C.V., Stainless Steel '77, Publ. Climax Moly. Co., Conference (London 1977) Report, 247-253, 1978.

43. Joshi, A., Stein, D.F., Corrosion 28, 9, 321, 1972.

44. Huey, W.R., Trans. Am. Soc. Steel. Treat. 18, 1126, 1930.

45. Gillette, H.W., Sym. on Evaluation Tests for Stainless Steels, ASTM, STP 93, 40, 1949.

46. Recommended Practice for Detecting Susceptibility to Intergranular Attack in Stainless Steels, ASTM Designation A262-79. Published by American Society for Testing and Materials.

47. Streicher, M.A., ASTM STP 656, 3-84, 1978.

48. Hondros, E.D., J. Physique Coll. 36, C4-117, 1975

49. DeLong, W.B., Multiple Testing of Stainless Steel Specimens. ASTM STP No. 93, 211-214, 1949.

50. Shirley, H.T., Truman, J.E., JISI, 171, 354, 1952.

51. Kurtepov, M.M., Akimov, G.V., Doklady Akad, Nauk SSSR, 87, 625, 1952.

52. Truman, J E., J. Appl. Chem. 4, 273, 1954.

53. Kurtepov, M M., Akimov, G.V., Doklady Akad, Nauk SSSR, 87, 93, 1952.

54. Mc Intosh A.B., Chemistry and Industry, 22. 687, 1957

55. Brown, M.H., Corrosion 30, 1, 1-12, 1974.

56. Streicher, M A., ASTM Bulletin, 35-38, Feb. 1953.

57. Lena, A.J., Discussion in Trans ASM 45, 446, 1953.

58. Couriou, H., Grall, L., Kurka, G., Plante, G., Colloque de Metallurgy (IV), 75, 1960.

59. Tupholme, C.B., Boucher, H.G.C., ISI Spec. Report 86, 238-245, 1964.

60. Cowan, R.L., Tedmon, C.S., in Advances in Corrosion Science. Ed. Fontana, M.G., Stahle, R.W., Plenum Press, Vol. 3, 293-400, 1973.

61. Wiederisch, H., Okomato, P.R., Interfacial Segregation. Publ. Am.Soc. Met. p. 405, 1979.

62. Williams. T.M., Stoneham, A.M., Harries, D.R., Metal Sci., 10, 14, Jan. 1976.

63. McLean, D., Grain boundaries in Metals, p. 148, Oxford (Clarendon Press) 1958.

64. Hondros, E.D., Mechanics and Physics of Fracture, Inst. Phys., Cambridge, Paper 21, p. 201, 1975.

65. Inman, M.C., Tipler, H.R., Met. Rev. 8, 105, 1963.

66. Aust. K.T., Armijo, J.S., Koch, E.F., Westbrook, J.H., Trans. ASM 61, 270, 1968.

67. Kraai, D.A., Floreen, S., Trans. AIME 230, 833, 1964.

68. Aust, J.T., Hanneman, R.E., Niessen, P., Westbrook, J.H., Acta Met 16, 291, March 1968.

69. Doig, P., Flewitt, P.E.J., J. Micr. 112, 3, 257-267, 1978.

70. Armijo, J.S., Corrosion, 21, 235-244, 1965.

71. Aust, K.T., Armijo, J.S., Koch, E.F., Westbrook, J.H., Trans. Am. Soc. Met. 60, 360, 1967.

72. Devine, T.M., Briant, C.L., Drummond, B.J., Scripta Met 14, 1175, 1980.

73. Armijo, J.S., Corr. Sci. 7, 143-150, 1967.

74. Tromans, D., Nutting J., Corrosion 21, 143, 1965.

75. Abe, S., Ogawa, T., Met. Prog. 116, 4, 61-65, 1979.

76. Armijo, J.S., Wilde, B.E., Corr. Sci. 8, 649-664, 1968.

77. Fontana, M.G., Met. Trans 1, 3251, 1970.

78. Hondros, E.D., Seah, M.P., Scripta Met. 6, 1007, 1972.

79. Coulomb, P., Leymonie, C., Lacombe, P., Acta Met. 7, 691, 1959.

80. Howard, R.E., Lidiard, A.B., Phil. Mag, 11, 1179, 1968.

81. Aust, K.T., Iwao O., NACE - 3, U.R. Evans, Conf. on Localised Corr. Williamsburg, p. 62-75, 1974.

82. Seah. M.P., Surf. Sci. 53, 168-212, 1975.

83. Evans, U.R., Corrosion and Oxidation of Metals, publ. E. Arnold, London, 1960.

84. Braun, I., Frank, F.C., Meyrick, G., Phil. Mag 3, 1312, 1958.

85. Vermilyea, D.A., Tedmon, C.S., Met. Trans. 1, 1076, 1970.

86. Westbrook, J.H., Met. Rev., 9, 36, 415, 1964.

87. Danyluks, Park, J.Y., Busch, D.E., Scripta Met 13, 857, 1979.

88. Abe, S., Private Communication, 1981.

89. Clarke, D.R., Electron and Positron Spectroscopies in Material Science and Engineering. Publ. Academic Press, p. 315-334, 1979.

90. Cliff, G., Lorimer, G.W., Proc. 5th Eur. Congr. Electr. Micr., Manchester, IOP, London,p140, 1972.

91. Cliff, G., Lorimer, G.W., J. Micr. 103, 2, 203, 1975.

92. Lorimer, G.W., Razik, N.A., Cliff, G., J. Micr. 99, 2, 153, 1978.

93. Lyman, C.E., Manning, P.E., Duquette, D.J., Hall, E., SEM 1, 213-220, 1978.

94. Lorimer, G.W., Al-Salman, S.A., Cliff, G., Inst. Phys. Conf. Ser. No. 36, Chapter 9, 369, 1979.

95. Goldstein, J.I., Proc. Workshop on Anal. Electr. Micr. SEM 1977 (ITT Research Inst. Chicago) 315-324, 1977.

96. Goldstein, J.I., Williams, D.B., SEM 1, 427-434, 1978.

97. Hall, T.A., J. Micr. 110, 2, 103-106, 1977.

98. Nicholson, W.A.P., Robertson, B.W., Chapman, J.N., Inst. Phys. Conf, Ser. No. 36, Chapt. 9, 373, 1977.

99. Kenik, E.A., Bentley, J., Influence of x-ray induced Fluoresecence on Energy Dispersive Analysis of thin foils. Proc 8th ICXOM 12th Annual MAS Conference, No. 114A 1977.

100. Faulkner, R.G., Hopkins, T.C., Norrgard, K, X-ray Spectrometry 6, 2, 73-79, 1977.

101. Kyser, D., Geiss, R.H., Proc. 8th Int. Conf. X-ray Opt. Microanalysis, Boston, Mass, 110 a-d, 1977.

102. Solomon, H.D., Corrosion 36, 7, 356, 1980

103. Mykura, N., MSc Thesis, University of Aston, 1978.

104. Hooper, R.A.E., Unpublished work.

105. Goldstein, Y.E., et al. Met. Sci. Heat Treat. (USSR) 20, 11, 1978.

106. Hatfield, W.H., JISI 127, 380-383, 1933.

107. Chadwick, G.A., Metallography of Phase Transformations, publ. Butterworth London. p.106, 1972.

108. Szummer, A., Corrosion NACE 35, 461, 1979.

109. Brown, M.H., Corrosion 29, 10, 384, 1973.

110. Pickering, F.P., Int. Met. Rev. 21, 227, 1976.

111. Masumoto, I, Tamaki, K., Katsuna, M., J.Japan Welding Soc., 41, 1306-1314, 1972.

112. Gooch, T.G., Brit. Welding J., 15, 345-357, 1968.

113. Bannerjee, B.R., Dulis, E.J., Hauser, J.J., Trans. ASM, Vol. 6, 103, 1968.

114. Chen, W.Y.C., Stephens, J.R., Corrosion NACE, 35, 10, 443-450, 1979

115. Pickering, F.B., The Metallurgical Evolution of Stainless Steels, published by ASM, 1979, Editor Pickering F.B., 274-283.

Bibliography

This list contains material used during the preparation of this work that is not directly referred to in the text.

Armijo, J.S., Law, J.R., Wolff, U.E., Radiation effect on the mechanical properties and microstructure of Type-304 stainless steel. Nucl. Applic. Vol. 1, 462 - 477, Oct . 1965.

Ball, M.D., Morris, P.L., The scanning transmission electron microscope - a versatile tool for the materials scientist. The Met. and Mat. Tech., 11 , 327 , June 1979.

Barbi, N.G., Judd G., Microstructure and microsegregation effects in the intergranular corrosion of austenitic stainless steel. Met. Trans., 3, 2959-2964, Nov. 1972.

Briant, C.L., Banerji, S.K. Intergranular failure in steel: the role of grain boundary composition. Int. Met. Rev., No. 4, 23 , 164-199, 1978.

Colombier, L., Hochmann J., Stainless and Heat Resisting Steels, publ. E. Arnold Ltd., 1967.

DeBold, T.A., Which corrosion test for stainless steel? Mat. Eng., 92 , 67-72, 1980.

Dhirendra, Sanyal, B., Effect of oxidising agents on the passivation of stainless steel AISI 321 in sulphuric acid. Br. Corr. J., 13, 2, 88-92, 1978.

Doig, P, Flewitt, P.E.J., Wild, R.K., A comparison of x-ray (STEM) and auger electron spectroscopy for the analysis of grain boundary segregation. Phil. Mag. A, 37, 6, 759-768, 1978.

Edeleanu, C., A potentiostatic technique for studying the acid resistance of alloy steels., J.I.S.I., 122-132, 188, Feb. 1958.

Fontana, M.G., Greene, N.D., Corrosion Engineering, 2nd Edition, publ. McGraw-Hill Book Co., N.Y., 1978.

Hahin, C., Stoss, R.M., Nelson B.H., Reucroft, P.J., Effect of cold work on the corrosion resistance of non-sensitized austenitic stainless steels in nitric acid. Corrosion, 32, 6, 229-238, 1976.

Heeley, E.J., Corrosion resistance of some austenitic Cr-Ni steels of 18/8/Ti composition, J.I.S.I., 182, 241-256, 1956.

Henry, G., Philibert, J., Mechanism of the action of boron in austenitic stainless steels. Memoires Scientifiques Rev. Met, 67, 4, 233-251, 1970.

Kirkby, H.W., Morley, J.I., Sigma phase in duplex chromium-nickel-molybdenum, corrosion resisting steels J.I.S.I.,158,289-294, March 1948.

Lea, C., Stress corrosion cracking and temper brittleness: effect of phosphorus grain boundary segregation in a low alloy steel. Metal Sci., 14, 107, March 1980.

Lewis, M.H., Hattersley, B., Precipitation of $M_{23}C_6$ in Austenitic Steels. Acta Met, 13, 11, 1159-1168, 1965.

Loginow , A.W., Evaluation of intergranular corrosion in stainless steel, J. of Test. and Eval., 4, 6, 434 - 439, Nov., 1976.

Low, J.R., Impurities, interfaces and brittle fracture Trans. Met. Soc. AIME, 245, 2481, 1969.

Lyman, C.E., Analytical electron microscopy of stainless steel weld metal, Welding Research Supplement (Welding J.), 189s - 194s, July 1979.

Maher, D.M., Joy, D.C., The scanning transmission electron microscope: a Micro-area Analytical System, J.Met. 29 Feb. 1977, 26 - 30.

Nockolds, C., Cliff, G., Lorimer, G.W., Characteristic x-ray Fluorescence correction in Thin Foil Analysis. Micron 11, 325-326, 1980.

Ogura, T., Makino, A., Masumoto, T., Comparison of Auger electron spectroscopy and etching method for grain boundary segregation of phosphorus, Scripta Met., 14, 887, 1980.

Phillips, V.A., Modern Metallographic Techniques and Their Applications, publ. Wiley-Interscience 1971.

Rosenfeld, I.L., Danilov, I.S., Oranskaya, R.N., Breakdown of the passive state and repassivation of stainless steels. J. Electrochem. Soc. 125,1729, Nov. 1978.

Shibad, P.R., Corrosion properties of nickel free austenitic stainless steel as compared with 18/8 steel. J. Electrochem Soc. India, 27, 1, 53-57, 1978.

Shreir, L.L. (Ed.), Corrosion, Vol. 1 and 2, 2nd Edition, publ. Newnes-Butterworth, London, 1976.

Skoulikidis, T., Vassiliou, P., Symniotou, E., Critique of corrosion potential/time and potentiostatic polarization curves as a method of predicting the general corrosion of metals and alloys (Fe,Al). B. Corr. J. 14, 3, 149-154, 1979.

Smallman, R.E., Ashbee, K.H.G., Modern Metallography, publ. Pergamon Press, Oxford, 1966.

Stein, D.F., Joshi, A., Laforce, R.P., Studies utilising Auger electron emission spectroscope on temper embrittlement in low alloy steels. Trans ASM, 62, 776, 1969.

Terao, N., Sasmal, B., Precipitation of $M_{23}C_6$ type carbide on twin boundaries in austenitic stainless steels. Metallography 13, 117-133, 1980.

Theus, G.J., Staehle, R.W., Review of stress corrosion

cracking and hydrogen embrittlement in the Austenitic Fe-Cr-Ni alloys.

Thompson M.N.,Doig P.,Edington J.W.,Flewitt, P.E.J. The influence of specimen thickness on x-ray count rates in STEM microanalysis. Phil. Mag. 35, 6, 1537-1542, 1977.

West. J., Electrodeposition and Corrosion Processes. Publ. Van Nostrand Reinhold Co., London, 1970.

Wilson, F.G., Mechanisms of intergranular corrosion of austenitic stainless steels - literature review. Br. Corr. J., 6, 100-108, May 1971.

Auger Electron Spectroscopy Handbook, Eds. Davis, Macdonald, Palmberg, Riach, Weber. Publ. Phys. Electronic Industries Inc., Minnesota, 1976.